

DISS. ETH NO. 23836

# **Synthesis and Properties of High Molecular Weight Poly(*m,p*-phenylene)s**

A thesis submitted to attain the degree of  
DOCTOR OF SCIENCES of ETH ZURICH  
(Dr. sc. ETH Zurich)

presented by

BERND DEFFNER

Diplom-Chemiker, University of Mainz

born on 10.10.1986

citizen of Germany

accepted on the recommendation of

Prof. Dr. A. Dieter Schlüter, examiner

Prof. Dr. Jan Vermant, co-examiner

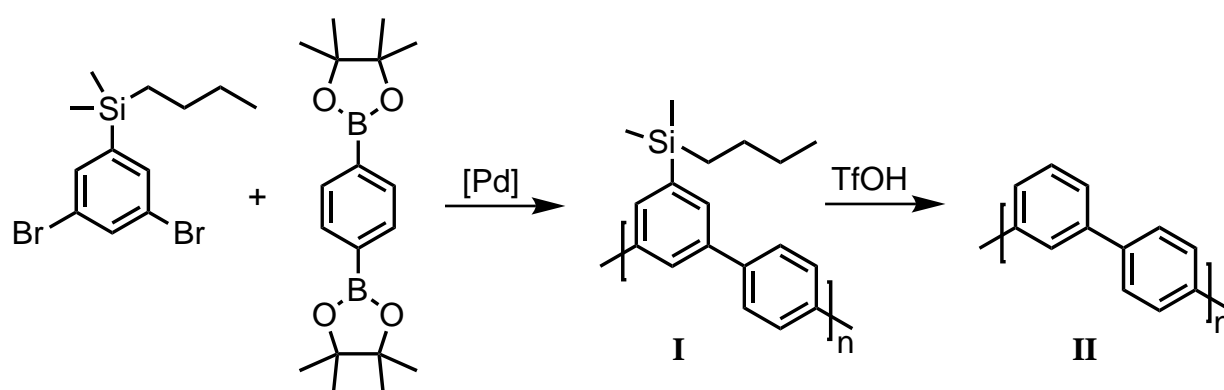
Prof. Dr. Massimo Morbidelli, co-examiner

2016



## Abstract

This thesis, to the best of our knowledge, is the first report on the mechanical properties of side chain free, high molecular weight poly(*m,p*-phenylene)s. For that purpose a precursor polymer I bearing acid cleavable silyl side chains was synthesized by Suzuki polycondensation (SPC) with a molecular weight of up to 300 kDa. The side chains have two functions: First they prevent early precipitation of the growing polymer chains from the reaction mixture, which is a common issue in the synthesis of rigid polymers, secondly they render it possible to obtain the parent polymer by acid treatment (Scheme I).



**Scheme I.** Example of a polymerization towards an high molecular weight poly(*m,p*-phenylene) and the subsequent removal of the solubilizing side chains for achieving the parent polymer.

In order to achieve the aforementioned outstanding molecular weights for polymer I, a reliable supply of pure monomers was essential. Therefore the present thesis also reports on the synthesis of new monomers for SPC with purities exceeding 99.5%. Using these monomers, the polymerization conditions were optimized concerning monomer concentration, catalyst, stoichiometry and scale aiming at the highest molecular weights possible. After optimization polymer I could be obtained in amounts of up to 14 g.

In all polymerizations cyclic oligomers were observed as byproducts. Such macrocycles are known to occur during the synthesis of polyphenylenes containing *meta* connected repeating units due to intramolecular ring closure. In case of polymer I these low molecular weight byproducts prevented the formation of mechanically stable films which were necessary for tensile stress resistance tests. Therefore a purification process was developed focusing on the efficient and selective removal of these cyclic oligomers.

Upon synthesis and purification, polymer I was processed into films by solution casting and

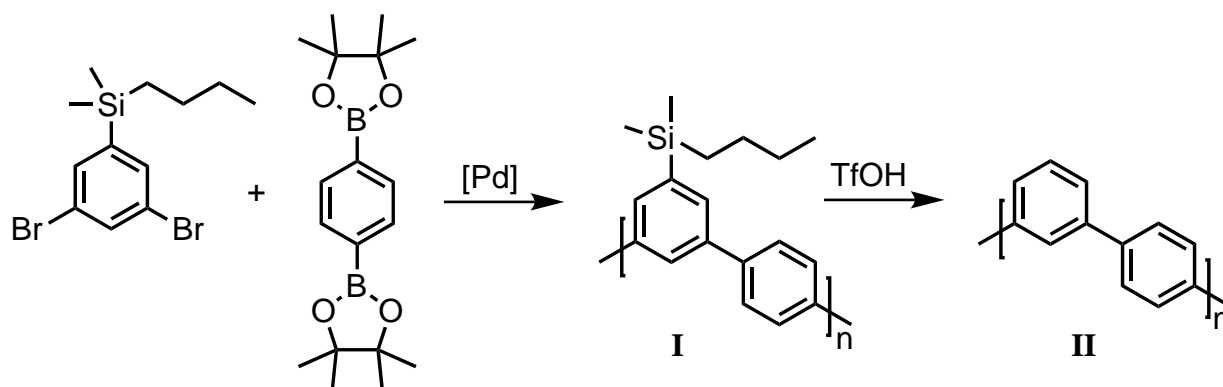
## Abstract

---

subsequent hot compression molding. Upon heating, these films demonstrate an extended plasticity above their  $T_g$  of 180 °C. This plasticity enabled us to produce threads of different draw ratios by hot drawing. Within the drawn samples, the polymer chains orient along the direction of elongation. This results in an increased crystallinity, an increase of Young's modulus from 1 GPa to 5 GPa and an improved yield strength from 40 MPa to 140 MPa. Finally it was shown by TGA as well as IR- and solid state NMR spectroscopy, that the acid cleavable side chain can be removed quantitatively even from processed polymer films by exposing them to TfOH. The resulting materials of undecorated polyphenylene **II** show an increased tensile stress resistance with a Young's modulus of up to 7.5 GPa and a maximum strength of 300 MPa.

## Zusammenfassung

Die vorliegende Arbeit ist, soweit uns bekannt, der erste Bericht über die mechanischen Eigenschaften von seitenkettenfreien, hochmolekularen poly(*m,p*-phenylen)en. Zu diesem Zweck wurde ein Vorläuferpolymer I, welches säurespaltbaren Seitenketten trägt, mit einem Molekulargewicht von bis zu 300 kDa synthetisiert. Die Seitenketten haben zwei Funktionen: Erstens verhindern sie ein frühzeitiges ausfallen der wachsenden Polymereketten, was ein bekanntes Problem bei der Synthese von kettensteifen Polymeren ist; und zweitens ermöglichen sie den Zugang zum seitenkettenfreien Polymer durch Säurebehandlung (Schema I).



**Schema I.** Beispiel für eine Polymerisation von einem hochmolekularem Poly(*m,p*-phenylen) sowie die darauf folgende Abspaltung der löslichkeitsfördernden Seitenkette um das unfunctionalisierte Polymer zu erhalten.

Um Polymer I mit den oben erwähnten, außergewöhnlich hohen, Molekulargewichten herzustellen, war eine verlässliche Versorgung mit reinen Monomeren unerlässlich. Die Synthesen von neuen Monomeren für SPC, mit Reinheiten jenseits von 99.5% sind deshalb ebenfalls Bestandteil dieser Arbeit. Diese Monomere wurden dann verwendet um die Polymerisationsbedingungen bezüglich Konzentration, Katalysator, Stoichiometrie und Ansatzgröße zu optimieren. Das Ziel war hierbei die höchst mögliche molare Masse zu erzielen. Nach der Optimierung konnten bis zu 14 g von Polymer I hergestellt werden.

In allen Polymerisationen wurden zyklische Oligomere als Nebenprodukt beobachtet. Es ist bereits bekannt, dass bei Polyphenylenen welche in *meta* Stellung verbundene Wiederholungseinheiten beinhalten, solche Makrozyklen durch intramolekulare Ringschlüsse entstehen können. Da solche niedermolekularen Nebenprodukte die Bildung von mechanisch stabilen filmen, für die Bestimmung von Zugspannungseigenschaften verhindert, wurde

eine Aufreinigungsmethode entwickelt welche gezielt und effektiv diese Makrozyklen entfernt. Nach der Synthese und Aufreinigung wurde Polymer **I**, durch gießen aus Lösung und anschließendes Heißpressen, zu filmen weiterverarbeitet. Anschließend wurde gezeigt, dass dies Filme oberhalb ihres  $T_g$  von 180 °C eine große Dehnbarkeit besitzen. Diese Dehnbarkeit wurde genutzt um Fasern mit verschiedenen Reckverhältnissen herzustellen. Innerhalb dieser gezogenen Proben orientierten sich die Polymerketten entlang der Zugrichtung. Dies führte sowohl zu einer erhöhten Kristallinität also auch zu einem anstieg des Youngschen Moduls von 1 GPa auf 5 GPa und der Zugfestigkeit von 40 MPa auf 140 MPa. Anschließend wurde sowohl mittels TGA als auch mittels IR- und NMR Spektroskopie gezeigt, dass die säureabspaltbaren Seitenketten sogar aus verarbeiteten Filmen und Fasern quantitativ entfernt werden können. Die so erhaltenen Materialien aus dem seitenkettenfreien Polymer **II** zeigten eine erhöhte Zugfestigkeit von bis zu 300 MPa sowie ein Youngsches Modul von bis zu 7.5 GPa.

---

## Contents

Abstract . . . . .	III
Zusammenfassung . . . . .	V
Contents . . . . .	VII
<b>Introduction</b>	<b>1</b>
<b>1 Polymers</b> . . . . .	<b>3</b>
1.1 Polymerization reactions . . . . .	5
1.2 Molecular weights and molecular weight distribution . . . . .	9
1.3 Important thermal parameters . . . . .	14
1.4 Mechanical properties of polymers . . . . .	17
<b>2 Conjugated polymers – a special class of materials</b> . . . . .	<b>19</b>
2.1 Synthesis of conjugated polymers . . . . .	20
2.2 Polyphenylenes . . . . .	21
2.3 Suzuki polycondensation . . . . .	25
2.4 Cycle formation in Suzuki polycondensation . . . . .	33
<b>3 Aim of the work</b> . . . . .	<b>35</b>
<b>Results &amp; Discussion</b>	<b>37</b>
<b>4 Monomer synthesis</b> . . . . .	<b>39</b>
4.1 Dibromo monomers . . . . .	39
4.2 Diboron monomers . . . . .	41
4.3 Monomer purity . . . . .	42
<b>5 Polymer synthesis</b> . . . . .	<b>46</b>
5.1 Optimization of the reaction conditions . . . . .	47
5.2 Molecular weight determination . . . . .	56
5.3 Polymerization using biphenyl monomers . . . . .	58

## Contents

---

<b>6</b>	<b>Properties of polymers carrying solubilizing side chains</b>	<b>63</b>
6.1	Glass transition, melting point and crystallinity	63
6.2	Thermal stability	70
6.3	Mechanical properties	71
<b>7</b>	<b>Removal of solubilizing side chains from bulk polymer</b>	<b>77</b>
7.1	Influence of film thickness	79
7.2	Influence of acid exposure time	80
7.3	Side chain cleavage of films from polymers 32 and 33	84
<b>8</b>	<b>Properties of unsubstituted polyphenylene</b>	<b>86</b>
8.1	Thermal stability	87
8.2	Mechanical Properties	88
<b>9</b>	<b>Summary and conclusions</b>	<b>91</b>
	<b>Experimental</b>	<b>93</b>
<b>10</b>	<b>Materials and methods</b>	<b>95</b>
<b>11</b>	<b>Synthesis</b>	<b>98</b>
<b>12</b>	<b>Polymer processing</b>	<b>111</b>
	<b>Appendix</b>	<b>113</b>
<b>13</b>	<b>List of abbreviations</b>	<b>115</b>
<b>14</b>	<b>References</b>	<b>117</b>
<b>15</b>	<b>Acknowledgements</b>	<b>129</b>
	<b>Curriculum Vitae</b>	<b>131</b>
	<b>Publications</b>	<b>133</b>



# Introduction



# 1 Polymers

Since the introduction of the polymer concept by Staudinger in 1920,<sup>[1]</sup> polymers have become an essential part of our everyday life and therefore have great economical importance.<sup>[2]</sup> Due to their low price, light weight and great variability, the world market for polymers and resulting materials has been growing rapidly since the 1950s (Figure 1.1). The main fields of application for the global production of 311 megatons in 2015 were packaging, building and construction as well as automotive. Aside from these established markets the ongoing research on polymers and related materials continuously opens new areas of application.

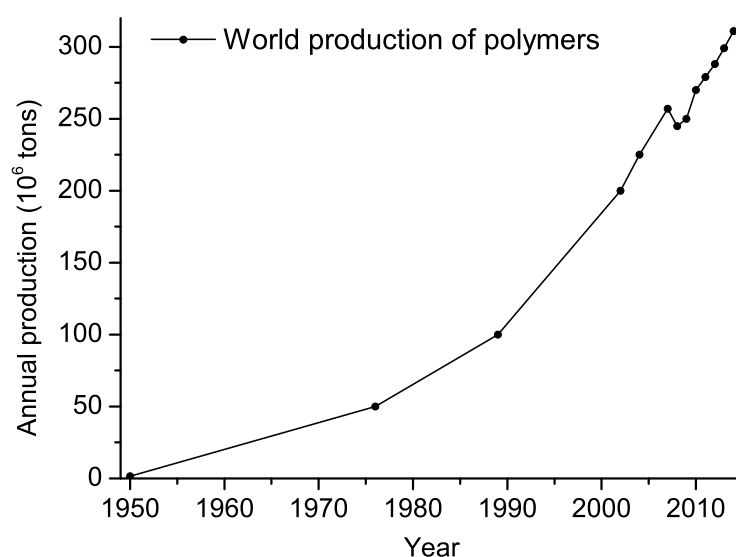


**Figure 1.1.** Annual global production of polymers since 1950. The development shows the increasing demand in polymers and related materials.

The term polymer (Greek: *poly* + *meros*, many parts) in general describes a macromolecule which is composed of many small molecules, which are called monomers (Greek: *mono* + *meros*, single part). The most general case is shown in Figure 1.2a, where all monomers have several reactive sites which allow them to react with other monomers to a randomly cross-linked three dimensional network<sup>[3]</sup>. The number of monomers incorporated into a polymer is called the degree of polymerization (DP) and the monomers once incorporated into the polymer are referred to as repeating units. Such complex networks are mostly insoluble, infusible and difficult to characterize in terms of their exact composition. However, depending on the monomers, they show useful mechanical and thermal

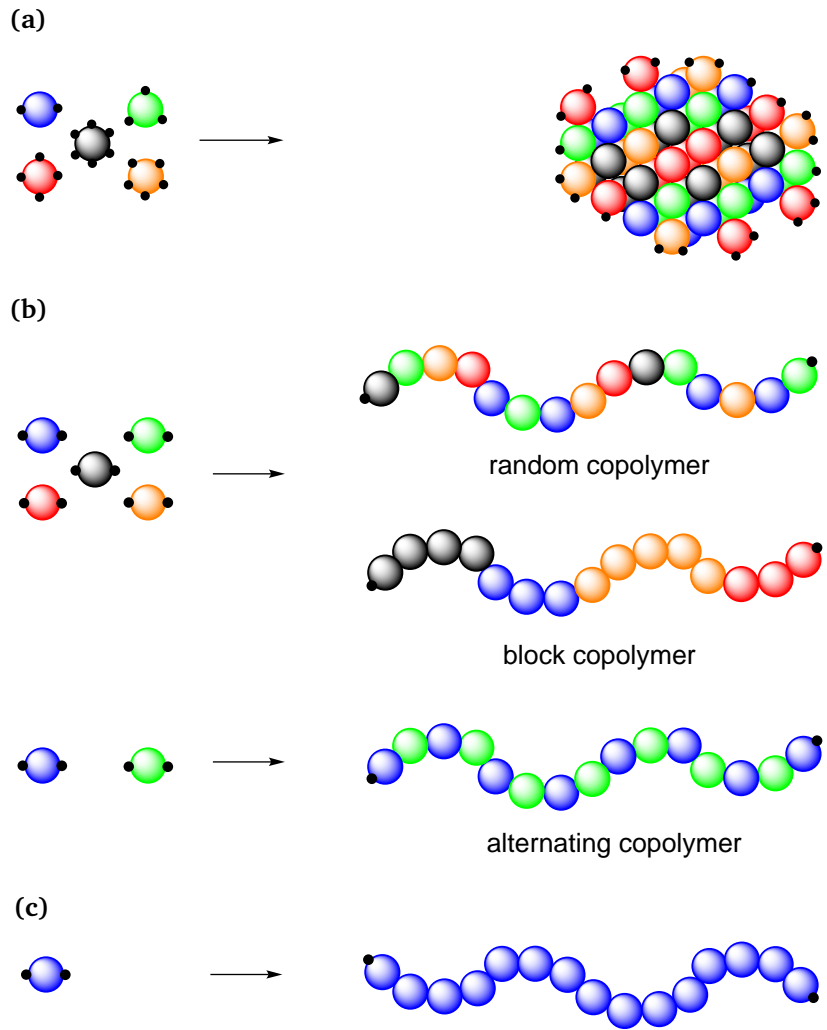


**Figure 1.2.** a) Randomly cross-linked polymer network consisting of different monomers. b) Different types of linear copolymers. Their main difference is the sequence of monomer incorporation. c) linear homopolymer consisting of a single type of monomer.

properties and are therefore used as so called duroplasts for example to fabricate parts for aviation and automotive.<sup>[4,5]</sup> A structurally simpler class of polymers are linear copolymers as shown in Figure 1.2b. In this case, the monomers have only two reactive sites under the applied polymerization conditions and thus react to chain like macromolecules. Depending on the reactivity of the different monomers and the reaction conditions, the sequence of monomer incorporation can vary. Prominent examples are random copolymers<sup>[6]</sup>, block copolymers<sup>[7,8]</sup> and alternating copolymers<sup>[9,10]</sup> the latter of which consist only of two different repeating units. Depending on the type and ratio of monomers as well as the sequence of incorporation, the properties of this class of polymers are highly tunable and therefore they are of great interest for a broad field of academic and industrial

research.<sup>[11–13]</sup>

Finally, the simplest and most explored and applied class of polymers are the linear homopolymers consisting only of one type of repeating unit (Figure 1.2c). A famous representative of this class of polymers is for example polyethylene (PE), which is the most produced polymer in the world with a annual amount of 80 megatons.<sup>[14]</sup> In addition polypropylene(PP), polystyrene(PS) and polyvinyl chloride (PVC) are further representatives, which commonly appear in everyone's day-to-day life. One feature that is displayed in all the polymers of Figure 1.2 are the unreacted sites at the borders or chain ends of the polymers. These groups can be functionalized<sup>[15,16]</sup> and therefore play an important role in the modification of polymers for specific applications.<sup>[17,18]</sup>

An additional class of macromolecules, which should be mentioned for completeness, are oligomers (Greek: *oligo* + *meros*, few parts). They are closely related to the above described polymers and differ structurally solely in the amount of repeat units. While polymers usually consist of several hundreds or thousands of repeat units, oligomers usually comprise between 2 and 50 monomer units. Because the border between these two classes is somewhat blurry, one common way of differentiation is the change of physical properties that occurs upon the addition of additional monomers. While in the case of oligomers the extension of the chain by a few repeating units has a significant impact on the properties, in the case of polymers the impact is negligible.<sup>[19]</sup>

## 1.1 Polymerization reactions

There are plenty of different methods for the synthesis of polymers and an in detail treatment of all of them would by far exceed the scope of this thesis. Therefore a brief overview of two general concepts, on how a polymer chain growth can proceed, will be explained in the following. All reactions which are used to obtain polymers can be divided into two categories. In particular, there are polymerization reactions, which proceed according to a chain-growth mechanism and such which proceed according to a step-growth mechanism. Although each group comprises several different types of reactions, within each group the reactions have common features.

### 1.1.1 Chain-growth polymerizations

Famous representatives of chain-growth polymerizations are for example radical polymerization<sup>[20]</sup>, anionic polymerization,<sup>[21]</sup> cationic polymerization<sup>[22]</sup> and coordinating polymerizations like ring opening polymerization<sup>[23]</sup> or Ziegler-Natta polymerization.<sup>[24]</sup> Although they all follow their individual mechanisms, they all proceed along characteristic steps.

- 1. Initiation:** This is the first step of every chain growth polymerization. During Initiation an initiator molecule is generated which is reactive towards the monomers. Depending on the type of polymerization, the initiation results in radicals, reactive ions or an active metal catalyst. Because these are very reactive species, they are usually generated *in situ* from a precursor molecule.
- 2. Propagation:** Once the initiation has occurred the first monomer reacts with the initiator leaving a reactive site at the just appended monomer to which the next monomer can add. Thus more and more monomers are added to the reactive chain end.
- 3. Termination:** Depending on the type of polymerization, termination of the growing chains can occur in different ways. Aside from reactions which quench a reactive species ultimately, termination can also proceed via a chain transfer. In this case the termination of one chain causes the initiation of another one, by a transfer of the reactive functionality to a monomer or solvent molecule. At which stage of the chain-growth a termination occurs is individual for each chain, and therefore a resulting polymer always consists of a mixture of chains with different degrees of polymerizations.

For clarification the three steps are displayed in Figure 1.3a, where the reactive sites are marked with \*.

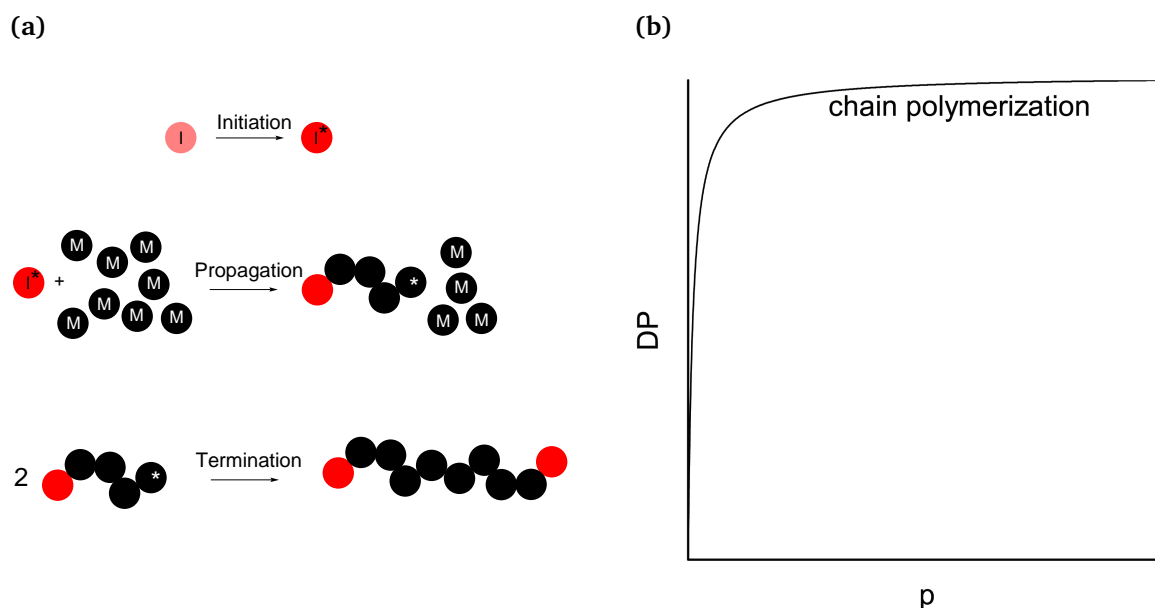
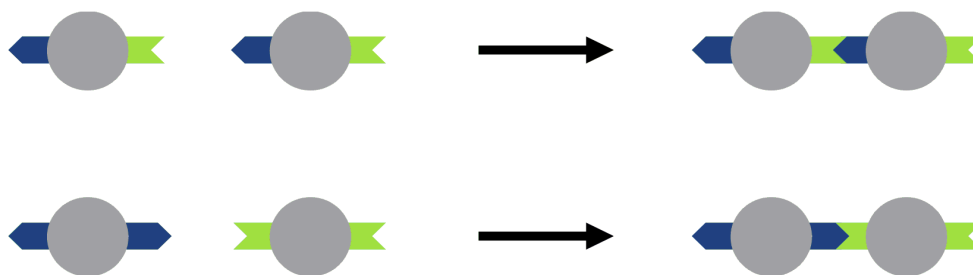


**Figure 1.3.** a) The three characteristic steps of an chain growth polymerization, initiation, propagation and termination. The reactive sites are marked with \*. For the termination the recombination of two active chain was chosen as an example. b) Development of degree of polymerization with conversion for chain-growth polymerizations.

In Figure 1.3b the degree of polymerization in dependence of the monomer conversion for a single polymer chain is shown. In the case of a conventional chain-growth polymerization, only few active chains are present compared to the amount of monomers. Therefore the length of an active chain increases rapidly until its termination occurs. After that termination the degree of polymerization stays constant and further conversion only leads to the growth of more chains.

### 1.1.2 Step-growth polymerizations

In contrast to chain-growth polymerizations, the step-growth polymerizations do not require an initiation because a reaction can occur between all the monomers ideally with an equal probability. A prerequisite for this to occur is that at least two complementary groups per monomer are present in the reaction.<sup>[25]</sup> As shown in Scheme 1.1, this can be realized either with a monomer carrying two complementary groups (AB-type) or by two different monomers each carrying one of the complementary functionalities twice (AA/BB-type). For completeness, it should be mentioned that of course also scenarios with more than two functional groups per monomer are known.



**Scheme 1.1.** First step of an AB-type (top) and AA/BB-type (bottom) step-growth polymerization. Both reactions lead to a dimer carrying again both complementary end groups.

In such cases, hyperbranched polymers result as products.<sup>[26]</sup> The fact that every monomer and intermediate of a step-growth polymerization, has the chance to react with almost every other molecule inside the reaction has direct consequences on the development of the degree of polymerization with increasing conversion. As displayed in Figure 1.4a, this for example means that at 50 % conversion the reaction mixture contains in average only dimers. The average degree of polymerization  $\overline{DP}$  for step-growth reactions with an equimolar amount of both functional groups was mathematically described by Wallace H. Carothers<sup>[27]</sup> and can be expressed according to Equation (1.1) in which  $p$  represents the conversion.

$$\overline{DP} = \frac{1}{1-p} \quad (1.1)$$

The plot of the Carothers equations in Figure 1.4b illustrates that high degrees of polymerizations can only be achieved at very high conversions. Consequently, causes which limit the maximum achievable conversions can either be used for tuning the polymer chain length or need to be eliminated in order to obtain high degrees of polymerization.



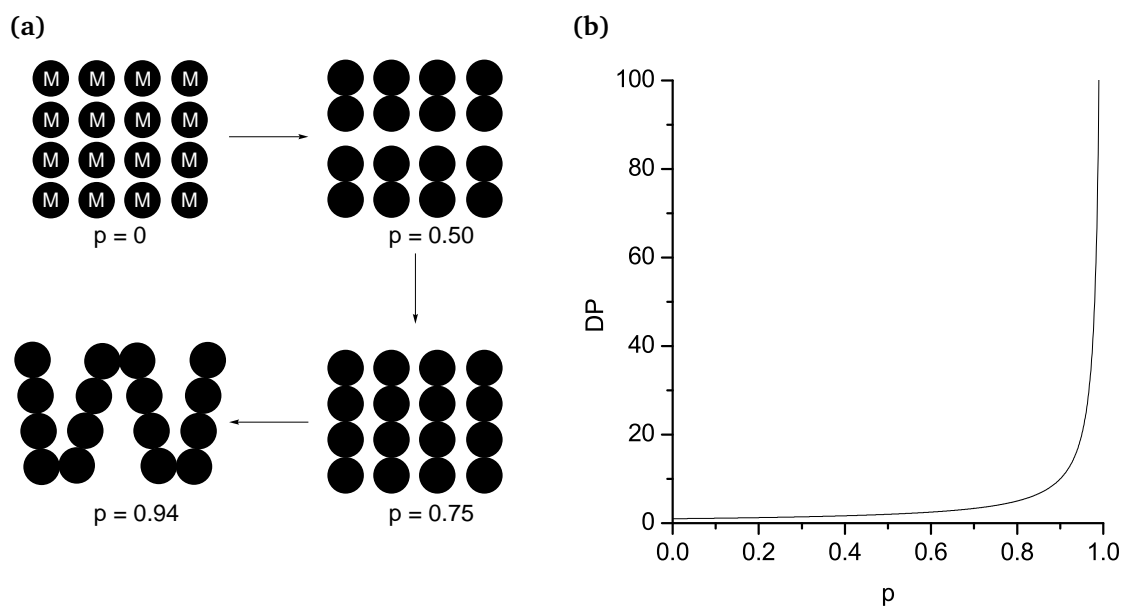


**Figure 1.4.** a) Schematic illustration of the step-growth process. b) Development of degree of polymerization with conversion. Only at very high conversions large degrees of polymerizations can be achieved.

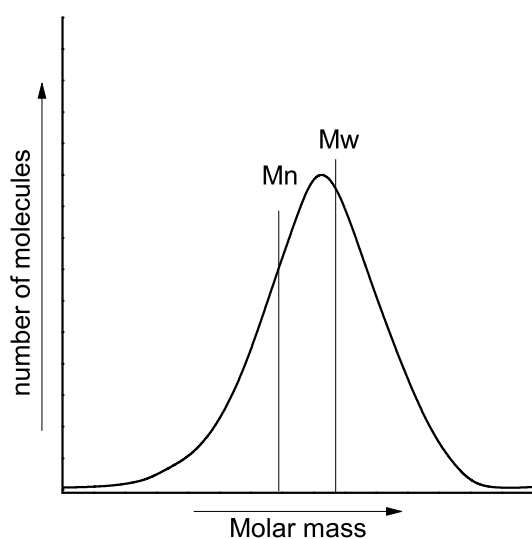
A mismatch of the stoichiometry between the complementary groups can be a reason for an incomplete conversion. Obviously, with one functionality in excess, the reaction stops after the consumption of the minor one. This can be prevented by using the AB-approach, where the stoichiometry of the functionalities is balanced naturally. However, other factors can also lead to a stoichiometric mismatch. The presence of impurities, for example, can either lead to uncertainties in measuring the amount of monomers or to capping reactions if the impurity is reactive towards one of the relevant functionalities. Lastly, also side reactions might prevent a high conversion and therefore procedures and conditions which reliably result in the desired bond formation are preferred for step-growth polymerizations.

## 1.2 Molecular weights and molecular weight distribution

The molecular weight of a single polymer chain is calculated by multiplying the molar mass of one repeating unit by the amount of repeating units in this chain. Thus, the knowledge of the molecular weight gives direct access to the number of monomers incorporated into a polymer chain. Unfortunately, the above mentioned step- and chain growth polymerizations all result in polymers consisting of many chains with different numbers of repeating units. Consequently, the molar mass of polymers is commonly given as an

average molecular weight of the different contributing chains.

In Figure 1.5, an exemplary number distribution of molar masses of a polymer is shown. The average molecular weights are usually given as ratios of different moments of such a distribution.<sup>[28]</sup> In particular, the ratio of the first and zeroth moment is called the number average molecular weight  $M_n$  and is calculated according to Equation (1.2). In that case all polymer chains with the same molar masses  $M_i$  are weighted by the amount of molecules  $N_i$  that have that molar mass. The ratio of the second and first moment is called the weight average molecular weight  $M_w$ . In this case, all contributing chains of the same molar mass  $M_i$  are weighted by the mass  $m_i$  they contribute to the overall polymer mass (Equation (1.3)). Another important parameter which is used to describe the width of the molecular weight distribution is the polydispersity index PDI. It is calculated according to Equation (1.4) using  $M_n$  and  $M_w$ . In an ideal case were all the chains of a polymer batch have the same molar mass,  $M_n$  would be equal  $M_w$  and thus the PDI would be 1.



$$M_n = \frac{\sum N_i M_i}{\sum N_i} \quad (1.2)$$

$$M_w = \frac{\sum m_i M_i}{\sum m_i} = \frac{\sum N_i M_i^2}{\sum N_i M_i} \quad (1.3)$$

$$PDI = \frac{M_w}{M_n} \quad (1.4)$$

**Figure 1.5.** Typical number distribution of molecular weights for a polymer and the resulting averages  $M_n$  and  $M_w$ .

The knowledge of the molecular weight and the distribution allows conclusions about the progress and completion of a polymerization reaction. Furthermore, many properties of polymers depend on their molecular weight. Hence, methods for its determination are of utmost importance and various techniques have been developed.<sup>[29,30]</sup> A selection of methods important for this work is presented in the following.

### 1.2.1 Determination of molecular weights

#### Colligative properties

Colligative properties are characteristics of a solution, which solely depend on the number of solvent and solute molecules and not on their chemical nature. Examples for such properties are osmotic pressure, melting point and boiling point. Therefore the comparison of one of these values of a solution with the corresponding value of the pure solvent allows the calculation of the number of solute particles.

Consequently, by dissolving a known amount of polymer, the number of chains within this solution and thus the number average molecular weight  $M_n$  can be determined.<sup>[31–33]</sup>

#### Static light scattering (SLS)

The determination of molecular weight by static light scattering relies on measuring the intensity of scattered light from very dilute polymer solutions (Figure 1.6a). The contribution of the dissolved polymers can be extracted, by subtraction of the scattering intensity of the pure solvent. In an ideal solution and for a constant scattering angle  $\Theta$ , the intensity contribution from the dissolved polymers is proportional to their mass and can be described by the Zimm equation (Equation (1.5)). Here  $R$  is the rayleigh ratio, which is an absolute scattering intensity independent of the scattering volume and detector distance. Further  $K$  is the scattering power of one individual particle and  $q$  corresponds to the scattering vector, which is closely related to the scattering angle. Unfortunately, ideal solutions are rare and only occur at theta conditions<sup>[34]</sup> or infinite dilution ( $c = 0$ ). Further, with increasing scattering angle  $\Theta$ , the contribution of longer polymer chains gets underestimated and only at a scattering angle of  $0^\circ$  this effect can be excluded.

$$\frac{Kc}{R} = \frac{1}{M_w} \left( 1 + \frac{q^2 R_g^2}{3} \right) + 2A_2c \quad (1.5)$$

with

$$K = \frac{4\pi^2}{\lambda^4 N_A} n_{D,0}^2 \left( \frac{\partial n_D}{\partial c} \right)^2 \quad (1.6)$$

and

$$q = \frac{4\pi n_D \sin(\Theta/2)}{\lambda} \quad (1.7)$$

In order to determine the molecular weight of a real solutions, light scattering experiments therefore have to be conducted at several concentrations and scattering angles. By a double extrapolation to  $\Theta = 0$  and  $c = 0$ , this method gives direct access to the weight average molecular weight  $M_w$  (Figure 1.6b).<sup>[35–37]</sup>

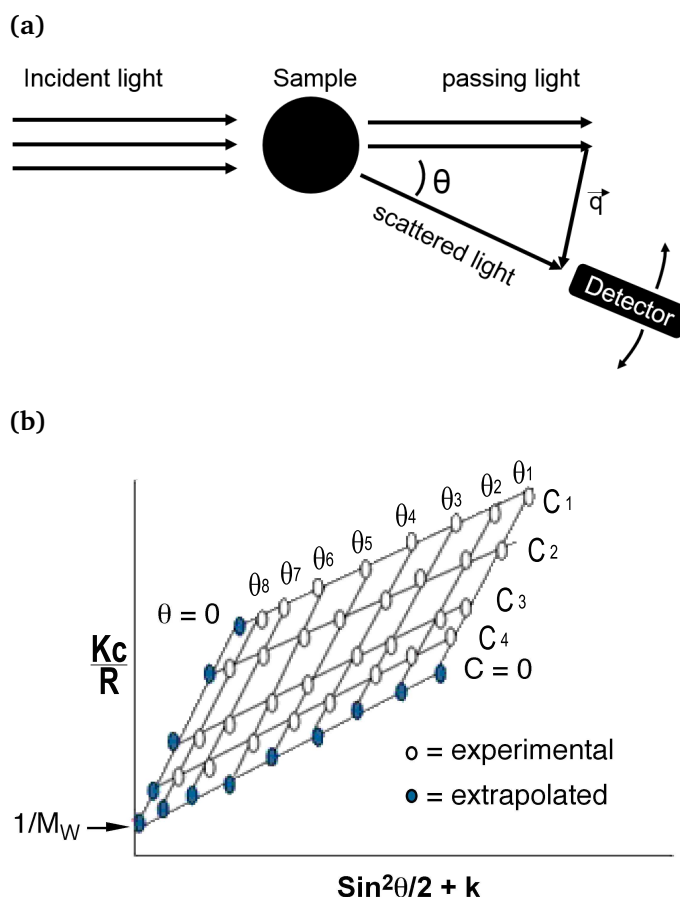


**Figure 1.6.** a) Schematic depiction of a light scattering setup. Only the scattered fraction of the incident beam is detected. b) Data points for scattering intensities at different angles and concentrations as well as the extrapolations to  $c = 0$  and  $\Theta = 0$ .

### Gel permeation chromatography

The above described methods give direct access to the values of the average molecular weights  $M_n$  and  $M_w$  and in combination ultimately also a conclusion about the width of the distribution. However, they do not provide an exact picture of the distribution curve of molecular weights. In contrast, gel permeation chromatography (GPC) can provide  $M_n$ ,  $M_w$  and the exact distribution like in Figure 1.5. Gel permeation chromatography is based on the separation of particles in solution by hydrodynamic radii. The essential part is the chromatographic column, which is filled with porous beads having a defined

pore size.<sup>[38]</sup> If a mixture of small and large particles is subjected to this column, small particles will diffuse further into the pores of the column material. Consequently, their retention time gets prolonged and large particles elute first (Figure 1.7a).<sup>[39]</sup> Therefore, a polymer solution containing polymer chains of different chain lengths will be separated accordingly and high molecular weight chains will elute faster than short chains. In order to gain information from this separation the eluting solution needs to be analysed by a detector. The most popular detectors used are UV-Vis, refractive index, light scattering and viscosimetry,<sup>[40]</sup> which need to be chosen depending on the polymer. By recording the detector signal over retention volume, the distribution of the hydrodynamic radii can be extracted. Finally, this information has to be translated into molecular weight, which is done by using a calibration curve. For the calibration, several polymers from the same species but with different known molecular weights and a very narrow distributions are subjected to the GPC. By recording their retention volumes, a calibration curve between molecular weight and elution volume can be generated. This calibration curve can now be applied to the distribution of the unknown polymer to extract the molar mass data. The advantages of this method are obvious, as in a relatively short time a very comprehensive picture of the molecular weight distribution of a polymer sample can be generated.

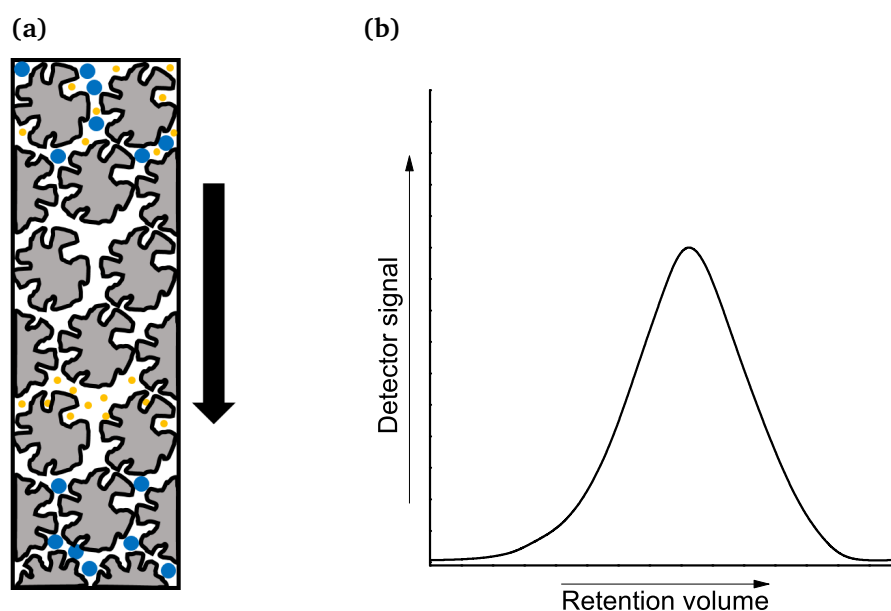


**Figure 1.7.** a) Schematic depiction of a GPC column filled with porous beads. The blue and yellow particles get separated by size during their way through the column. b) Elution curve of an GPC detector showing the distribution of hydrodynamic radii.

On the down side, the results always rely on the quality of the calibration curve. Strictly speaking, exact results can only be obtained by using the same type of polymer for the calibration and for the measurement. However for a wide range of polymers it was shown by Benoit et al. that there is a universal calibration,<sup>[41,42]</sup> which allows the use of one calibration curve for various polymers.

### 1.3 Important thermal parameters

Like for other materials, also for polymers thermal parameters are important for a complete description of the material. Further, the thermal properties determine the temperature range in which a material can be used and processed. The most obvious parameter is of course the melting point  $T_m$ , at which a material changes its state from a crystalline solid to liquid. Although polymers are not purely crystalline materials, depending on structure and processing, polymers can have a significant portion of crystallinity.<sup>[43]</sup> After melting, the liquid state of polymers is still rather viscous and not comparable to the melt of small molecules, the transition however fulfills all criteria for a first order phase transition. In particular, this means that there are discontinuities in enthalpy and volume. In Figure 1.8 the specific volume ( $V_m$ ) of a polyethylene sample is recorded during heating.

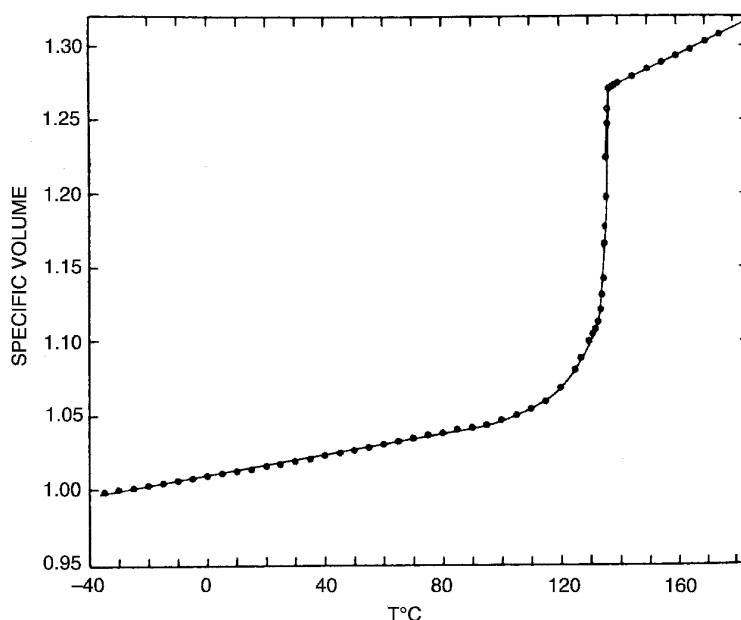


**Figure 1.8.** Specific volume of a polyethylene sample over temperature at constant pressure. At the melting point, the volume shows a discontinuous course.<sup>[43]</sup>

As the mass does not change during the experiment, it directly displays the change in vol-

ume. At  $T_m$  of 130 °C it shows the typical discontinuous course for a first order transition. As mentioned above, the crystallinity of polymers can vary to a large degree,<sup>[44,45]</sup> which means that most polymers consist of crystalline and amorphous domains. Therefore below the melting point many polymers show a glass transition temperature  $T_g$ . At this temperature an amorphous material undergoes the transition from a brittle glassy state into a softer rubbery state. From a thermodynamic point of view, this is a second order transition. Consequently, at  $T_g$  there are no discontinuities in volume or enthalpy but rather in their temperature and pressure derivatives *i.e.* expansion coefficients  $\alpha$  and heat capacities  $C_p$ . Figure 1.9 shows the development of the volume and expansion coefficient as well as enthalpy and the heat capacity around  $T_g$ .

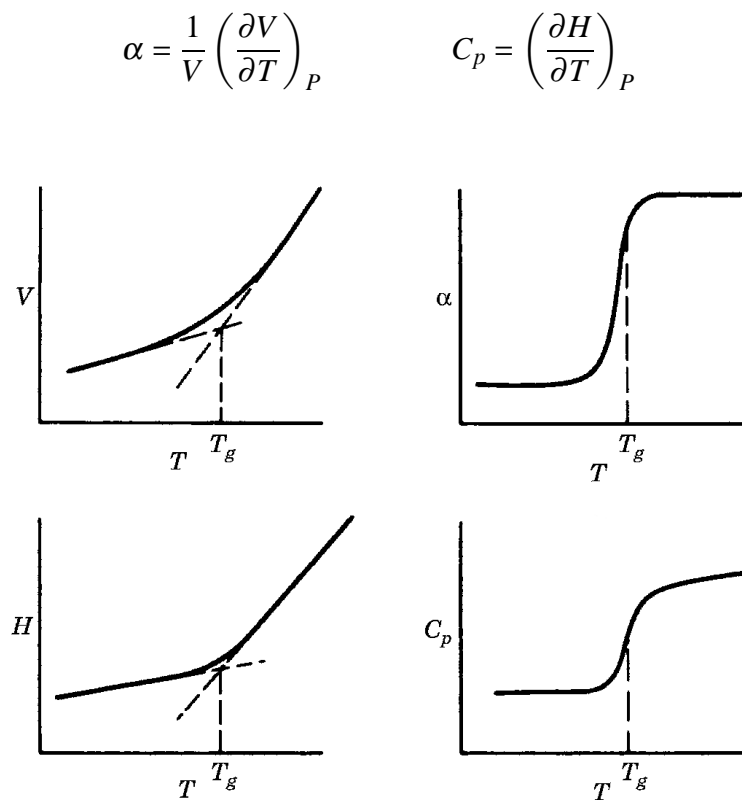


**Figure 1.9.** Volume and Enthalpy and their temperature derivatives expansion coefficient and heat capacity as a function of temperature around the glass transition temperature.<sup>[46]</sup>

While for the volume and the enthalpy the transition only causes a change in the slope, for their temperature derivatives  $\alpha$  and  $C_p$  it causes a discontinuity. As mentioned the glass transition leads to a softening of the polymer, which can be explained by an increased

mobility of the polymer chains. It should be noted that in addition to the thermodynamic description also other theories, based on free volume and kinetics, have been developed to describe the glass transition.<sup>[46]</sup>

### 1.3.1 Differential scanning calorimetry

For the determination of phase transitions, differential scanning calorimetry (DSC) is an important and widely used method. In a DSC experiment, a sample (pan with polymer) and a reference (empty pan) are heated separately with the same heating rate. The difference in heat flow for heating the sample and for heating the reference at the same rate is recorded. In case of a phase transition in the sample, *e.g.* melting, the enthalpy of transition (*e.g.*  $\Delta H_m$ ) adds to the heat flow in order to keep the heating rate constant. This deviation in heat flow is recorded in a thermogram.

A typical thermogram for a semicrystalline polymer is displayed in Figure 1.10. Upon heating, the first transition that occurs is the glass transition, which can be identified as a change in the slope of the heating and cooling cycle. This change of the slope can be attributed to the second-order nature of the glass transition. As mentioned above, at  $T_g$  only the heat capacity changes, not the enthalpy itself. Upon further heating, an exothermic peak can be observed, which in contrast to the glass transition shows a distinct change of the enthalpy. This peak can be assigned to a crystallization process. Due to the increased mobility above  $T_g$ , the polymer has the chance to partially rearrange into the energetically more favourable crystalline state. Additional heating finally leads to the melting of the polymer, which results in a clear endothermic peak in the thermogram.

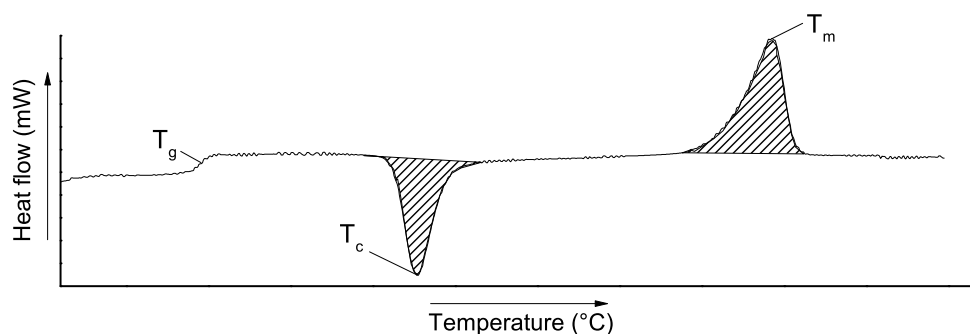


**Figure 1.10.** Typical DSC curve of a semicrystalline polymer showing a glass transition temperature, a crystallization peak and a melting point. The areas under the peaks allow for the calculation of the transition enthalpies.



Finally, it should be mentioned that in addition to the temperatures of the phase transitions, also the energy of the transition can be determined from the peak area. This way the degree of crystallinity of a polymer can be estimated, by comparing the found transition energy with the theoretical value for a 100 % crystalline material.<sup>[47]</sup>

#### 1.4 Mechanical properties of polymers

It is obvious that for most applications a polymeric material is chosen based on its mechanical properties. Depending on the polymer and the conditions under which an experiment is conducted, polymers can show different responses to mechanical stress. These range from a glassy brittle behaviour over a rubber-like elastic behaviour to a viscous liquid like behaviour. Because of this variability polymers are called viscoelastic materials.<sup>[48]</sup> Although there are plenty of mechanical characteristics which can be determined by shear, compression, impact or abrasion it is very common to determine the mechanical behavior of polymers in tensile stress experiments. Here the tensile modulus also called Young's modulus ( $E$ ) reflects how strong a material responds to tensile stress and defines the stiffness at the given experimental parameters like temperature and rate of the experiment.

In Figure 1.11 three typical behaviours of polymers are displayed. In the case of a brittle plastic, the resulting strain  $\epsilon$  upon applying a tensile stress  $\sigma$  increases linearly and the material fails already after a few percent of elongation. This is usually the case for polymers well below their  $T_g$ . At a slightly increased temperature but still below  $T_g$  the same polymer can show the behaviour of a tough plastic. This means that after an initial stiff response the sample yields and can be stretched up to several hundred percent before its failure. The toughness of such a polymer is expressed by the area under the stress-strain curve. Well above  $T_g$ , polymers usually behave like elastomers or rubbers and can be stretched already at very low stress by up to over 1000 % in some cases. It should be noted that plastic elongation of a sample is often referred to as draw ratios, which is the final length of a elongated sample divided by its original length.

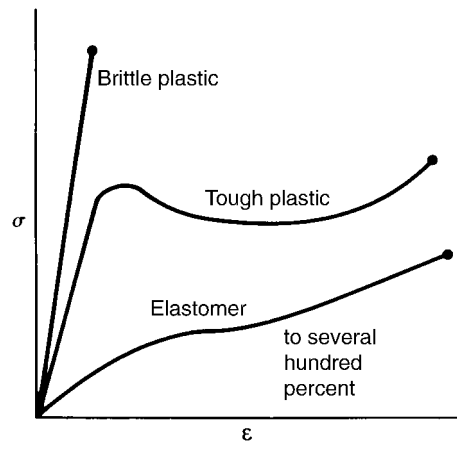


**Figure 1.11.** Typical tensile stress behaviours of polymers. Depending on the temperature and the rate of the experiment, polymers can show brittle, tough or rubber-like performance. <sup>[49]</sup>

## 2 Conjugated polymers – a special class of materials

Conjugated polymers are organic macromolecules, which consist of alternating single and double bonds throughout the molecule's backbone. The overlap of the  $\pi$ -orbitals along the whole polymer chain brings about the conjugation and results in unique properties.<sup>[50,51]</sup> The structurally simplest example for a conjugated polymer is polyacetylene **1**.<sup>[52]</sup> This and other famous examples for conjugated polymers are depicted in Figure 2.1. In addition to the homopolymers, also copolymers of the depicted repeating units gained considerable attention.<sup>[53,54]</sup> By far the most attention, in academia and industry, is devoted to ability of conjugated polymers to serve as an electrically conducting material.<sup>[55]</sup> Although in the neutral state conjugated polymers are usually insulators like most other polymers, upon addition or withdrawal of electrons by reduction or oxidation, their electrical conductivity can be tuned over a wide range.<sup>[56–58]</sup>

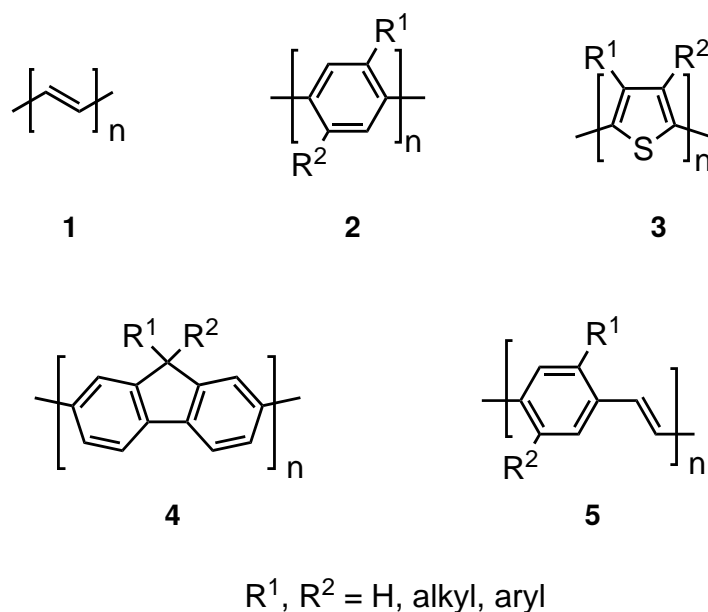
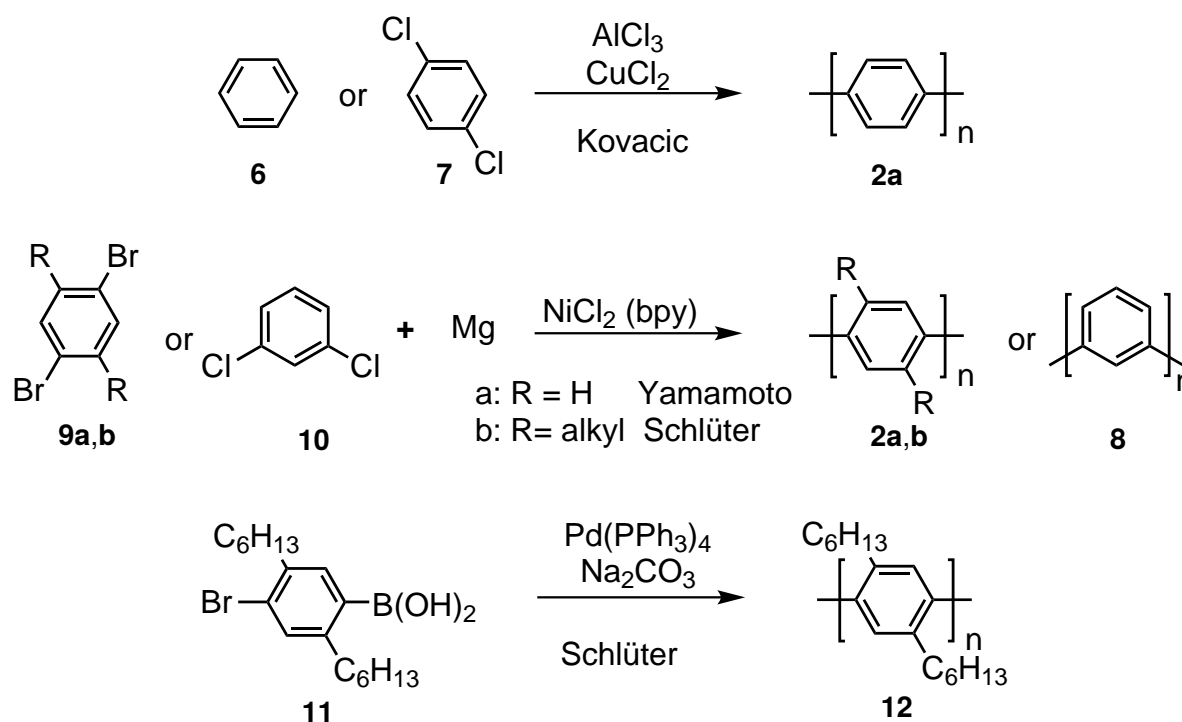


**Figure 2.1.** Prominent examples of conjugated polymers are polyacetylene **1**<sup>[52]</sup>, polyphenylenes **2**<sup>[59]</sup>, polythiophenes **3**<sup>[60]</sup>, polyfluorenes **4**<sup>[61]</sup> and polyphenylenevinylenes **5**<sup>[62]</sup>.

In most cases, conjugated polymers consist of directly linked aromatic units. As a result, the overall structure of such polymers is rigid. This high rigidity strongly influences the chemical and physical properties such as solubility, fusibility and liquid crystalline behaviour.<sup>[63]</sup> Consequently, conjugated polymers also arouse interest as mechanically<sup>[64,65]</sup>, chemically and thermally<sup>[66]</sup> robust materials.

## 2.1 Synthesis of conjugated polymers

Due to the great interest in conjugated polymers over the last decades, several strategies have been developed for their synthesis. Aside from polyacetylene, which is usually synthesized by a Ziegler-Natta type reaction of gaseous acetylene,<sup>[67]</sup> the syntheses of conjugated polymers rely on C-C coupling chemistry between aromatic  $sp^2$  carbons. First approaches by Kovacic et al. aimed at the synthesis of polyphenylene from benzene **6** or polyhalogenated benzenes **7** via oxidative procedures (scheme 2.1).<sup>[68,69]</sup> Unfortunately, most of these approaches resulted in low molecular weight products with significant amounts of structural irregularities and branching. In 1978, Yamamoto et al. were able to synthesize poorly soluble polyphenylenes **2a** and **8** with high structural perfection by using transition metal catalyzed Kumada-coupling<sup>[70]</sup> with *p*-dibromobenzene **9a** and *m*-dichlorobenzene **10** as starting materials.<sup>[71]</sup> Later, this method was applied by Schlüter and Wegner et al. to dibromobenzenes **9b** carrying solubilizing alkyl side chains, which led to soluble poly(*p*-phenylene)s (PPP) **2b**. While this was an important success for the field, the degrees of polymerization did not exceed 15 repeating units. Further, the dihalogenated starting compounds can react on both sides and thus a head-to-tail selectivity is not provided.



**Scheme 2.1.** Different approaches for the synthesis of conjugated polymers. First attempts predominantly aimed at polyphenylenes.

Finally, in 1989, Schlüter et al. utilized the now famous Suzuki-Miyaura cross-coupling (SMCC) chemistry<sup>[72]</sup> for the synthesis of polyphenylenes **12**. The asymmetrically functionalized monomer **11** provided a strict regioselectivity and the mild conditions under which the reaction proceeded opened the field for a broad variety of functional groups within the side chains. This so-called Suzuki polycondensation (SPC) is nowadays among the most-used reactions for the preparation of conjugated polymers<sup>[73]</sup> and will be discussed in more detail in Chapter 2.3. Since the introduction of SPC, other cross-coupling protocols like Stille-coupling,<sup>[74]</sup> Nigishi-coupling<sup>[75]</sup> and direct arylation<sup>[76]</sup> have also been used for the synthesis of conjugated polymers. The last reaction has the advantage of producing less toxic side products due to the absence of organometallic compounds. In addition to the classical synthetic approaches, electrochemical polymerization procedures are also known.<sup>[77]</sup>

### 2.2 Polyphenylenes

Amongst conjugated polymers, polyphenylenes have been on the radar of materials science for several decades and were among the first aromatic polymers studied.<sup>[78–80]</sup> Initially, electrical conductivity of these polymeric materials was in the focus. This focus then slowly shifted towards optoelectronic applications in *e.g.* organic light emitting diodes or photovoltaics.<sup>[81–84]</sup> In addition to their unique electronic properties, their application as high performance materials was also investigated.<sup>[85,86]</sup> For example, Friedrich et al. showed that commercially available PPP<sup>[87]</sup> can be processed via injection molding resulting in a material with outstanding stiffness, strength and abrasion resistance reaching into the region of fibre reinforced materials.<sup>[88–90]</sup> Due to these properties, industrial interest increased<sup>[91,92]</sup> and applications in prosthetics and aerospace were contemplated.<sup>[87,93,94]</sup> The by far most investigated polyphenylenes are the all-straight poly(*p*-phenylene)s **2** in which the phenylene units in the backbone are connected through the 1- and 4- positions. The high main chain rigidity of PPP causes a melting point beyond its degradation temperature and low solubility in common organic solvents (Figure 2.2).<sup>[95]</sup> Both of these properties are caused by the high crystallization energy and the low entropy gain upon dissolution or upon melting.<sup>[96,97]</sup>

The introduction of side chains attached to a polymer backbone is a common method for

## 2 Conjugated polymers – a special class of materials

the enhancement of the solubility and fusibility of rigid-rod polymers. Further, side chains are useful to enhance solubility during polymer chain growth.<sup>[98,99]</sup>

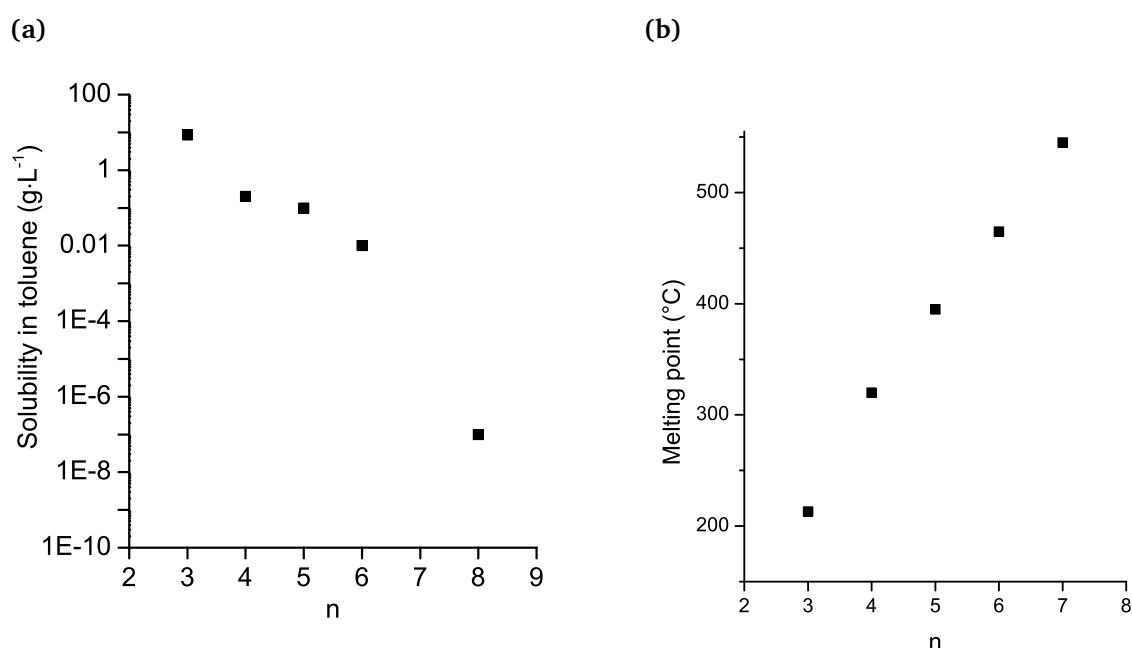


**Figure 2.2.** Solubilities a) and melting points b) of PPP with n repeating units.<sup>[98,100]</sup> Already at a DP of 8 PPP becomes insoluble and degrades before its melting point.

While decoration with flexible side chains is useful whenever solubility of a polymer is an issue, side chains also have a downside: not only do they dilute the intrinsic backbone properties,<sup>[101]</sup> but they can also detrimentally affect the stability of polymers towards thermal and chemical impact. In regard to polyphenylene, side chains further affect the dihedral angle between two adjacent phenylene units. As shown in Figure 2.3, the steric repulsion of the substituents can result in variation of the dihedral angle between 23° and 80°. <sup>[102,103]</sup> Unfortunately, this torsion reduces the overlap of the  $\pi$ -orbitals and thus lowers the conjugation. In order to address the issues introduced by the solubilizing side chains, mainly two approaches were investigated. The first one concerns the dihedral angle and thus the conjugation and the spectroscopic properties. In ladder-type polyphenylenes **13** (Figure 2.3), two adjacent phenylenes are connected with different bridging groups X. Depending on the size of these groups, the torsion angle can be tuned.<sup>[104–106]</sup> The second approach relies on the removal of the flexible side chains after synthesis and processing of the material. A recent success in this regard was reported by

Sakamoto et al.<sup>[107]</sup> using acid cleavable silyl side chains. Their approach is shown in scheme 2.2. By treating a solution of **14a** with trifluoromethanesulfonic acid (TfOH), the side chains are cleaved and the parent insoluble polyphenylene **14** precipitates in a very fast and quantitative manner. Thus this approach in principle facilitates access to side chain-free polyphenylenes of high molar mass and is therefore an attractive addition to the repertoire of polymer chemistry.

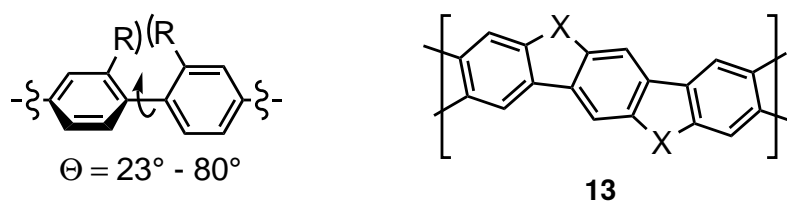
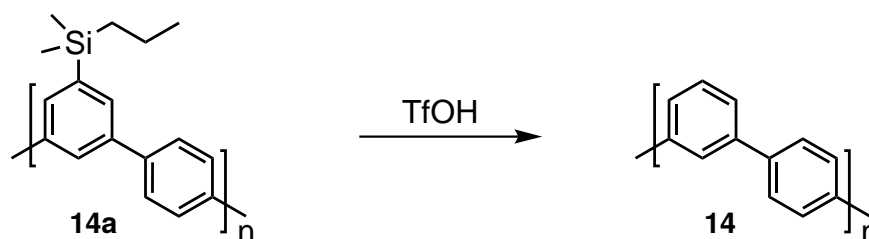


**Figure 2.3.** The torsion angle between two adjacent phenylene units has an important influence on the spectroscopic properties. It can be tuned by connecting the rings with different bridges.

As indicated in Scheme 2.2 and Figure 2.4, in addition to the all-*para* PPP **2** also polyphenylenes containing *meta* connected phenylene units (**8**) are known. On top of the increased flexibility, which comes through the 1,3 connectivity, also the spectroscopic and electronic properties change.<sup>[108-110]</sup> This change in properties can be explained by the interruption of conjugation which occurs at every *meta* repeating unit.<sup>[111,112]</sup> In Figure 2.4 this lack of conjugation is displayed by the missing mesomeric structure.

Synthetically poly(*m*-phenylene)s **8**<sup>[113]</sup>, poly(*o*-phenylene)s **15**<sup>[114]</sup> as well as the mixed species such as polymer **14**<sup>[115]</sup> have been described in the literature. While reports about poly(*o*-phenylene)s are scarce<sup>[116-118]</sup> due to their tedious synthesis, poly(*m*-phenylene)s have been studied in greater detail.



**Scheme 2.2.** Cleavage of the solubilizing silyl side chains of a poly(*m,p*-phenylene) using trifluoromethanesulfonic acid.<sup>[107]</sup>

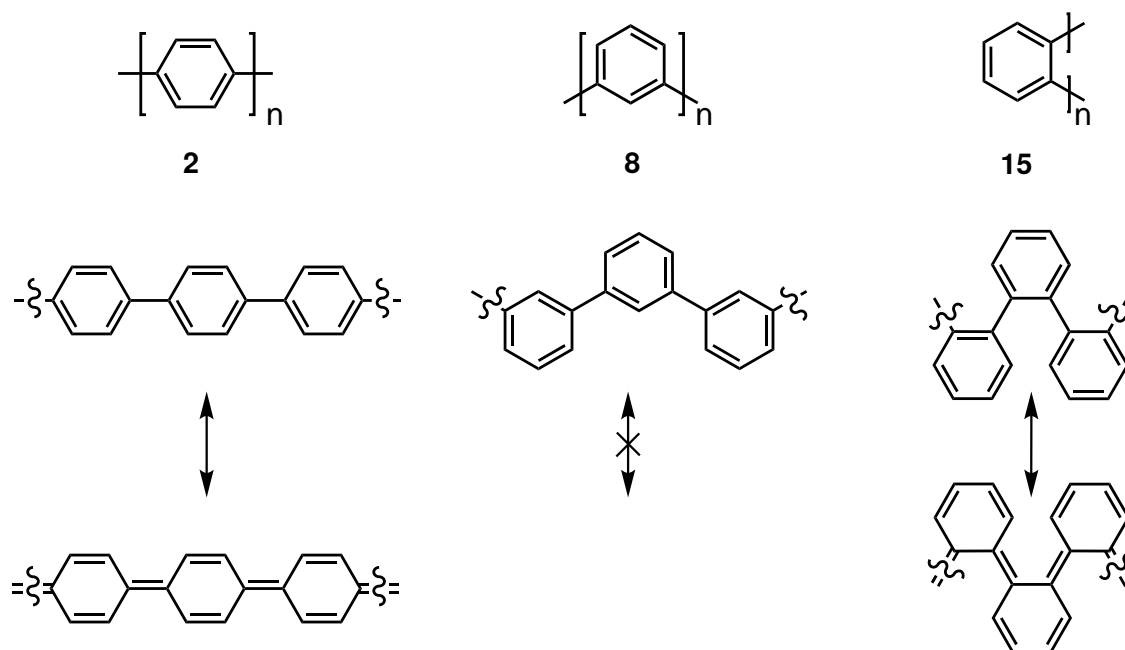


**Figure 2.4.** Different connection patterns in polyphenylenes and their influence on the conjugation. Phenylenes connect in *meta*-fashion do not allow for resonance structures within the octet rule.

The kinked structure of **8** and **15** lends a certain degree of flexibility to the backbone, which results in a decrease of glass transition temperature and melting point and also an improved solubility as compared to PPP.<sup>[71,119]</sup> From a processing point of view, these property changes are desirable, which is why poly(*m*-phenylene)s recently also were studied concerning their application as high performance materials.<sup>[120]</sup> In particular, for polymer **16** it was found that at high degrees of polymerization the polymer is predominantly amorphous with a  $T_g$  of around 165 °C. Upon hot compression molding of this polymer, a homogeneous film formed, which at room temperature showed a tensile stress behavior comparable to a tough, commercially available polycarbonate (Figure 2.5).<sup>[120]</sup> Upon heating above the glass transition, this material could be stretched up to 800%.<sup>[121]</sup>



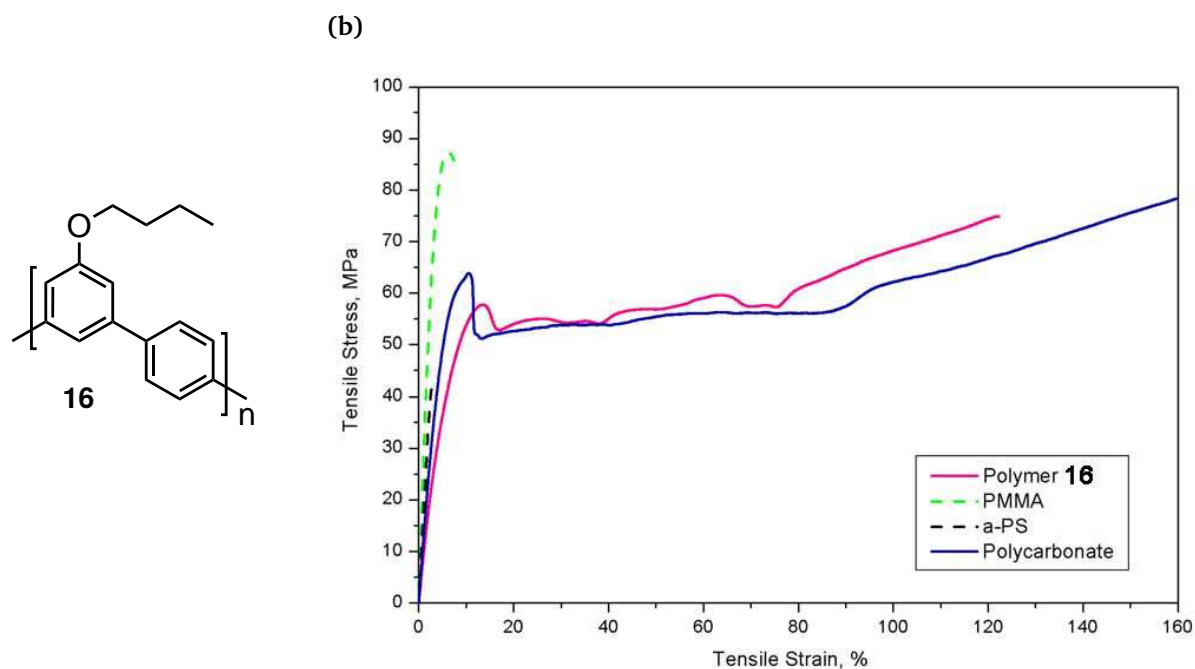
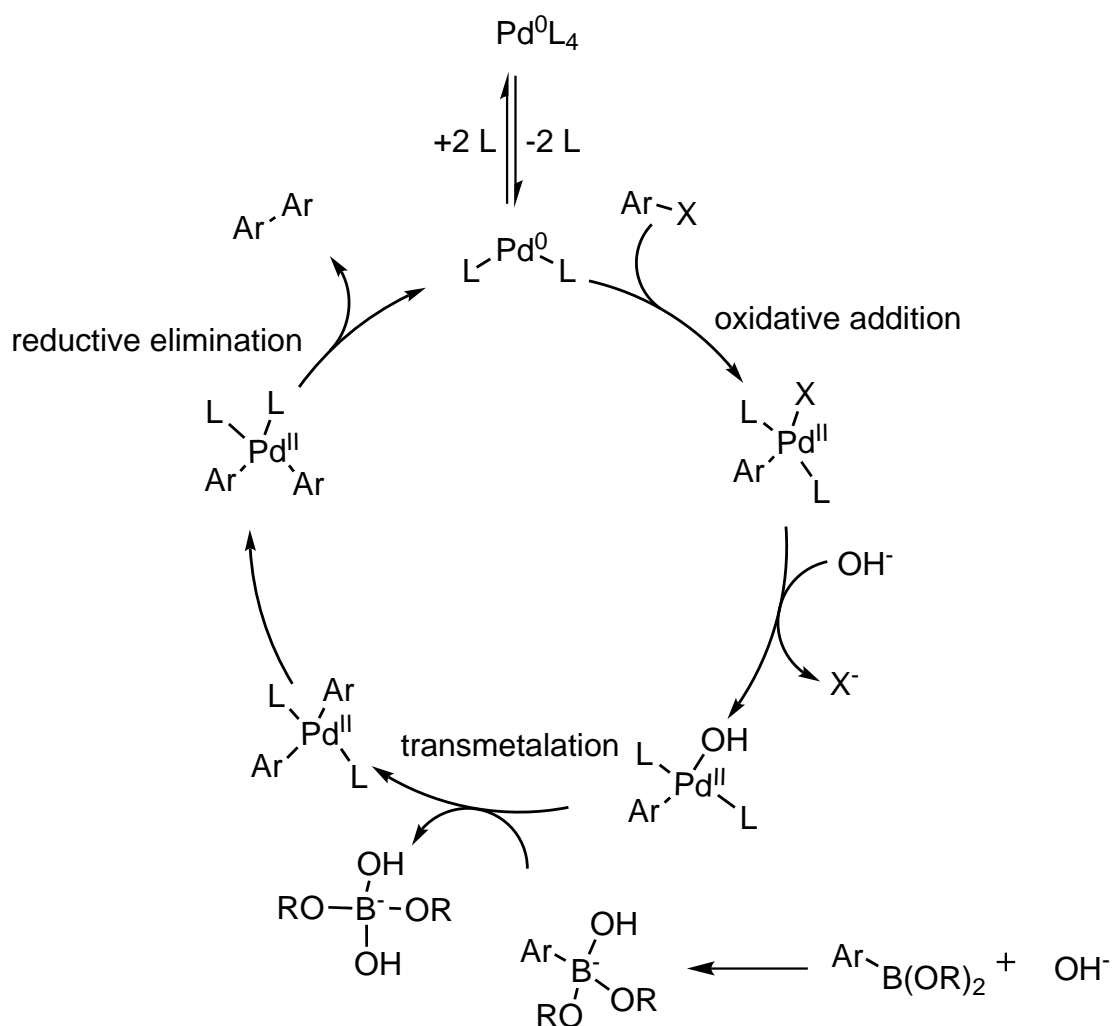


**Figure 2.5.** Stress-Strain curves of polymer **16** (pink) and commercially available amorphous polymers. The behavior of polymer **16** is comparable to a tough polycarbonate.

### 2.3 Suzuki polycondensation

Suzuki polycondensation is a widely used method for the synthesis of conjugated polymers which was introduced by Schlüter and Wegner et al. in 1989.<sup>[122,123]</sup> As the name reveals, it is based on the very famous Suzuki-Miyaura cross-coupling reaction (SMCC), which takes place between an aryl halide and an aryl boronic acid derivative in the presence of a base and a palladium catalyst.<sup>[72]</sup> Due to numerous investigations, the mechanism of the SMCC is very well understood.<sup>[124,125]</sup> As shown in scheme 2.3, the catalytic cycle comprises three main steps: oxidative addition, transmetalation and reductive elimination. The catalytic cycle starts with the formation of the active catalytic species  $\text{Pd}^0\text{L}_2$  by dissociation of two ligands. The active catalyst subsequently undergoes oxidative addition, which is an insertion into the C-X bond of the aromatic halogen, whereby the catalyst changes its oxidation state. After the oxidative addition, the resulting palladium complex engages in the transmetalation, in which the palladium complex replaces the boron group of the aromatic boron compound. For the exact mechanism of this step, several pathways have been proposed which depend on the combination of base, catalyst and substrates.<sup>[126,127]</sup>



**Scheme 2.3.** Proposed mechanism for Suzuki cross-coupling between an aryl halogen and aryl boronic compound (X = halogen, L = Ligand).

Nevertheless, an essential prerequisite for a transmetalation is the activation of the aromatic boron compound by the base. After both coupling partners are attached to the same palladium, an isomerization occurs which allows for the reductive elimination to occur.<sup>[128]</sup> In this step, the final product is released and the catalyst is recovered in its original oxidation state. While this step proceeds very quickly, the rate determining step of the catalytic cycle is usually the oxidative addition. This can change however towards the transmetalation, depending on the substrates and reaction conditions.<sup>[129]</sup> Therefore, usually these two steps need to be optimized in order to increase the reaction rate.

In order to utilize this reaction for the synthesis of polymers, Schlüter et al. in the beginning used the difunctionalized starting material **12** bearing both necessary groups for bringing about Suzuki coupling in one molecule (Scheme 2.1). More generally spoken,

there are actually two approaches for the polymerization via SPC, which are presented in Figure 2.6. First, there is the AB-type approach, in which both necessary functionalities (halogen and boronic acid derivative) are present in one molecule. Second, there is the AA/BB-type approach, in which a dihalogen is employed into polymerization in the presence of equimolar amounts of a bisboronic compound.<sup>[121]</sup> Both cases have their advantages and disadvantages and both have been successfully applied in academia and industry for the synthesis of polymers.<sup>[113,130–132]</sup>

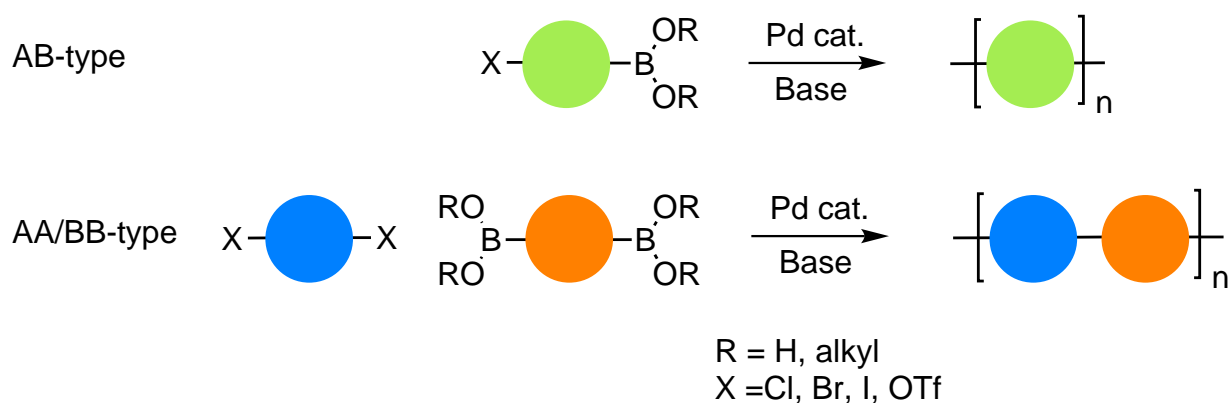


**Figure 2.6.** The two approaches of Suzuki polycondensation. In analogy to a classical polycondensation reaction they are named AB- and AA/BB-approach.

In the AB-type SPC, the obvious advantage is the built-in stoichiometric match of the functional groups, which is essential for the synthesis of high molecular weight polymer in polycondensation reactions (Chapter 1.1.2). While this appears to be ideal, the synthesis of AB-type monomers involves tedious desymmetrization steps, which often have monofunctionalized side products. As these side products would act as capping agents with a detrimental effect on the degree of polymerization, very careful and often lengthy purification is necessary to achieve the desired pure starting material.<sup>[133]</sup> In comparison, the AA and BB-type monomers can often be synthesized easily and in large scales. Further, the dihalogen monomer, usually dibromo, can be used as a starting material for the synthesis of the boron compound. The downside of this approach is that several prerequisites have to be fulfilled in order to guarantee for an exact stoichiometric ratio of the two monomers. First, a quantitative transfer of an exactly determined amount of monomer into the reaction vessel has to be accomplished. Second the purity of both monomers need to be determined precisely in order to know exactly how much monomer is used.

Nevertheless, most of the reported SPCs are following the AA/BB-type approach. Not only

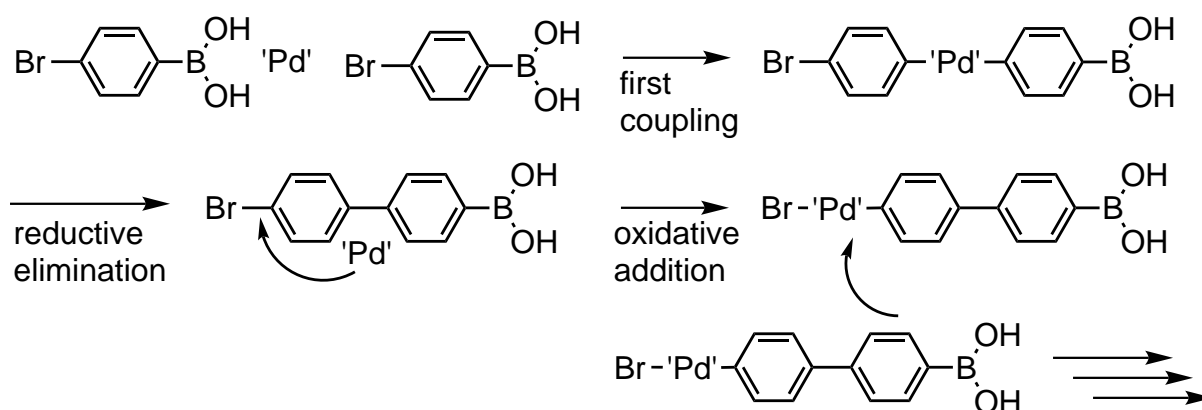
## 2 Conjugated polymers – a special class of materials

because of the fast monomer synthesis but also because of the possible structural variety that are associated with the use of two independent monomers. In particular the AA/BB-type approach gives access to perfectly alternating copolymers.

While there is a vast amount of reported SPCs using all sorts of different monomers, only a few take advantage of considering the above discussed aspects of stoichiometry and monomer purity.<sup>[134,135]</sup>

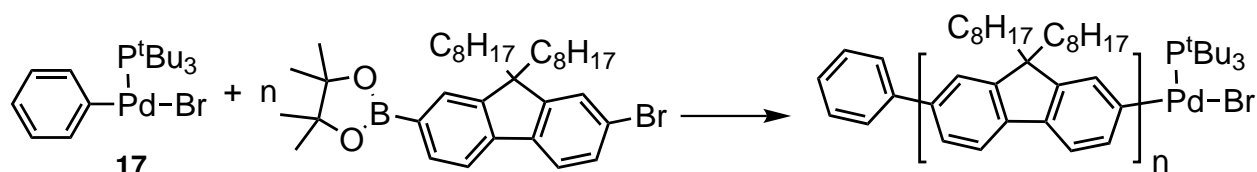
### 2.3.1 Mechanistic Considerations

In general, SPC is presented as a step-growth polymerization, which means in theory that after the first monomers are coupled by the catalyst, dimers with again two complimentary end groups are formed. These dimers can then react with other dimers or monomers to give higher oligomers always with two complementary end groups. However, it has been shown that some palladium catalysts after reductive elimination undergo the next oxidative addition, preferentially at the newly formed molecule.<sup>[136]</sup> This means e.g. that a newly formed dimer is more likely to grow further than that the Pd involved, couples two new monomers. As shown in Scheme 2.4, it does however not prevent the reaction of two oligomers. This would liberate one of the catalyst molecules, which would then be available for the coupling of two new monomers. Therefore SPC using exclusively bifunctional monomers does not qualify for a mechanism in which every catalytic cycle leads to a chain growth by one monomer unit.



**Scheme 2.4.** After reductive elimination the following oxidative addition preferentially takes place at the same molecule. A coupling of oligomers however leads to a liberation of a catalyst molecule. For clarity, the ligands at the palladium are omitted.

The effect of preferential oxidative addition however triggered some research groups to design experiments which they describe as chain-growth SPC.<sup>[137–139]</sup> By using mono-functionalized initiators (**17** Scheme 2.5), the coupling of oligomers is prevented and only monomers can add to the growing chain. End group analysis revealed that all polymers bear the initiating group. Unfortunately the reported cases were limited to molecular weights up to 30 kDa and to strictly defined polymerization conditions and monomers.<sup>[140]</sup>



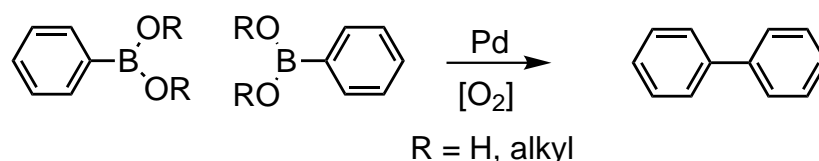
**Scheme 2.5.** AB-type SPC presented as a chain-growth polymerization. The mono-functionalized initiator **17** is crucial as it allows only for the addition of monomers.

### 2.3.2 Side reactions

As mentioned above, the presence of equimolar amounts of complementary groups is essential for a successful SPC. Consequently, all side reactions which could compromise this prerequisite during the reaction need to be considered and ruled out.

#### Homocoupling of aryl boronic compounds

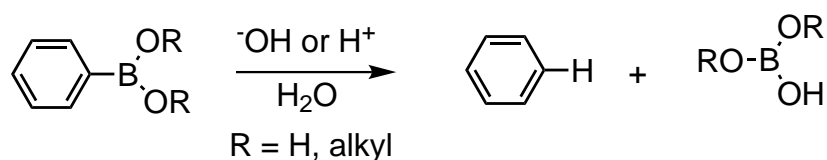
A very well-known side reaction for SMCC is the oxidative homocoupling of aryl boronic compounds (Scheme 2.6), which takes place in the presence of oxygen and a palladium catalyst.<sup>[141,142]</sup> Consequently, the exclusion of oxygen is of utmost importance when conducting SPC, as otherwise a premature consumption of the boronic species would occur. While the exclusion of oxygen is important for all Suzuki couplings when high yields are desired, especially in SPC this can be a challenge due to long reaction times and the severe impact the loss of coupling groups has on the achievable molar mass.



**Scheme 2.6.** Homocoupling of aryl boronic acids in the presence of oxygen. This side reaction leads to a premature consumption of the boron species.

### Protodeboronation

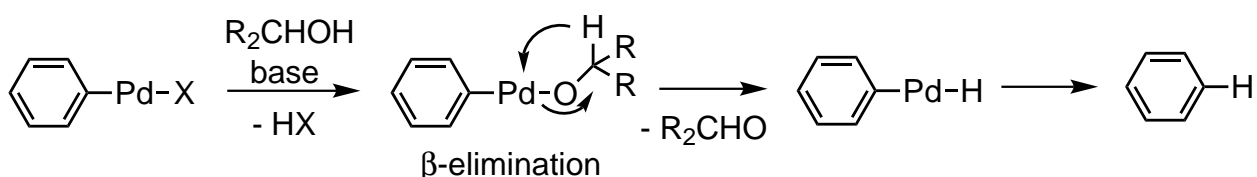
Another known side reaction in SPC is protodeboronation. This occurs in the presence of water and leads to the substitution of boron by hydrogen (Scheme 2.7). It has been shown that especially in the presence of acids or strong bases this reaction can proceed rapidly and quantitatively.<sup>[143,144]</sup> This is an important aspect as SMCC as well as SPC are performed in the presence of a base. Luckily, under mildly basic conditions, protodeboronation is retarded, which is in favor of SPC. Unfortunately, already minor losses of the boron species already have a detrimental effect on the outcome of SPC. Therefore, it is commonly understood that a small excess of the boron species in order to account for the protodeboronation is beneficial for a successful polymerization.<sup>[145,146]</sup>



**Scheme 2.7.** Acid- or base- promoted protodeboronation of an aryl boronic compound. In SPC this leads to a mismatch in stoichiometry.

### Dehalogenation

While the two side reactions discussed above both concern the boron species, the aromatic halogen can also be affected by side reactions in transition metal catalyzed cross-couplings. In particular, it is known that dehalogenation can occur in the presence of primary or secondary alcohols due to  $\beta$ -hydride elimination at the catalyst (Scheme 2.8).<sup>[147]</sup> While alcohols are not commonly used in SPC, they can result from the hydrolysis of boronic esters;<sup>[148]</sup> aryl boronic esters are preferred substrates for SPC compared to the free boronic acids for solubility reasons. In order to prevent dehalogenation triggered by hydrolyzation products, tertiary alcohols like pinacol are used for esterification of the boron compounds. Due to the absence of a  $\beta$ -hydrogen, dehalogenation can be prevented.

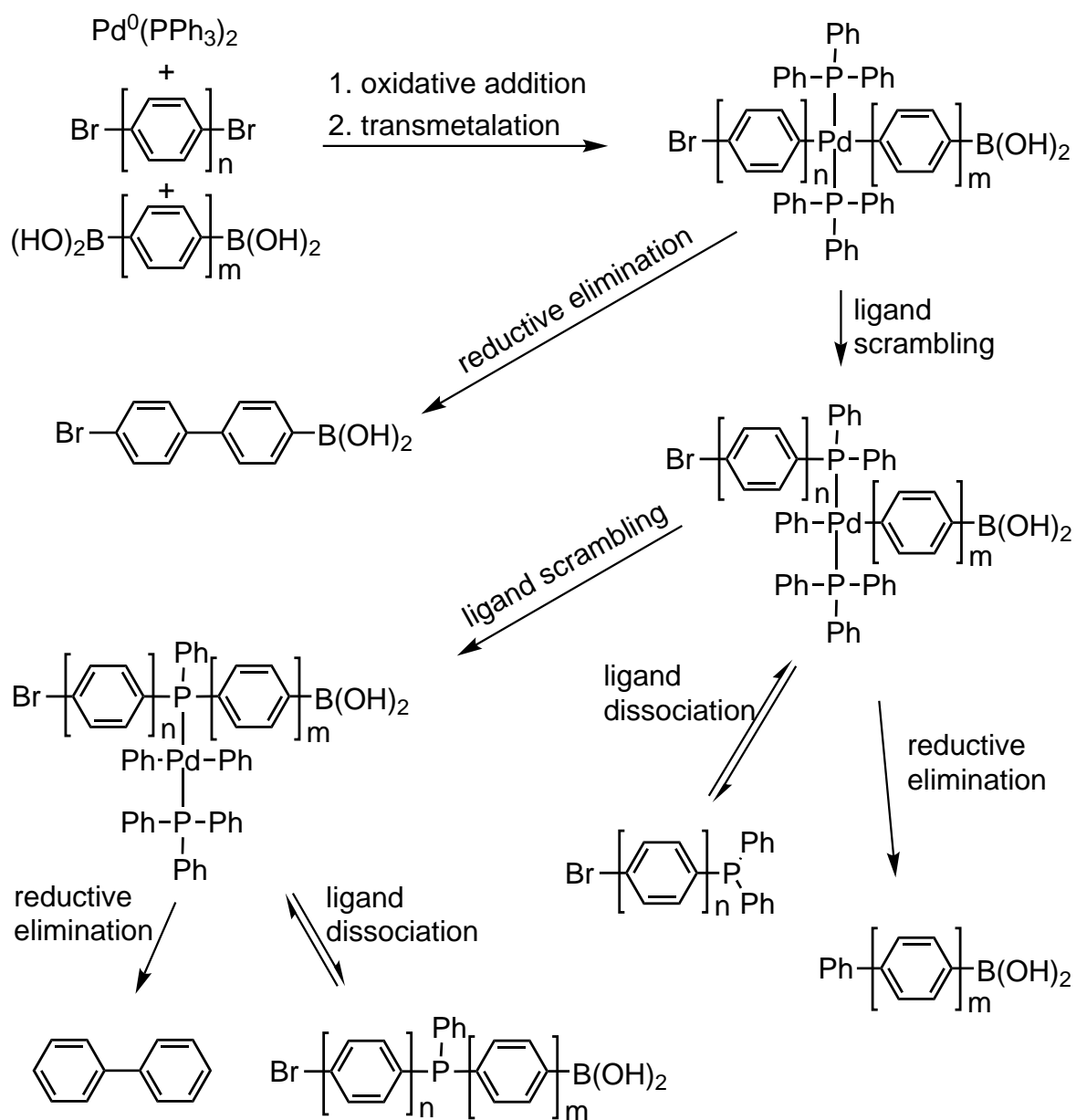


**Scheme 2.8.** Dehalogenation of the aryl halogen in the presence of a secondary alcohol. The loss of the halogen is due to a  $\beta$ -hydride elimination.

### Ligand scrambling

Another side reaction that has been observed especially for transition metal catalyzed cross-coupling reactions involving phosphine ligands is the exchange of aryls between the transition metal center and the phosphine ligand.<sup>[149]</sup> As shown in Scheme 2.9, this so-called ligand scrambling can impact SPC in several ways. Prior to reductive elimination, the aryls at the palladium can perform an exchange with the aryls attached to the phosphine ligand. After a first ligand scrambling, a reductive elimination or a dissociation of the ligand involved in the scrambling lead to end-capping of the polymer chain. In addition to these two options, another ligand scrambling can occur, which would finally result in the incorporation of phosphorous into the polymer chain. It should be noted that the ligand dissociation is of course reversible and the released ligands shown in Scheme 2.9 can participate in further ligand scrambling. This way, the incorporated phosphorous can even serve as branching point with three polymeric arms.<sup>[150]</sup> Gratefully, it has been shown that this side reaction only plays a minor role in SPC<sup>[151]</sup> and that it can be suppressed by using bulky ligands or phosphine-free palladium sources.<sup>[150,152]</sup>

## 2 Conjugated polymers – a special class of materials



**Scheme 2.9.** Aryl-aryl exchange between the phosphine ligands and the palladium center can lead to incorporation of phosphorous into the polymer chain as well as to chain termination.



## 2.4 Cycle formation in Suzuki polycondensation

In a step growth polymerization 100 % conversion is reached if all end groups are consumed. In a polymer chain there are always two chain ends left and therefore the theoretical state of full conversion can only be reached if exclusively cycles are formed during polymerization. While this fact has been neglected in the first theories by Carothers and Flory,<sup>[153,154]</sup> a few years later Jacobson, Stockmayer and others presented theories, which consider cycle formation as a competing reaction during step-growth polymerization (Figure 2.7).<sup>[155,156]</sup> In general, two different cases can be considered: One in which the bond formation during polymerization is reversible and therefore a thermodynamic equilibrium between open chains and rings can be reached (e.g. polyester formation),<sup>[157]</sup> and one where the bond formation is irreversible and therefore the formation of cyclic byproducts is kinetically driven (e.g. polyurethane formation or SPC).<sup>[158]</sup> For the latter case, it has been shown by Kricheldorf and others that cyclization can occur throughout the whole polymerization and even at high concentrations, given that solubility is maintained.<sup>[159,160]</sup> However, ring formation strongly depends on the chain stiffness and the favoured conformations of the polymer.<sup>[161,162]</sup>

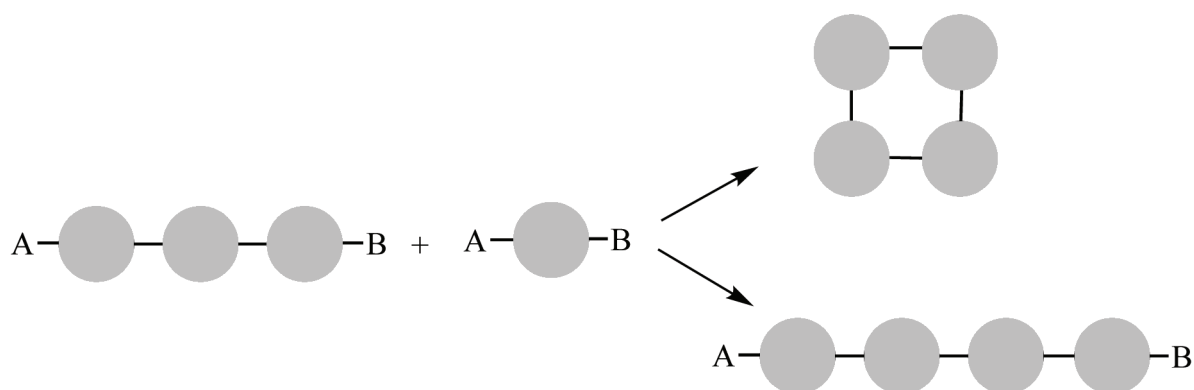


**Figure 2.7.** Cycle formation and linear chain growth are two competing reactions in step-growth polymerization. The degree of cycle formation depends on chain stiffness, preferred conformation and reaction conditions.

SPC predominantly uses monomers where the angles between the reactive sites are close to 180° (see Figure 2.8 **18** and **19**). Furthermore, the growing chain with its directly connected aromatic units is rather stiff. Both factors result in a low probability of two chain ends of the same chain to meet and form a ring. For monomer **20** and other *meta*-phenylene-containing monomers however, the angle between the functional groups differs

## 2 Conjugated polymers – a special class of materials

from  $180^\circ$  and renders the formation of cyclic oligomers more likely.

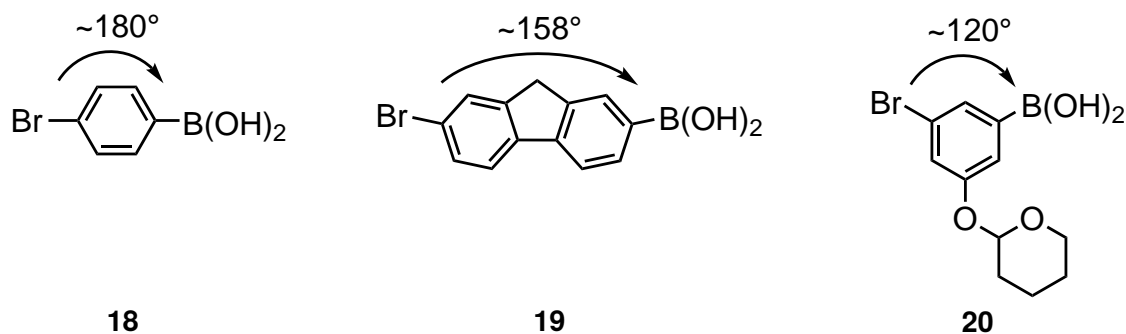


**Figure 2.8.** Different monomers for SPC with varying angles between the reactive sites.

A representative GPC curve of a poly(*m*-phenylene) polymerized from monomer **20** is displayed in Figure 2.9a and shows a typical bimodal distribution. By fractionation the low molar mass fraction was isolated and subjected to MALDI-TOF analysis. Thus the low molar mass signal in GPC could be assigned predominantly to cyclic byproducts (Figure 2.9b). From these and alike results Sakamoto and Schlüter concluded that cyclic byproducts mainly occur in the low molecular weight range. Further their formation can be controlled by concentration, choice of ligand and mode of monomer addition. [113,134]

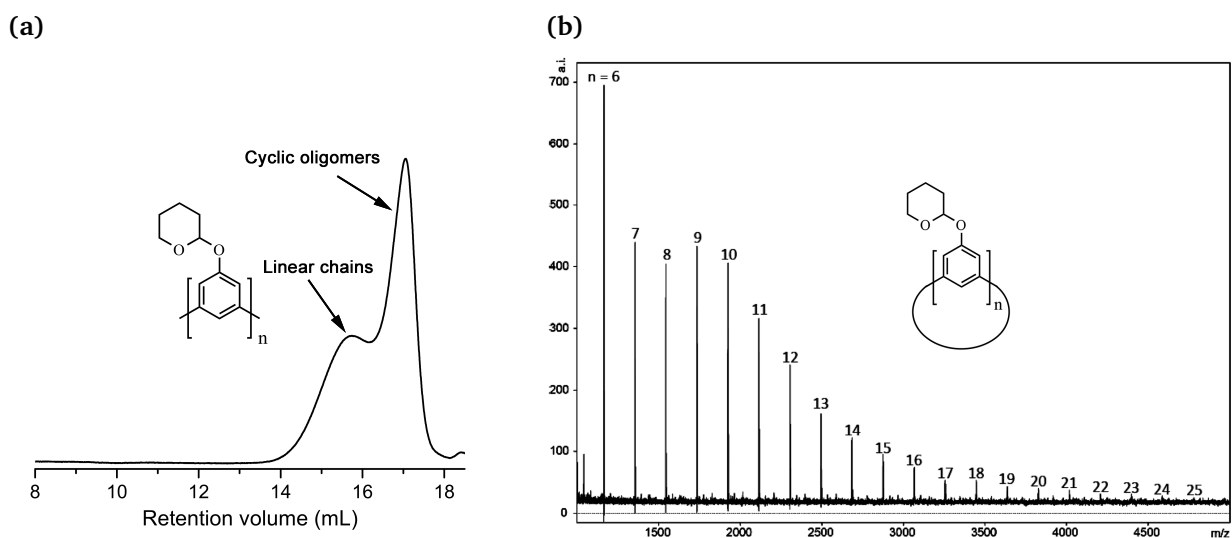


**Figure 2.9.** a) GPC curve of a poly(*m*-phenylene) showing a bimodal molar mass distribution due to the formation of macrocyclic byproducts. The MALDI-TOF spectrum of the isolated low molecular weight material b), shows predominantly the presence of cyclic oligomers.

### 3 Aim of the work

From the beginning the present work focused on two main goals.

First and foremost the aim was to establish a scalable Suzuki polycondensation procedure, which reliably yields high molar mass polyarylenes. Through the example of poly(*m,p*-phenylene)s the enormous potential of SPC as a method for the synthesis of structure perfect aromatic polymers well above the threshold of 100 kDa should be proven.

Second, the goal was to create a novel material based on high molar mass side chain free poly(*m,p*-phenylene)s which would exhibit properties attractive for applications as high-performance fibers, strong films and the like.

These two main goals result in several milestones to be achieved. They include:

1. to devise and realize multigram access to appropriately designed monomers for SPC. Thereby a particular focus had to be placed on the choice of side groups with respect to their quantitative removability after polymerization.
2. to develop procedures that would allow to purify these novel monomers to a level not commonly encountered in previous work.
3. to develop robust polymerization protocols which –despite the unavoidable need for removal of cyclic side products– nevertheless provide access to high molar mass products on scales of several grams.
4. to investigate the molecular structures of the novel polymers by state-of-the-art methods and determine the molar masses not only by routine GPC measurements but also by advanced light scattering techniques.
5. to produce films and drawn fibers from the polymeric products still containing the removable side chain.
6. to study the removal of the side chains from the polymers after processing into films and drawn fibers and to prove that this important step can be performed virtually quantitatively.
7. to investigate the mechanical properties of the specimen obtained under 6. after removal of the side chains.



## **Results & Discussion**



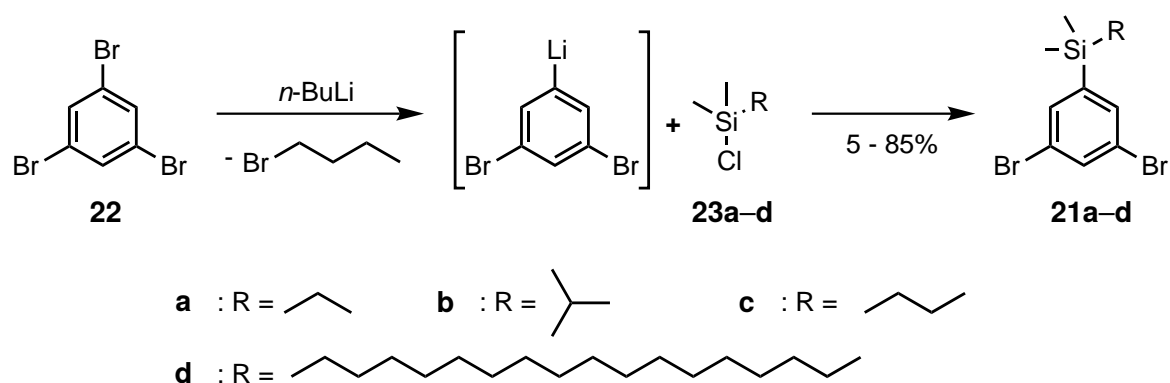
## 4 Monomer synthesis

The basis for the successful development of polymers is a solid and sufficient supply of pure monomers. Uncertainties concerning purity result in uncertainties in the amount of functional groups present in the polymerization. Due to the detrimental effect a stoichiometric mismatch has on the outcome of SPC, a reproducible high purity is particularly important. In order to guarantee this prerequisite, a straight forward synthesis with a minimal amount of steps is needed. Most of the reported procedures for AB type monomers involve multiple steps and lengthy purifications,<sup>[73,133]</sup> which is why an AA/BB type approach was chosen for the present thesis. In this case two monomers are necessary, one bearing two halogen groups and one bearing two boron functionalities. In the following section we describe several syntheses of AA- and BB type monomers. A characteristic of the dibromo compounds is that they all bear acid cleavable side groups, which facilitate solubility during polymerization but can be cleaved off afterwards. Different silyl side chains were introduced and investigated concerning their solubility enhancement of the resulting polymer.

### 4.1 Dibromo monomers

For the synthesis of the dibromo monomers **21a–d**, 1,3,5-tribromobenzene **22** was chosen as a starting material. In order to achieve a high degree of purity for the final product, impurities should be avoided from the very beginning. Therefore the commercially available compound **22** was recrystallized from ethanol or acetic acid to give the pure starting material as colorless crystals. According to Scheme 4.1 compound **22** was mono-metallated, by a lithiation with *n*-butyllithium. The very reactive lithiated intermediate was finally quenched *in situ* with one of the alkylated chlorosilanes **23a–d**. Four different alkyl side chains were introduced, in order to investigate their influence on the solubility of the resulting polymer. The results of the syntheses are summarized in Table 4.1. The synthesis of monomer **21a** has already been reported<sup>[163]</sup> and could be reproduced on a scale of 7 g. The same procedure also led to satisfying yields (>70 %) for monomers **21c** and **21d**. In the case of monomer **21c** the synthesis was even scaled up to 40 g of product. In all cases the raw product was distilled three times until no further increase of purity could be observed by NMR. Although this purification procedure lowered the overall yields

## 4 Monomer synthesis



**Scheme 4.1.** Reaction scheme of symmetric dibromo monomers **21a-d** with different alkyl side chains.

somewhat, product purity was prioritized. For monomer **21b** however, the chosen synthesis turned out to be more difficult and the yields after distillation did not exceed 6 %. One possible explanation for this poor result might be the use of a partially hydrolyzed batch of compound **23b**. The purchased hygroscopic<sup>[164]</sup> compound had already a gel-like, instead of a solid appearance, which is the reason for that assumption. After first polymerization tests with the resulting low amount of monomer **21b** this compound was no longer of interest due to the low solubility of the resulting polymers (see Chapter 5). Therefore the optimization of its synthesis was not pursued.

**Table 4.1:** Results of the synthesis of different dibromo monomers

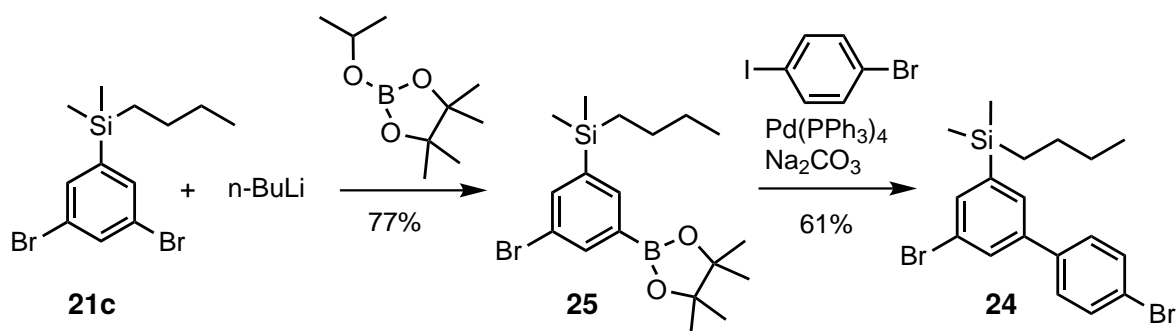
Monomer	Scale [g]	Yield <sup>a</sup> [%]
<b>21a</b>	7.20	67.4
<b>21b</b>	0.62	5.6
<b>21c</b>	40.0	72.7
<b>21d</b>	11.0	84.5
<b>24</b>	6.55	34.1

<sup>a</sup>Overall yields starting from 1,3,5-tribromobenzene **22**

In order to broaden the scope of monomers and possible polymers, the monomer set of symmetric dibromo compounds was extended by the biphenyl monomer **24** (Scheme 4.2). Compared to the monomers **21a-d** the two brominated carbons in monomer **24** are not equivalent, which is why they allow for a *head-to-tail* isomerism when incorporated into a polymer. The synthesis comprises two additional steps starting from compound



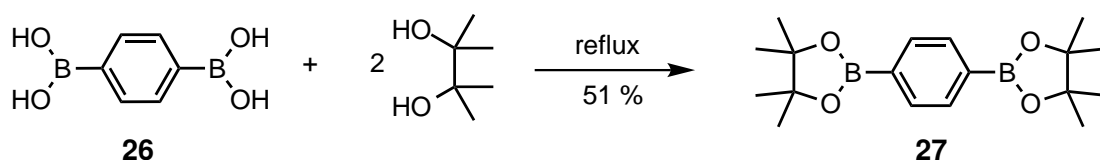
**21c.** After mono-lithiation and subsequent quenching with isopropyl pinacol borane, the desymmetrized compound **25** was obtained in 77% yield. A final Suzuki coupling with *p*-bromoiodobenzene yields monomer **24**. Including the synthesis of **21c**, the total three step synthesis, starting from **22**, has an overall yield of 34 %.



**Scheme 4.2.** Synthesis of biphenyl monomer **24**. The two different halogenated sides of this compound introduce a directionality into the resulting polymer.

## 4.2 Diboron monomers

For synthesis of the diboronated monomers different synthetic approaches were used. The commercially available benzene-1,4-diboronic acid (**26**) was used as a starting material for the synthesis of the *para*-substituted monomer **27**. By a simple esterification reaction with pinacol this monomer could be obtained in scales up to 50 g (Scheme 4.3).<sup>[165]</sup> In this case the low yield of 51% can be explained by losses associated with the recrystallization which had to be repeated in order to achieve the required high purities. However this yield suggests that further investigations concerning the recrystallization conditions would be beneficial before a further scale up is attempted.



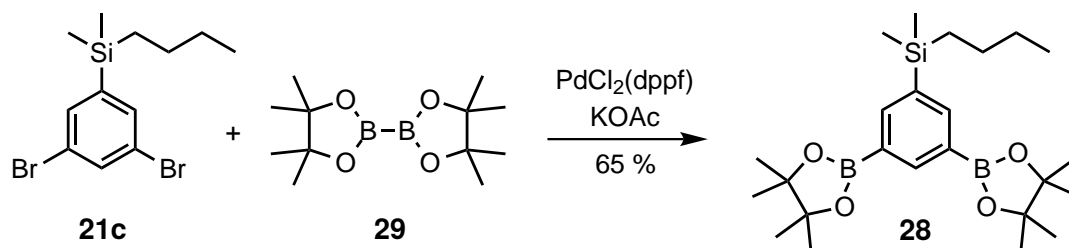
**Scheme 4.3.** Esterification of 1,4-phenyldiboronic acid. The low yield is attributed to repeated recrystallization.

The other boron monomer, **28**, was synthesized by a palladium catalyzed Miyaura borylation of monomer **21c** with bis(pinacolato)diboron **29** (Scheme 4.4). The reaction proceeds *in situ* via a stepwise borylation of the two brominated carbons. A competing SMCC of the

## 4 Monomer synthesis

---

mono borylated intermediate with the starting material is prevented by using KOAc. This very weak base is not sufficient to activate an arylboronic compound for a SMCC.<sup>[166]</sup> Monomer **28** could be obtained on a 8 g scale.



**Scheme 4.4.** Borylation of monomer **21c** via palladium catalyzed Miyaura borylation with bis(pinacolato)diboron **29**.

### 4.3 Monomer purity

As mentioned above, Carothers equation implies that high molecular weights in Suzuki polycondensation can only be achieved if a perfect stoichiometric ratio between the two different monomers is achieved. Therefore the monomer purity is of crucial importance in order to know the exact amount of functional groups present. NMR spectroscopy and gas chromatography (GC) were utilized for determining the purity of the above described monomers. In addition to these two methods all monomers gave correct values for elemental analysis (Table 4.2).

After synthesis and purification, all monomers were subjected to high resolution NMR spectroscopy. For determining the purity from the resulting spectra, the C-13 satellite method was used.<sup>[73,167]</sup> This method exploits that due to the natural abundance of C-13 of 1% and the nuclear spin quantum number of 1/2, the C-H coupling results in two satellite signals with an intensity of 0.5 % of the corresponding main signal. An example of such satellite signals are shown in the magnification in Figure 4.1 and are marked by asterisks. By comparing the integrals of the C-13 satellite signals with the integrals of the signal from an observed impurity it is possible to estimate the amount of impurity. Thus for all monomers a purity of  $\geq 99.5\%$  was determined. It should be noted that for the comparison of the integrals it was assumed that all impurity signals correspond to one

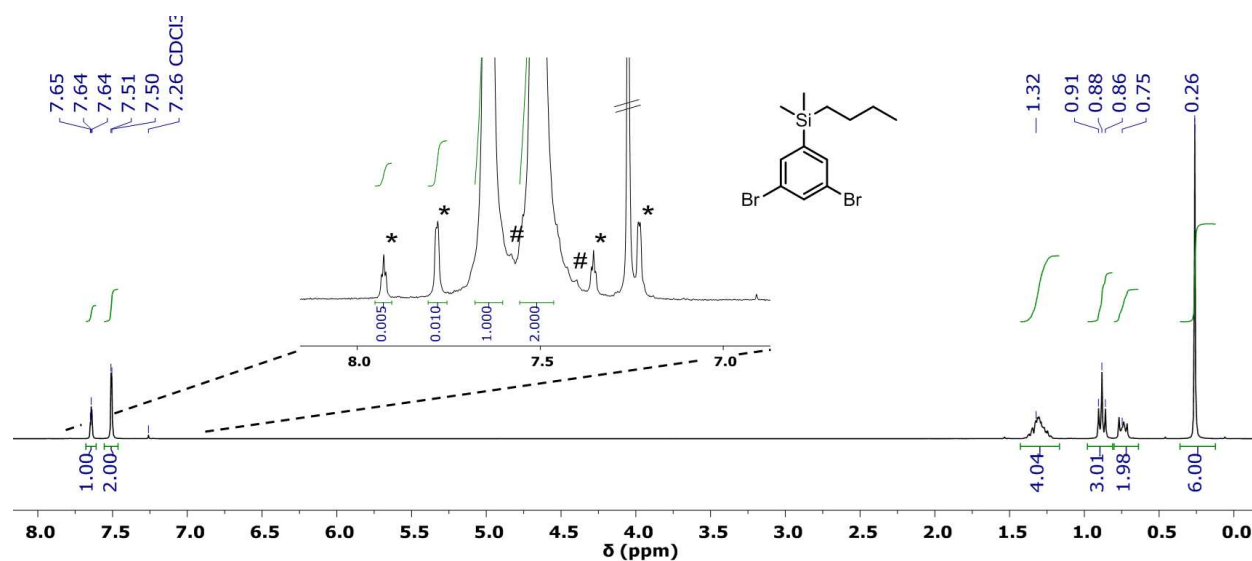


**Figure 4.1.**  $^1\text{H}$ -NMR spectrum of **21c** in deuterated chloroform with a magnification of the aromatic region. C-13 satellites are marked with \* and impurities with #.

proton. Therefore the determined purity values are expected to be the lower limit. The downside of this method is that the peaks in the spectrum are not baseline separated and the suggested impurity peaks overlap with the monomer peaks. Furthermore there could be more signals hidden beneath the monomers peaks. Therefore gas chromatography (GC) was chosen, to evaluate the reliability of the NMR method. For this purpose three dilute solutions (0.156 M, 78 mM and 15.6 mM) of **21c** in THF were subjected to GC. The resulting chromatograms are shown in Figure 4.2a and show a decrease of the monomer signal at around 16 minutes upon dilution. Further, it should be noted that aside from the injection- and the solvent signal at around 2 minutes retention time, no additional signals appear at these low concentrations even under high magnification. From these chromatograms the calibration curve (Figure 4.2b) for the dibromo monomer **21c** was generated. For the purity determination subsequently the pure monomer **21c** was injected into the GC, which resulted in the chromatogram in Figure 4.2c. Besides the oversaturated signal of the monomer, under strong magnification, some impurities can also be detected. After determination of the peak areas of these impurities, the theoretical peak area for the pure monomer was extracted from the calibration curve by extrapolation. The sum of the areas for the impurities could thus be divided by the theoretical area for the pure monomer. This procedure resulted in a purity of 99.96%, which is even higher than the one determined by NMR. It should be mentioned that for the described method, we assumed

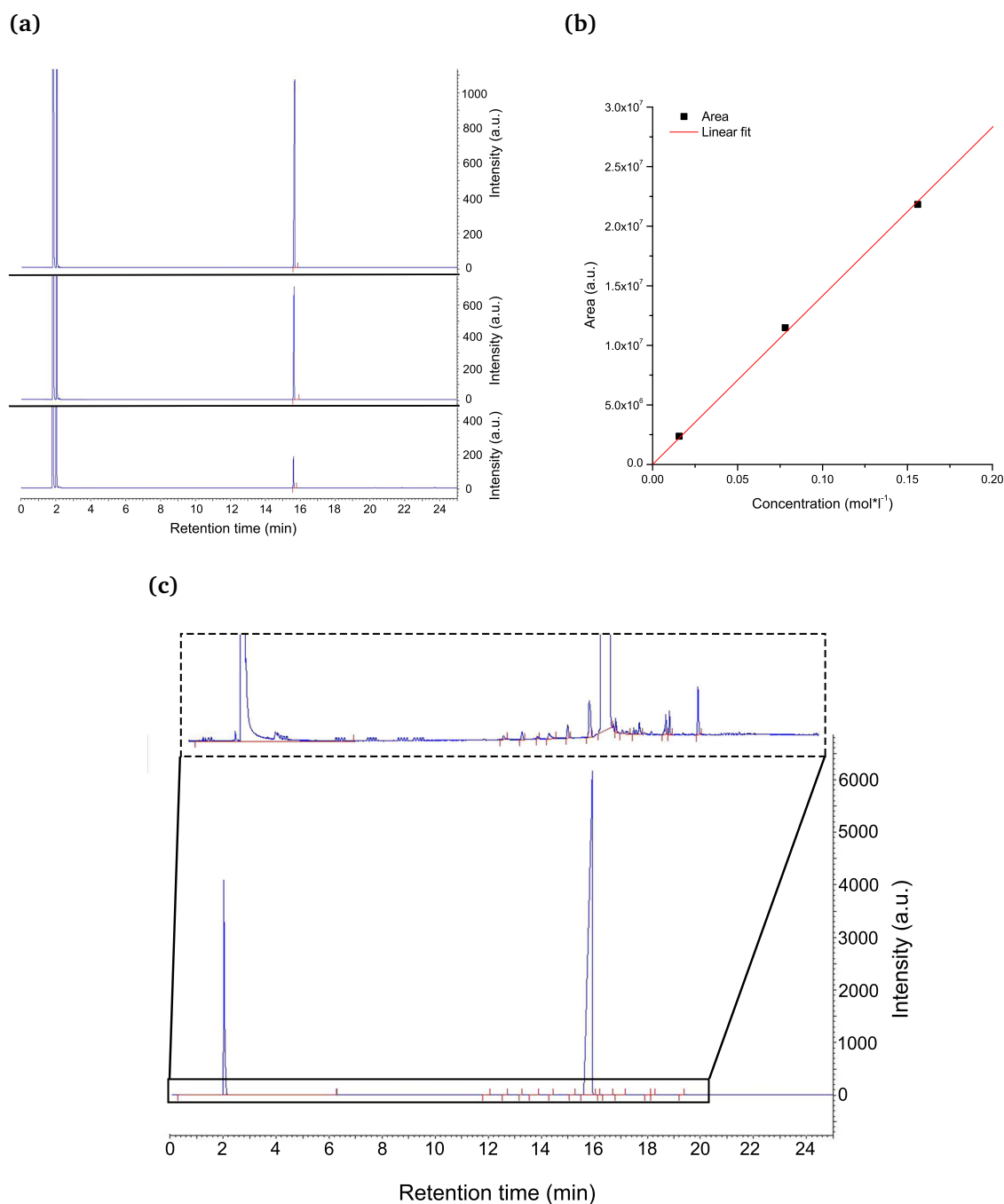


**Figure 4.2.** a) Gas chromatograms of diluted solutions of **21c** in THF. b) Calibration curve for **21c**. c) Oversaturated FID signal of the gas chromatographic analysis of undiluted **21c**.

the same sensitivity of the flame ionization detector (FID) towards the monomer and all impurities. Due to this encouraging finding, from there on we relied on the NMR method for all the other monomers. They were not used for polymerizations below a purity of 99.5%. In addition to the determined high purities, with one exception all monomers gave correct values in elemental analysis (Table 4.2). While this is not a method for purity

quantification, it nevertheless supports the high purities found by NMR spectroscopy and GC and confirms the synthesized structures.

**Table 4.2:** Values for the elemental analysis of the synthesized monomers. Calculated values in parenthesis.

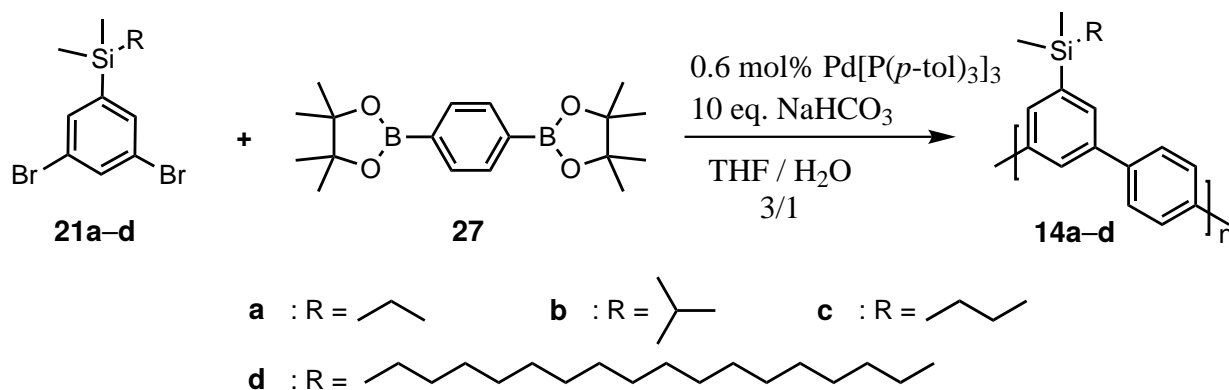
Monomer	C [%]	H [%]	Br [%]
<b>21a</b>	39.25 (39.31)	4.98 (4.80)	47.40 (47.54)
<b>21b<sup>a</sup></b>	-	-	-
<b>21c</b>	40.97 (41.16)	5.18 (5.18)	45.85 (45.64)
<b>21d</b>	57.64 (57.14)	8.65 (8.48)	28.49 (29.24)
<b>24</b>	50.97 (50.72)	5.48 (5.20)	37.39 (37.49)
<b>27</b>	65.36 (65.51)	8.50 (8.55)	-
<b>28</b>	64.63 (64.88)	9.83 (9.53)	-

<sup>a</sup>Due to the low yield an elemental analysis for **21b** could not be obtained.

## 5 Polymer synthesis

With the above described monomers in hand the next goal was to establish a method, which allows for a reproducible synthesis of high molecular weight polyphenylenes with acid cleavable silyl side chains. These polymers later should be used for investigating their mechanical properties when processed into films. From reports on polymers **14a** and **16**<sup>[120,163]</sup> we concluded that for this class of polymers, molecular weights beyond 100 kDa have to be achieved in order to exhibit interesting mechanical properties. Therefore, first polymerizations aimed at finding out whether the chosen silyl groups (**23a–d**) would enhance solubility sufficiently for synthesizing such high molar mass polymers.

As a starting point monomers **21a–d** were polymerized with the diboronic ester **27** under the already reported conditions (Scheme 5.1).<sup>[107]</sup> For **14a** the published results from Sakamoto et al.<sup>[107]</sup> could be reproduced and the polymer precipitated from the reaction mixture at a  $M_w$  of approximately 30 kDa. Next, polymer **14b** was synthesized using the same conditions. As expected, due to the fewer degrees of freedom of the *tert*-butyl group, the solubility was even worse and the growing polymer **14b** already precipitated at a  $M_w$  of 5 kDa. On the contrary, solubility was not an issue for polymer **14c**, which was obtained with a  $M_w$  of 35 kDa. While this finding was of course not satisfying, the fact that the obtained material stayed in solution caught our attention. We speculated that upon optimization of the conditions higher degrees of polymerization could be reached. Finally, we also polymerized **14d** for which solubility was also not an issue. However the cleavable side chain in this case makes up 67 % of the polymer's mass.



**Scheme 5.1.** Synthesis of poly(*m,p*-phenylene)s (PmpPs) with various side chains using the conditions already reported for **14a**.

This was considered too much for a subsequent removal, not only from an atom efficiency point of view but also because of the low chances to obtain an intact film after side chain cleavage from the bulk material. From the above described results it was concluded that an optimization of the reaction conditions using **21c** and **27** would be the most promising choice for both, a successful synthesis of high molar mass polyphenylenes as well as for the subsequently planned processing and cleaving procedure.

## 5.1 Optimization of the reaction conditions

The aim of the optimization of the above mentioned polymerization reaction was the synthesis of linear polyphenylenes of highest molecular weight possible. Therefore we relied on GPC using conventional polystyrene calibration throughout the optimization process, for the evaluation of the resulting polymers. The starting point for the optimization was the above described polymerization of **14c** using the reported conditions.<sup>[107]</sup> The result of this polymerization, which was carried out on a 1 g scale, is listed in Table 5.1, entry 1. It shows that the molar mass range remained practically the same (35 kDa) compared to **14a** (33kDa), although the solubilizing side chain was extended by one CH<sub>2</sub> group. The molecular weight values refer to a raw GPC elution curve still containing cyclic oligomers (see chapter 2.4). Interestingly though, the polymers **14c** stayed in solution, while in the case of **14a** they precipitated, which indicates an increased solubility of **14c** compared to **14a** and therefore a potential for higher molar masses upon optimization.

### 5.1.1 Monomer concentration

As described in Chapter 2.4 cycle formation is an inherent problem of polycondensation and can prevent the formation of long polymer chains by intramolecular ring closure of oligomers. According to the Ruggli-Ziegler dilution principle<sup>[168]</sup> it was assumed that this issue can be addressed by varying the monomer concentration. Therefore, that was the first parameter we tried to optimize. By stepwise increasing the monomer concentration in order to disfavour cycle formation, similar weight averages for the molar masses were obtained (Table 5.1). The GPC curves of the resulting polymers, however, showed significant differences (Figure 5.1). As described in Chapter 2.4 and 5.1.5 the macro cycles elute at higher retention times, therefore the bimodal distributions allow conclusion concerning

the ratio of linear to cyclic products. While in fact the ratio of cycles in the product could be reduced (as judged by the GPC signal at around 17 mL of retention volume), the molar mass of the linear material at a retention volume of around 14 mL somewhat decreased. The reason for that is an upcoming solubility issue at higher concentrations. Therefore it was concluded that under the given conditions there is a trade-off between reducing the amount of macrocycles and increasing the molecular weight of the linear polymers.

Because the goal was the maximization of the molar mass, we opted for the minimum concentration of  $12\text{g L}^{-1}$  for all following polymerizations. Thereby we ignored the issue of cycle formation in favor of an improvement of the linear fraction and relied on the possibility of an efficient separation of the cyclic and linear products.

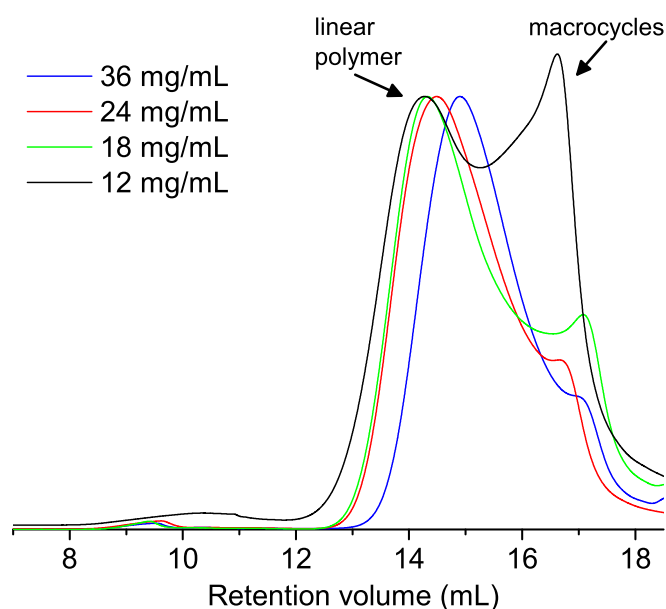


**Figure 5.1.** GPC elution curves for polymer **14c** obtained from polymerizations at different monomer concentrations. The bimodal distribution is attributed to the mixture of cyclic and linear products.

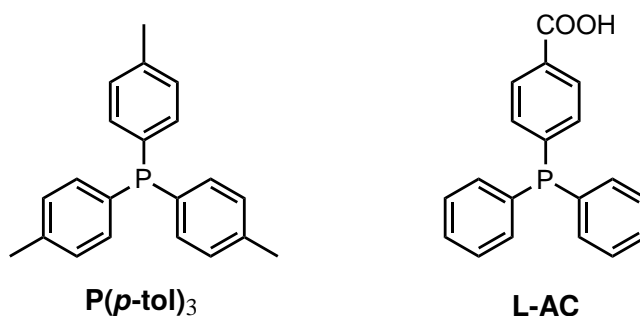


**Table 5.1:** Synthesis results of polymerizations between **21c** and **27** applying different monomer concentrations. The concentration values refer to monomer **21c**. The experiments were performed on a 1 g scale regarding monomer **21c**.

Entry	Catalyst	Conc. [g L <sup>-1</sup> ]	Base	M <sub>n</sub> [kDa]	M <sub>w</sub> [kDa]	Yield [%]
1	Pd( <b>30</b> ) <sub>3</sub>	12	NaHCO <sub>3</sub>	5.0	35	85
2	Pd( <b>30</b> ) <sub>3</sub>	18	NaHCO <sub>3</sub>	4.4	32	83
3	Pd( <b>30</b> ) <sub>3</sub>	24	NaHCO <sub>3</sub>	6.2	27	80
4	Pd( <b>30</b> ) <sub>3</sub>	36	NaHCO <sub>3</sub>	8.8	32	75

### 5.1.2 Catalyst

The fact that the polymerization was terminated, although polymer **14c** was still in solution, led us to the conclusion that the reactivity of the reported catalyst, based on the tris(*p*-tolyl)phosphine ligand, may not have been sufficiently high and thus leading to premature termination. Consequently, a different catalyst precursor, Pd(**L-AC**)<sub>3</sub>, was used with K<sub>2</sub>CO<sub>3</sub> as a base. For this combination Cheng et al.,<sup>[169]</sup> reported a particularly high reactivity. This Pd-complex carries the phosphine ligand **L-AC** (Figure 5.2) which improves the water solubility of the catalyst especially under basic conditions as is the case in SPC. First experiments using this catalyst were performed without implementing other changes and a representative result is shown in entry 3 of Table 5.2. As can be seen in Figure 5.3a, a significant increase in molecular weight was observed (55 kg mol<sup>-1</sup>). A kinetic comparison of both catalysts, Pd[**P(p-tol)**]<sub>3</sub> and Pd(**L-AC**)<sub>3</sub>, supported this finding. Figure 5.3b displays the increase of M<sub>w</sub> with reaction time for both catalyst/base combinations.

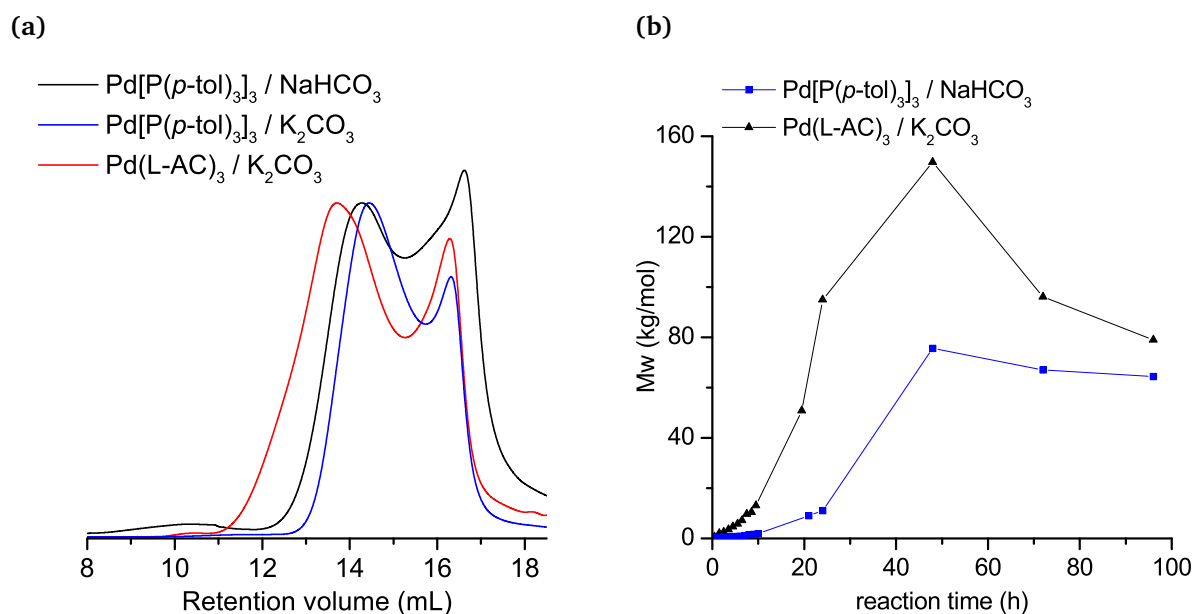


**Figure 5.2.** Previously used tris(*p*-tolyl)phosphine ligand (left) and the new acidic 4-diphenylphosphanobenzoic acid ligand (right).

**Table 5.2:** Polymerization results of monomers **21c** and **27** using different catalysts and bases. The experiments were performed on a 1 g scale regarding monomer **21c**.

Entry	Catalyst	Base	$M_n$ [kDa]	$M_w$ [kDa]	Yield [%]
1	Pd(P( <i>p</i> -tol) <sub>3</sub> ) <sub>3</sub>	NaHCO <sub>3</sub>	5.0	35	85
2	Pd(P( <i>p</i> -tol) <sub>3</sub> ) <sub>3</sub>	K <sub>2</sub> CO <sub>3</sub>	5.6	17	87
3	Pd(L-AC) <sub>3</sub>	K <sub>2</sub> CO <sub>3</sub>	6.0	55	85

It should be noted, that the drop of molar masses at long reaction times is due to precipitation of high molecular weight material, which was therefore not collected when taking samples with a syringe. Further it should be noted that molecular weight values were determined by GPC with a PMMA calibration, which explains the higher values as compared to Table 5.2. That the improved reactivity was in fact due to the change in catalyst and not the change in base (K<sub>2</sub>CO<sub>3</sub> instead of NaHCO<sub>3</sub>) can be concluded from entry 2, where only the base was changed but not the catalyst. The molar mass obtained in this case was even lower than in the previous entries. This might be due to an increased protodeboronation resulting from the stronger base K<sub>2</sub>CO<sub>3</sub>.

**Figure 5.3.** a) GPC curves of polymerizations using different base/catalyst combinations showing the molecular weight increase using Pd(L-AC)<sub>3</sub> / K<sub>2</sub>CO<sub>3</sub>. b) Development of  $M_w$  over reaction time for both catalysts showing a much faster increase using Pd(L-AC)<sub>3</sub> / K<sub>2</sub>CO<sub>3</sub>.

While the increased molar mass with the new conditions ( $\text{Pd}(\text{L-AC})_3/\text{K}_2\text{CO}_3$ ) was attractive, the fraction of cyclic products had not decreased much as judged by GPC.

### 5.1.3 Stoichiometry

It is routine in SPC to use the boronic acid ester component in slight excess to meet the required 1:1 stoichiometry despite eventual deboronation reactions.<sup>[143]</sup> Typically 1.02-1.03 equivalents are employed.<sup>[135,145]</sup> In our case however a smaller excess was beneficial. In a series of optimization experiments various monomer ratios were employed and the results are summarized in Table 5.3. As can be observed in Figure 5.4, the highest molar mass was obtained for 1.005 equivalents. This ideal monomer ratio was found for three independent monomer batches, which confirms the reproducibility of our monomer and polymer synthesis. This ratio was therefore considered reliable and used for all following experiments. These findings indicate, the vital importance of stoichiometry in Suzuki polycondensation. The strong emphasis on monomer ratio in this series of experiments led to the highest molecular weights achieved so far. The found combination of catalyst, base and stoichiometry from now on will be referred to as 'optimized conditions'.

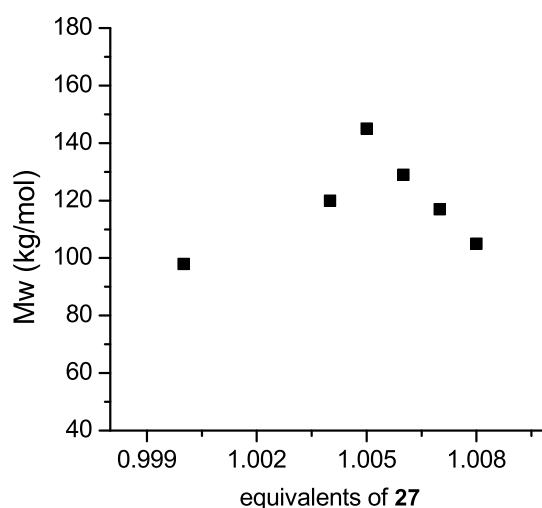


**Figure 5.4.** Dependence of  $M_w$  on the excess of **27**. The molecular weights show that also on a 1 g scale high molecular weights can be achieved, when stoichiometry is tuned very carefully.

## 5 Polymer synthesis

---

**Table 5.3:** Polymerization results of monomers **21c** and **27** using different stoichiometric ratios. The experiments were performed on a 1 g scale regarding monomer **21c**.

Entry	Amount of <b>21c</b> [eq.]	Amount of <b>27</b> [eq.]	$M_n$ [kDa]	$M_w$ [kDa]	Yield [%]
1	1.000	1.000	7.3	98	93
2	1.000	1.004	11	120	n.d.
3	1.000	1.005	13	145	98
4	1.000	1.006	12	129	n.d.
5	1.000	1.007	7.8	117	91
6	1.000	1.008	10	105	96

### 5.1.4 Scale-up

Due to the previous findings the reaction scale also seemed to be an interesting target of optimization. By increasing the scale, the relative error occurring during weighing and monomer transfer should decrease and therefore the targeted stoichiometric ratio can be met more accurately. Accordingly, the scale of the polymerization was gradually increased from 1 g to 18 g of monomer **21c**. The results of this series of polymerizations are summarized in Table 5.4 and Figure 5.5a, both of which show a steady increase of molar mass with polymerization scale. In the case where 18 g of monomer **21c** was used the  $M_w$  reached up to 151 kDa. In the case the molar masses are in fact so high, that aggregates formed which could not easily be dissolved even after extended shaking in chloroform at 35 °C. This aggregation leads to the obvious broadening of signal at low retention volumes. That the broadening is in fact due to aggregates can be seen in Figure 5.5b, were two samples of the purified\* material where prepared for GPC, one in chloroform and one in toluene. In the case of toluene, the aggregates are predominantly dissolved after prolonged shaking at 38 °C.

---

\*For purification procedure see chapter 5.1.5

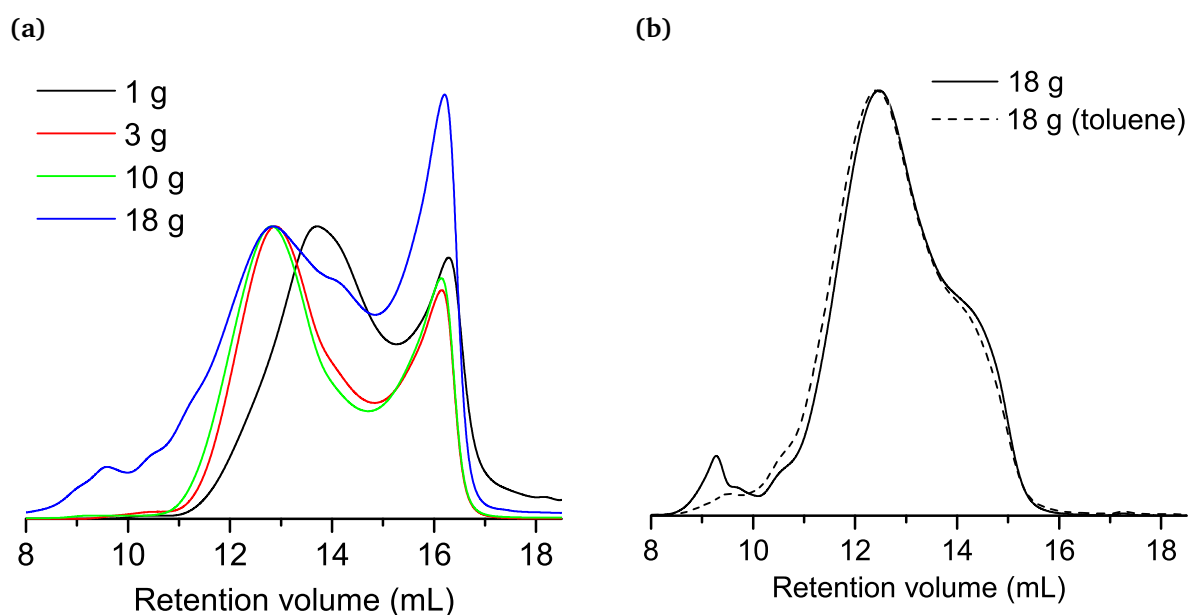


**Figure 5.5.** a) GPC elution curves for polymer **14c** obtained of polymerizations at different scales after macrocycle removal. Note that for the 18 g batch the signals at low retention volume are due aggregates of high molar mass material. They can be partially resolved by prolonged shaking in toluene at 38 °C b).

All in all, these results clearly indicate, that Suzuki polycondensation when prepared under properly optimized conditions is a powerful tool for synthesizing conjugated polymers with high degrees of polymerization on a large scale.

**Table 5.4:** Polymerization results of monomers **21c** and **27** on different reaction scales.

Entry	Amount of <b>21c</b>	$M_n$ [kDa]	$M_w$ [kDa]	Yield [%]	Amount of <b>14c</b> [g]
1	1	6.0	55	85	0.65
2	3	9.3	88	94	2.2
3	10	9.3	101	96	7.3
4	18	8.0	151	99	14.3

### 5.1.5 Removal of Macrocycles

As described in Chapter 2.4 the formation of macro cycles is known as a competing reaction to the growth of linear chains in step growth polymerizations.<sup>[155,156]</sup> Also Suzuki polycondensation is prone to this side reaction when performed with kinked monomers like **21a–d** or **24**.<sup>[113]</sup> More specifically, the formation of such cyclic products is the reason for the observed bimodal molar mass distributions in all GPC elution curves of the previous section. The probability that two chain ends of the same chain meet to form a ring is especially high for low degrees of polymerizations, which is why the cyclic product predominantly occur as oligomers and therefore elute at high retention volumes.

So far the focus has been on increasing the overall molar mass of the polymer **14c**. Therefore, it was necessary to find an efficient and selective purification method in order to separate the low molecular weight macrocycles from the high molecular weight linear polymer. We found that the low molar mass fraction, which contains the macrocycles, is slightly soluble in acetone whereas the high molar mass fraction is completely insoluble in this solvent. Consequently the cyclic oligomers can be extracted by soxhlet extraction using acetone. Figure 5.6a shows the GPC results of the polymerization in Table 5.4 entry 3, before (black curve) and after soxhlet extraction (red curve). Although the better part of the cyclic byproducts could be removed by that procedure, the GPC elution curve (Figure 5.6a, red curve) still shows a small residual low molecular weight signal even after 5 days of extraction. It was, however, possible to further improve this result by fractionating precipitation in acetone (Figure 5.6a, blue curve).

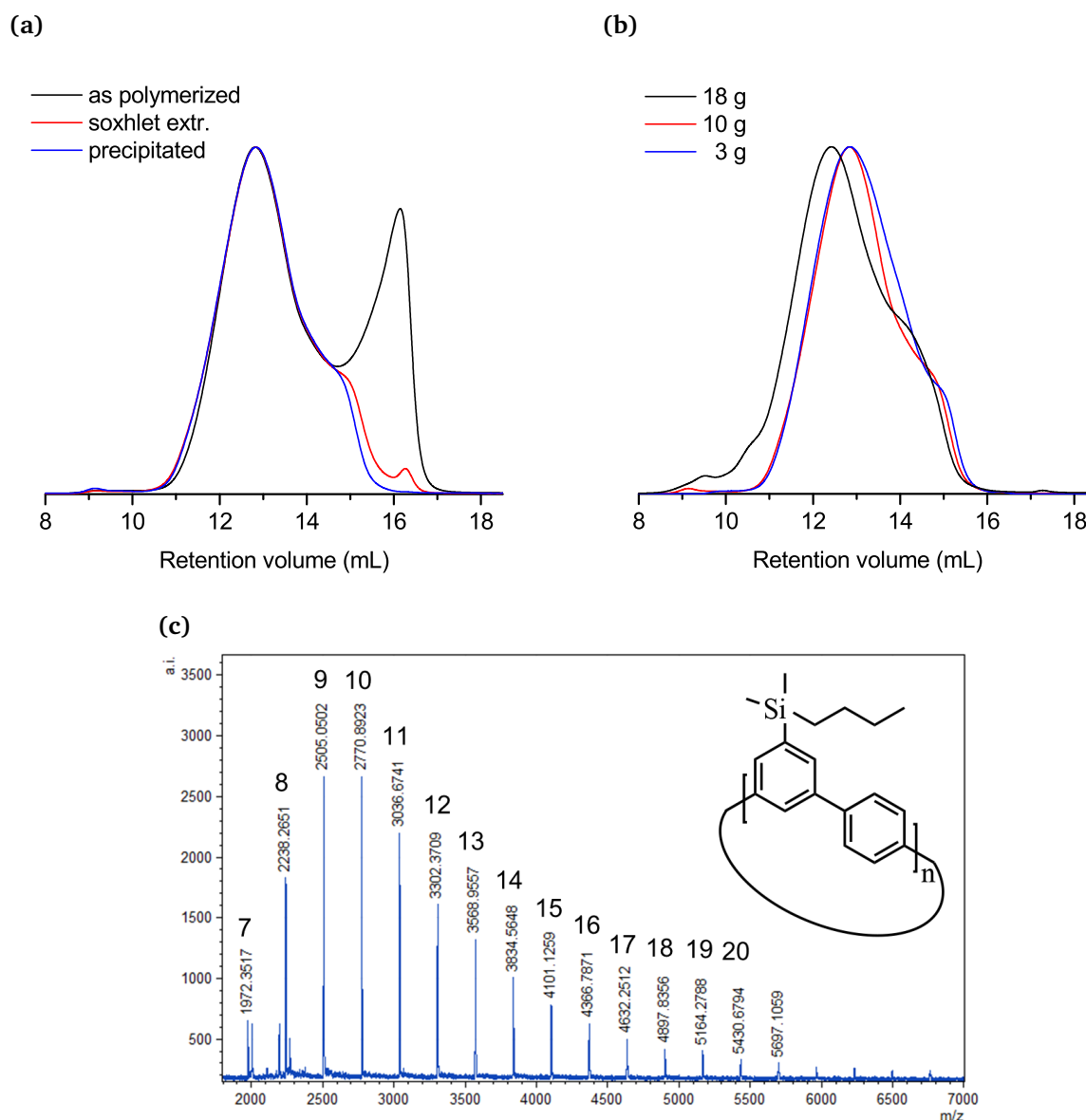


**Figure 5.6.** a) GPC curves of polymers after different purification steps aiming at the removal of cyclic byproducts. b) Polymer **14c** polymerized in different scales, after soxhlet extraction and precipitation. c) MALDI-TOF spectra of the low molecular weight fraction, showing the predominance of cycles.

Figure 5.6c shows the MALDI-TOF spectrum of the extracted low molar mass fraction. The observed signals can be assigned to endgroup free oligomers, which indicates that the extracted fraction contains nearly exclusively cyclic oligomers. Therefore we conclude, that the applied purification selectively targets the undesired macrocyclic byproducts.

The described purification procedure consisting of soxhlet extraction and subsequent precipitation was applied to all batches of polymer **14c** and showed reproducible success. Three representative batches of different polymerization scales are shown in Figure 5.6b

## 5 Polymer synthesis

and Table 5.5. These results illustrate even more clearly than before the increase of molar mass with polymerization scale. Once the undesired macrocycles are removed, the linear polymers reveal their exceptionally high molar masses of up to 304 kDa. However, it should be mentioned that this molecular weight comes on the expense of yield. It was found that the amount of removed cyclic byproduct was always around 30 % of the initial mass.

**Table 5.5:** Polymerization results between monomers **21c** and **27** using different reaction scales before and after purification.

Entry	Amount of <b>21c</b> [g]	$M_n$ [kDa]	$M_w$ [kDa]	Yield [%]	Amount of <b>14c</b> [g]
1	3	9.3	88	94	2.2
1a <sup>α</sup>	3	41	142	-	-
2	10	9.3	101	96	7.3
2a <sup>β</sup>	10	29	142	73	5.6
2b <sup>γ</sup>	10	42	147	53	4.1
3	18	8.0	151	99	14.3
3a <sup>β</sup>	18	25	277	76	10.9
3b <sup>γ</sup>	18	46	304	64	9.2

<sup>α</sup> Several batches were combined and purified by soxhlet extraction and subsequent precipitation into acetone.

<sup>β</sup> After soxhlet extraction with acetone.

<sup>γ</sup> After precipitation into acetone.

### 5.2 Molecular weight determination

All molecular weight values reported above were determined by GPC using conventional calibration with a polystyrene standard. For rigid polymers however using polystyrene calibrations can be misleading because of the significant difference in chain rigidity and therefore the hydrodynamic radii at a given molecular weight.<sup>[170]</sup> In order to confirm the above found molecular weights, static light scattering (SLS) was used as an independent and direct method for the determination of molecular weights. Therefore a fraction of the polymer batch from entry 2b in Table 5.5 was isolated by preparative recycling GPC (Figure 5.7a). This fraction showed a  $M_n$  of 105 kDa and a  $M_w$  of 241 kDa in analytical GPC using conventional polystyrene calibration. Before the actual SLS measurement, the



refractive index increment of the polymer **14c** in chloroform had to be determined in order

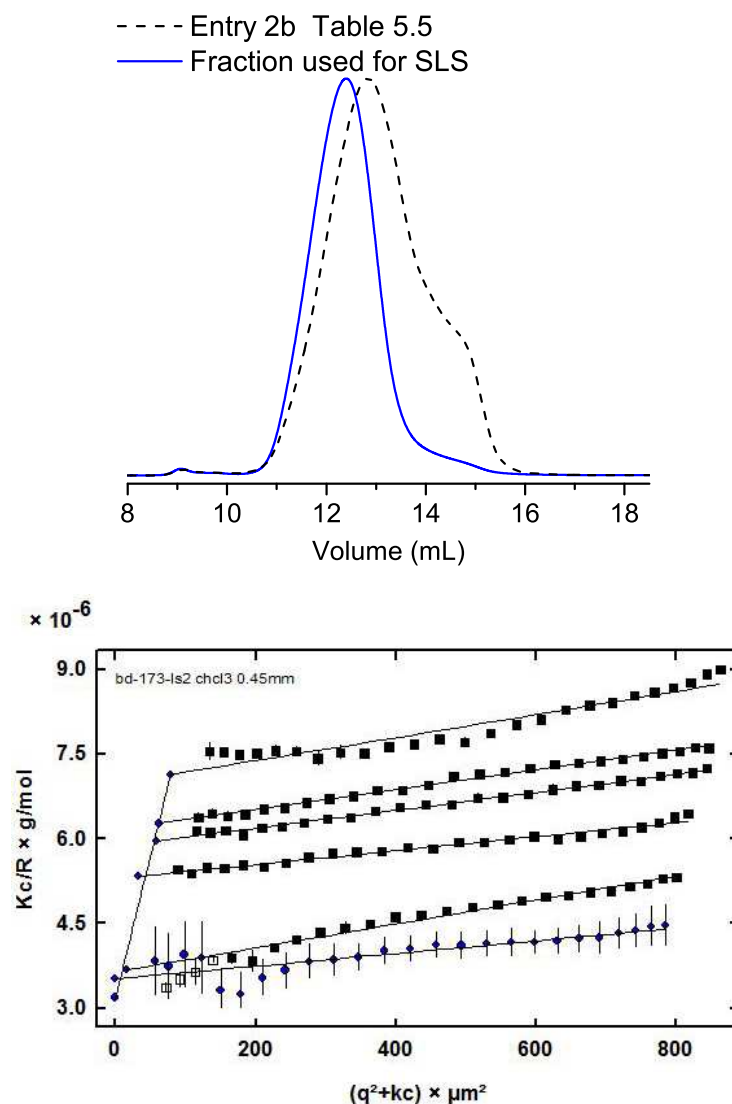


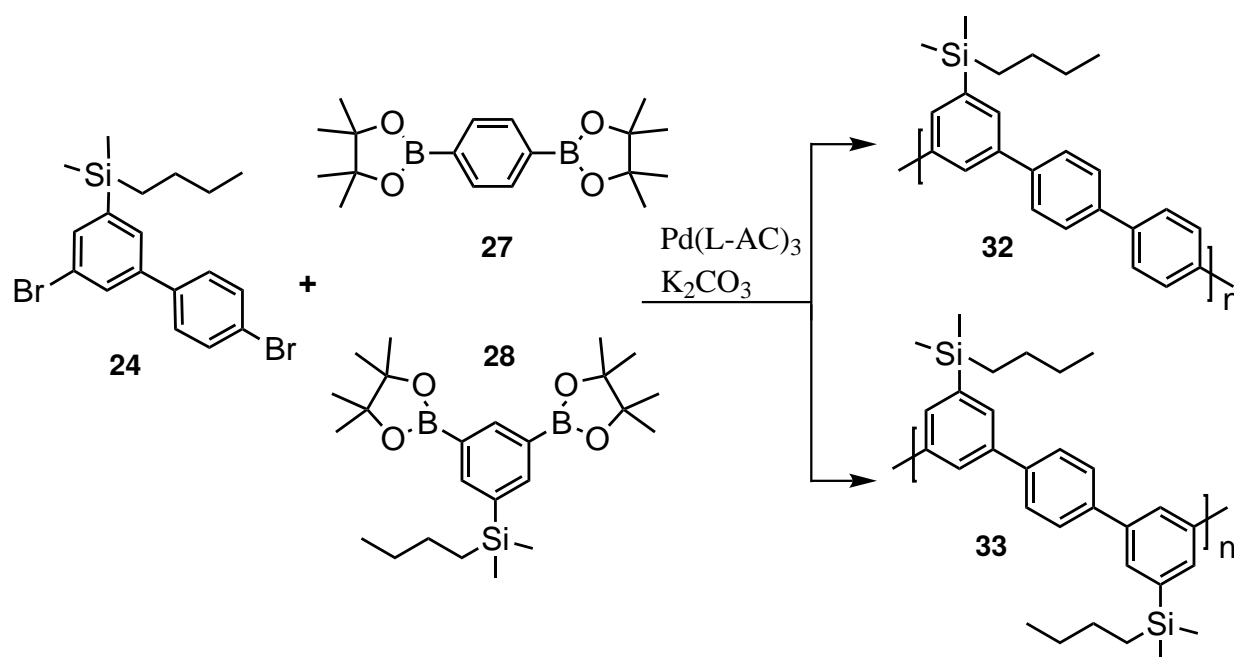
**Figure 5.7.** a) GPC curves of polymer **14c** (entry 2b, Table 5.5; black curve) and the fractionated sample for static light scattering (blue curve). The SLS fraction showed a  $M_w$  of 241 kDa by GPC 241 kDa. b) Zimm plot of polymer **14c** in chloroform. The black squares represent the measured data, while the blue dots are the extrapolated data for  $c = 0$  and  $q = 0$ . The plot suggests a  $M_w$  of 314 kDa.

to calculate the scattering power  $K$ . This was done with a Michelson interferometer at the scattering laser wavelength of 632.8 nm and resulted in a  $\frac{\partial n}{\partial c}$  of 0.1824 ml/g. Finally, static light scattering was used for the generation of a Zimm plot. For that, the average scattering intensity was measured for different scattering vectors  $q$  and concentrations  $c$  (black squares, Figure 5.7b). By linear extrapolation of the resulting data, two lines can be extracted. One at  $q = 0$  and one at  $c = 0$  (blue dots in Figure 5.7b). According to

the Zimm-equation (Equation (1.5)) the molecular weight can be determined from their y-intercept, which is at  $\frac{1}{M_w}$ . Thus a  $M_w$  of 314 kDa was found. Further, the second virial coefficient and the radius of gyration can be calculated ( $A_2 = 7.78 \cdot 10^{-7} \text{ dm}^3 \text{ g}^{-1}$ ,  $R_g = 30.9 \text{ nm}$ ). The positive value of  $A_2$  confirms chloroform as a good solvent for polymer **14c**. These results show that the molecular weights determined by GPC are not overestimated and therefore confirm the outstanding molecular weights for **14c**. Do to the error bars in both methods we however refrain from interpreting the results in the way that the molecular weights obtained from GPC are systematically underestimated. Rather these results imply that hydrodynamic radii for a given molecular weight are similar for polystyrene and polymer **14c**. This can be explained by the *meta* substituted phenylene units within the backbone, which give the polymer a high degree of flexibility.

### 5.3 Polymerization using biphenyl monomers

As a result of the previously achieved high molecular weight products the plan was to broaden the scope of the cleavable side chain approach. Of particular interest was to find out whether the intrinsic problem with cyclic contaminations could be circumvented. In other SPC's this issue was mainly addressed by varying the reaction conditions.<sup>[113]</sup> As indicated above the kinked nature of monomer **21c** is likely an important factor in cycle formation. At the beginning of the growth process of each chain it increases the population of conformations in which the two chain ends are close to one another. Therefore, if the two reactive sites of **21c** could be spaced out by the introduction of a *para*-phenylene unit into the monomer, the propensity of cycle formation ought to decrease. This was realized by the monomer **24** introduced in Chapter 4. By polymerization of this dibromomonomer either with the diboronic acid ester **27** or **28** under the previously found conditions two novel polymers **32** and **33** could be isolated (Scheme 5.2). These two polymers are both composed of terphenylene repeating units and differ in the amounts of kinks within the backbone as well as in the amount of side chains. While polymer **32** contains one *meta*-phenylene group and one side chain per repeating unit, polymer **33** contains two *meta*-phenylene groups and two side chains per repeating unit. The results of the conducted polymerizations are summarized in Table 5.6. They show that also with monomers **24** and **28** the optimized SPC conditions result in molecular weights above 100 kDa.



**Scheme 5.2.** Polymerization of monomer **24** with compounds **27** and **28** using the optimized reaction conditions. The resulting polymers **32** and **33** differ in their amount of kinks within the backbone as well as the amount of side chains.

It therefore confirms, that these conditions reliably deliver high molar mass polymers. The GPC curves of polymers **32** and **33** before Soxhlet extraction are depicted in Figure 5.8 (black solid curves). According to the expectations, they show a significant difference in the amount of formed macrocycles judged by the signal intensity between 15 and 18 mL retention volume. In particular, for polymer **33** the portion of formed low molecular weight byproduct is significantly higher than for polymer **32**. As described above this reflects the number of *meta* substituted phenylene units within the polymers backbone. The lower amount of *meta*-phenylene units in case of **32** as compared to polymer **33**,

**Table 5.6:** Polymerization results between monomers **24**, **27** and **28** using the optimized reaction and purification procedure.

Entry	Polymer	$M_n$ [kDa]	$M_w$ [kDa]	Yield [%]	Amount [g]
1	<b>32</b>	5.8	118	84	1.4
1a <sup>α</sup>	<b>32</b>	50	141	76	1.2
2	<b>33</b>	6.2	56	86	0.9
2a <sup>α</sup>	<b>33</b>	36	103	45	0.5

<sup>α</sup> After soxhlet extraction for 5 days.

drastically decreases the number of conformations for which cycle formation is possible. It should be noted that the concentration was kept constant for all polymerizations at  $35 \text{ mmol l}^{-1}$  regarding the bromo monomers. Therefore the difference in amount of cycles formed is in fact due to the structural differences of the polymer and not due to differences in concentration.

In summary, our findings are in line with earlier findings on cycle formation in classical polycondensations with rigid molecules by Kricheldorf et al.<sup>[161,162]</sup> The rate of macrocycles formation ( $v_{cy}$ ) decreases with increasing chain stiffness. In present case the amount of *meta*-phenylene determines the chain stiffness.

According to the approach described in the previous chapter, the two polymers **32** and **33** were subjected to a soxhlet extraction with acetone for five days in order to remove the formed macrocycles. In Figure 5.8 the GPC curves of the extracted residues (blue curves) as well as of the extracted fractions (black dashed curves) are depicted. In case of polymer **32** (Figure 5.8a) the elution curves suggest that the extraction worked rather selectively concerning the cyclic oligomers. Therefore it was possible to determine the mass fraction of cyclic oligomers to around 10%. In case of polymer **33** (Figure 5.8a) there is a strong overlap between the elution curves of the extracted fraction and the residue. This suggests that the linear polymers also exhibit slight solubility in acetone and therefore

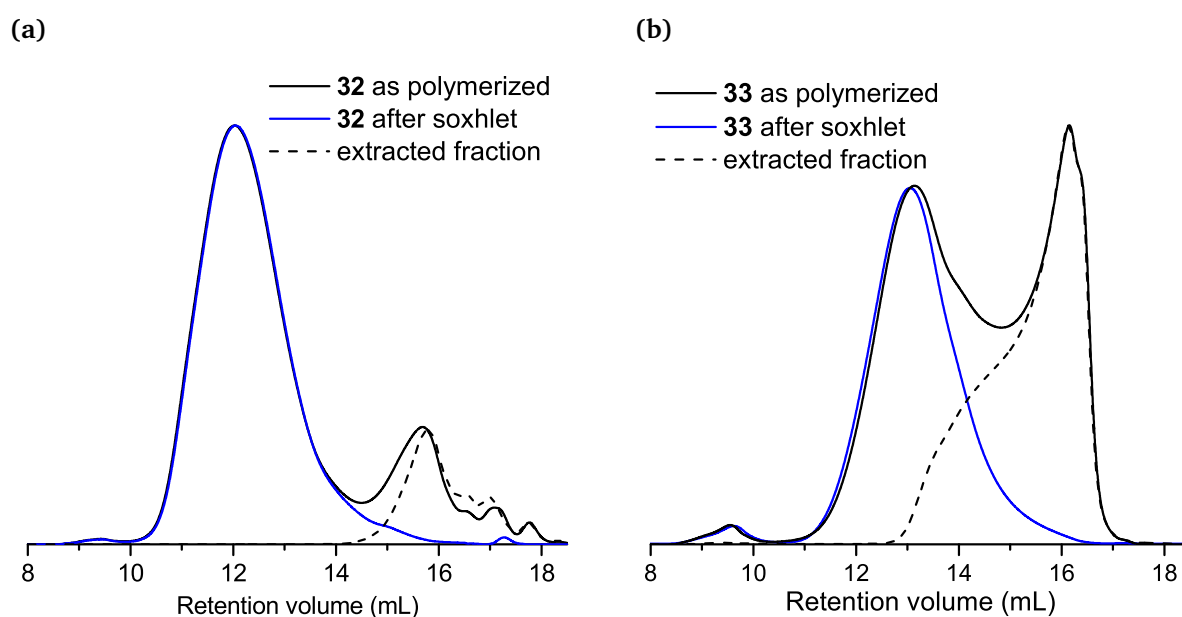


**Figure 5.8.** GPC elution curves of polymers **32** a) and **33** b). The black solid curves refer to the polymers as obtained after polymerization. The black dashed curves refers the soxhlet extracted fraction and the blue curves to the purified material.

get partially extracted along with the macrocycles. This different behavior of polymer **32** and **33** during extraction could be corroborated by MALDI-TOF analysis. The spectra of the extracted fractions for both polymers are shown in Figure 5.9 and Figure 5.10. They reveal that the extracted fraction from polymer **32** (Figure 5.9) shows nearly exclusively cyclic oligomers. The extracted fraction of polymer **33** (Figure 5.10) in contrast contains significant amounts of ligand capped linear chains. Obviously the increased frequency of *meta*-phenylene units and side chains in polymer **33** compared to polymer **32** improve the solubility of the linear polymer **33** in acetone. Therefore, assigning the extracted fraction of 47 wt.% to cyclic oligomers has to be considered an overestimation in the case of polymer **33**.

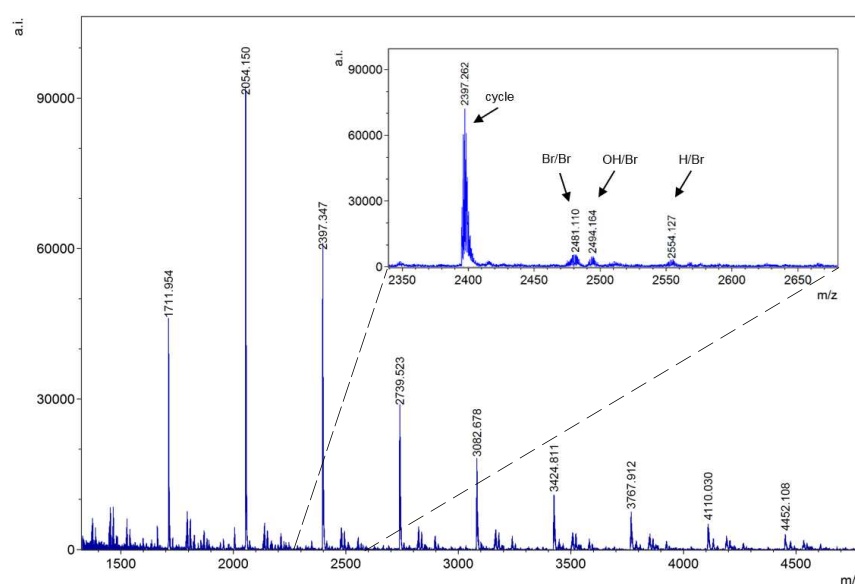


**Figure 5.9.** MALDI-TOF spectra of extracted fraction of polymer **32**. The appearing signals predominantly correspond to cyclic oligomers.

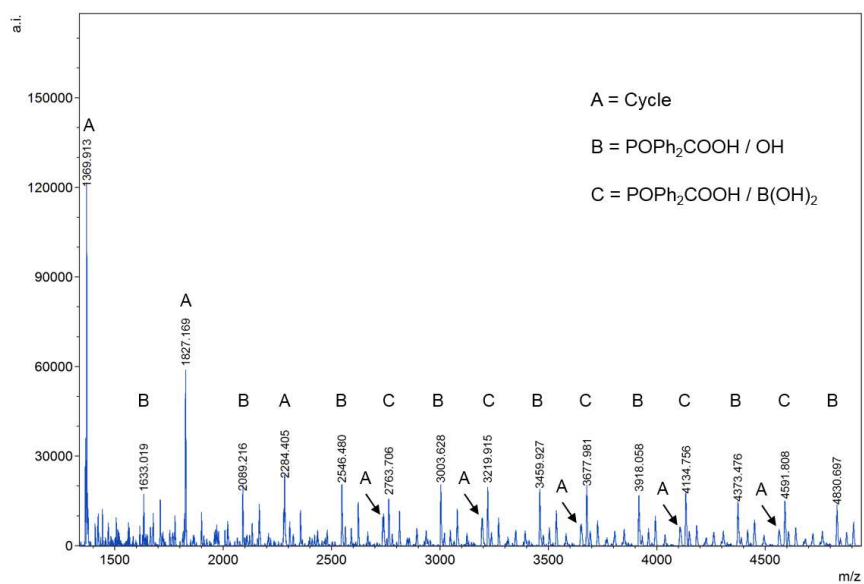


**Figure 5.10.** MALDI-TOF spectra of extracted fraction of polymer **33**. The spectra contains considerable amounts of ligand capped low molecular weight linear polymer.

## 6 Properties of polymers carrying solubilizing side chains

In order to evaluate the potential of the above described polymers in terms of applications and processing, the knowledge of some basic physical parameters is indispensable. For that purpose the synthesized polymers were investigated, concerning their glass transition temperature ( $T_g$ ), melting point ( $T_m$ ), thermal stability, crystallinity and mechanical properties. Differential scanning calorimetry (DSC) is a common method for the investigation of phase transitions and was therefore the method of choice. The results allowed for conclusions concerning  $T_g$ ,  $T_m$  and the crystallization behavior of the polymers. In addition TGA was used in order to draw conclusions about the thermal stability of the material. Of special interest was whether the polymers could be processed above the found  $T_g$  or if they would already start to degrade below that. Due to time constraints and the fact that we had the most material of polymer **14c** most of the experiments were conducted only with this polymer.

In addition it was also shown that polymer **14c** can be processed in to films by solution casting. With a tensile tester these films were then investigated concerning their tensile modulus, tensile strength and toughness.

### 6.1 Glass transition, melting point and crystallinity

During the optimization of the synthesis of polymer **14c** several batches of different molecular weights were obtained. As can be learned from Table 5.5 the purified polymers spread over a molecular weight range from 142 kDa to 304 kDa. As it is known that phase transition temperatures of polymers are dependent on molecular weight,<sup>[49]</sup> it was of interest to which degree the phase transition behavior changes over the molar mass range of the available samples. For that reason the two extreme cases,  $M_w = 142$  kDa at the lower end and  $M_w = 304$  kDa at the upper end were subjected to DSC after precipitation from chloroform in methanol. The resulting thermograms are displayed in Figure 6.1. They show a glass transition temperature between 175 °C and 180 °C for both samples. Although the onset of the softening might be a little earlier for the 142 kDa sample, the differences are only minor. This suggests that among the available samples, the dependence of  $T_g$  on the molecular weight is negligible.

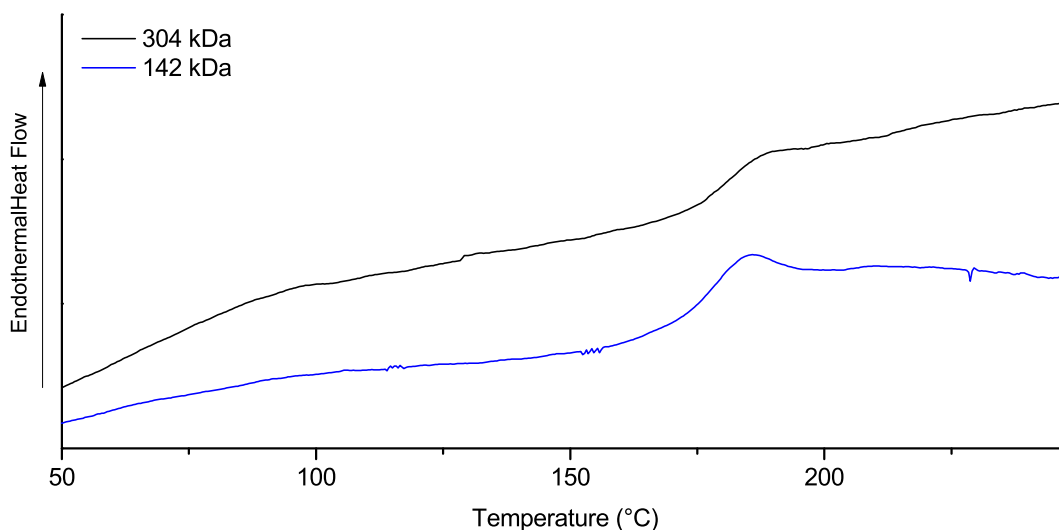


**Figure 6.1.** Thermograms of polymers **14c** of different molecular weights after purification. The data show no significant difference in  $T_g$ .

Aside from the molar mass, it is known that the properties of polymers are also depend on their processing history.<sup>[171,172]</sup> As mentioned the above described samples were prepared by precipitation from chloroform solution. This method leads to an immediate solidification, which could hinder the formation of larger ordered domains within the polymer and thus influence its phase transition behavior. In order to gain insight into this matter, new samples of polymer **14c** were prepared. For that purpose a chloroform and a toluene solution of polymer **14c** were made. Out of each solution one sample was prepared by precipitation in methanol and one by slow evaporation of the solvents at room temperature (rt) in covered petri dishes. Thus overall four samples were obtained two by precipitation from chloroform and toluene and two as  $\approx 0.1$  mm thick films by slow evaporation from the same solvents. All four samples were finally subjected to DSC and the results are shown in Figure 6.2. Interestingly, the four curves exhibited marked differences. In the case of the two precipitated samples, no melting point and a  $T_g$  of around 180 °C was observed. It is therefore concluded that in the tested cases (chloroform and toluene), the solvent influence on precipitated samples is negligible concerning the softening and melting behavior.



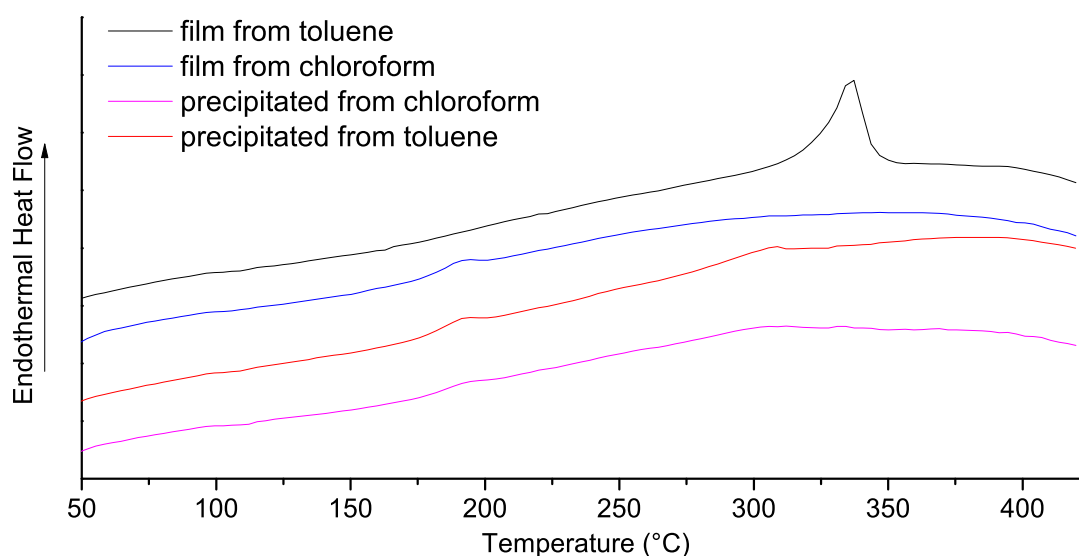


**Figure 6.2.** DSC in nitrogen atmosphere of **14c** solidified under different conditions.

The two films generated by slow evaporation behave as follows: The chloroform film again exhibits no melting point and a  $T_g$  at around 180 °C and thus behaves similar to the above described precipitated samples. In contrast, the toluene film has no observable  $T_g$ , but rather exhibits a distinct melting point at 335 °C. These data indicate that depending on the solvent the crystallinity of the film can vary considerably.

Aside from the DSC results the different crystallinity also affects the turbidity of the two studied films. While the film generated by chloroform evaporation is basically transparent, the film obtained from toluene shows significant cloudiness, which is typical for semicrystalline polymers (Figures 6.3a and 6.3b). Another common method for investigating the crystallinity of polymers is X-ray diffraction (XRD).<sup>[173]</sup> Therefore the aforementioned films were subjected to this method. The resulting XRD pattern for the chloroform and the toluene film are shown in Figures 6.3c and 6.3d respectively. For the toluene film the XRD pattern shows more and sharper rings as compared to the chloroform film, whose XRD pattern predominantly appears as one broad halo. This indicates that in the toluene film there is an increased degree of order, which supports the existence of crystalline domains. These results are in agreement with the DSC, which only shows melting and therefore crystalline domains for the toluene film.

The investigation of the morphology and how it can be tuned is a common approach when characterizing polymers.<sup>[174,175]</sup> Also polyphenylenes were partially covered by such studies.<sup>[176]</sup>

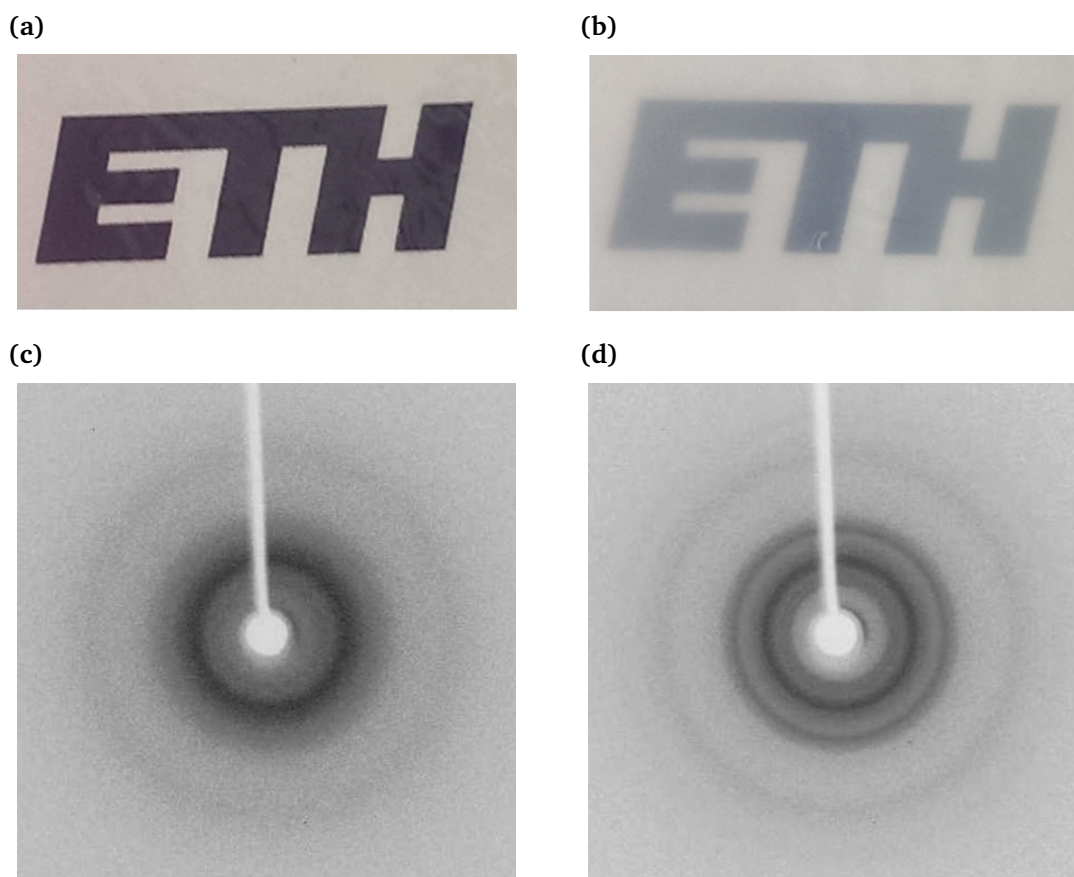


**Figure 6.3.** Photographs of films from polymer **14c** on the ETH logo. a) solution cast from chloroform and b) solution cast from toluene. They show a significant difference in turbidity. XRD patterns of solution casted films from chloroform c) and toluene d) confirming the higher crystallinity of the toluene film.

It is therefore commonly understood that the morphology of polymers can be tuned by different solvents and solidification rates. With this in mind the above found results led to the following conclusions concerning the different behavior of the toluene film. Either the slower evaporation of toluene compared to chloroform leads to the formation of the observed crystallinity, or rather the chemical difference between chloroform or toluene causes the observed difference. In order to investigate to which degree the difference in evaporation rate of the solvent plays a role in this regard, additional polymer films were prepared. This time the evaporation rate was varied for chloroform as well as for toluene by casting films at different temperatures. By DSC and XRD measurements it should thus be possible to gain insight into the dependence of crystallization on evaporation rate. First two chloroform were prepared by solution casting at 7 °C and 50 °C. The resulting film cast at 7 °C shows a slight cloudiness, whereas the 50 °C cast film is highly transparent (Figures 6.4a and 6.4b). This visual difference indicates a variation in crystallinity.

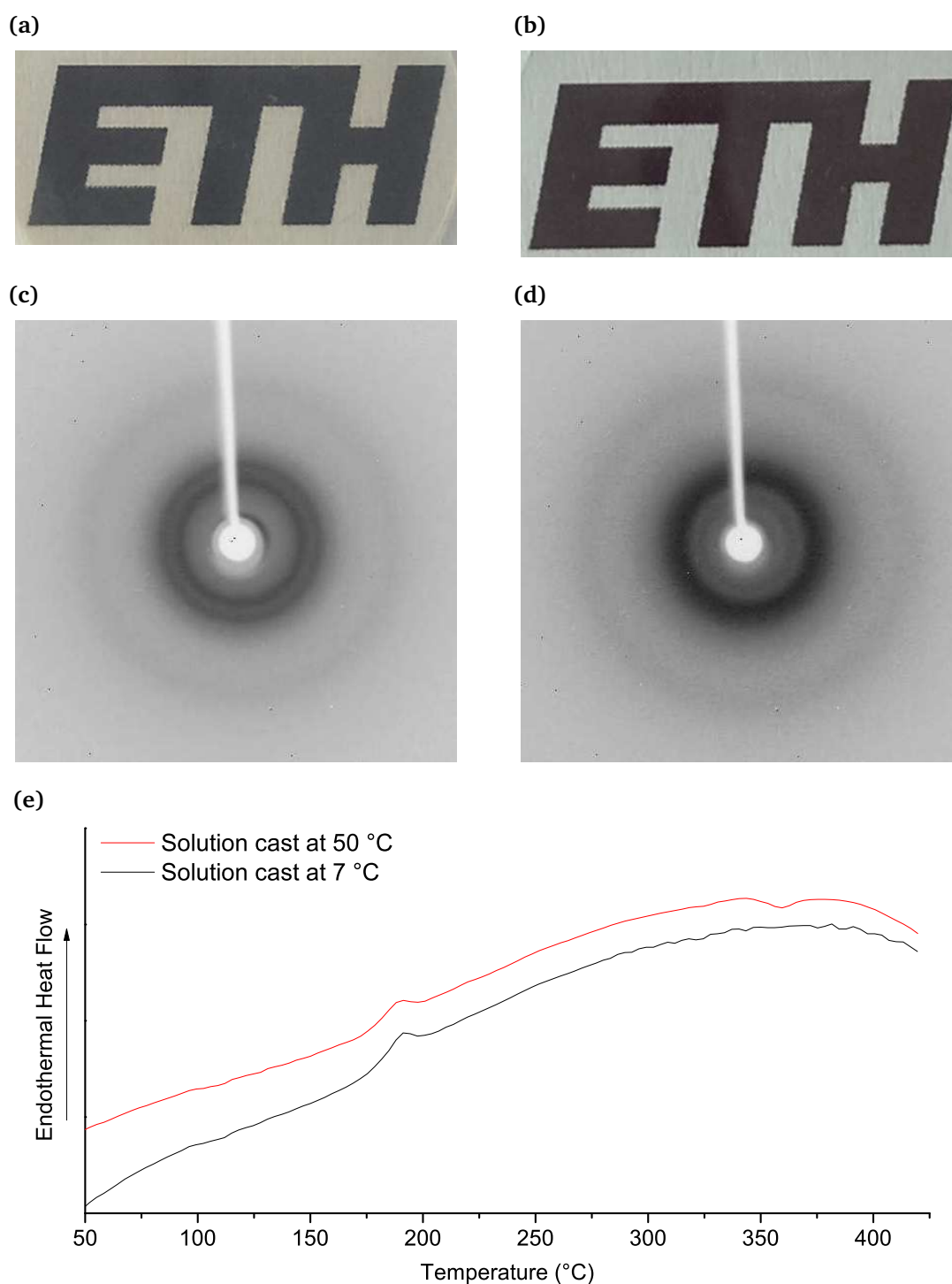


**Figure 6.4.** Photographs of films from polymer **14c** on the ETH logo cast from chloroform at 7 °C a) and 50 °C b). A slight increased turbidity for the former can be observed. XRD patterns of the same films from chloroform at 7 °C c) and 50 °C d) confirming the increased crystallinity due to slower evaporation at the lower temperature. The DSC curves of both samples e) do not show a distinct melting point, which is probably due to a still very low degree of crystallinity.

Consequently, the two films were subjected to XRD. The resulting diffraction patterns are shown in Figure 6.4c for the 7 °C cast film and in Figure 6.4d for the 50 °C cast film. The XRD pattern of the former exhibits more distinct reflections, while the latter is dominated by one broad signal. These results corroborate the visual impression and suggest an increase in crystallinity upon slow evaporation of chloroform. It should, however, be noted that the differences between the two samples in Figure 6.4 are less pronounced compared to the differences between the chloroform and toluene film in Figure 6.3. Further, the DSC results of both films still show a distinct  $T_g$  and no observable melting point (Figure 6.4e). It is therefore assumed, that the crystallinity even in the case of the chloroform film cast at 7 °C is still very low. To conclude this investigation, two further films were prepared. This time from toluene solution cast at room temperature and at 80 °C. Both films showed a cloudy appearance and were visually practically identical. These films were subjected to DSC measurements and the resulting thermograms are displayed in Figure 6.5. They indicate that the casting temperature did not have a significant influence on the crystallinity of these films. In both cases a distinct melting point is observed whereas glass transitions are absent.

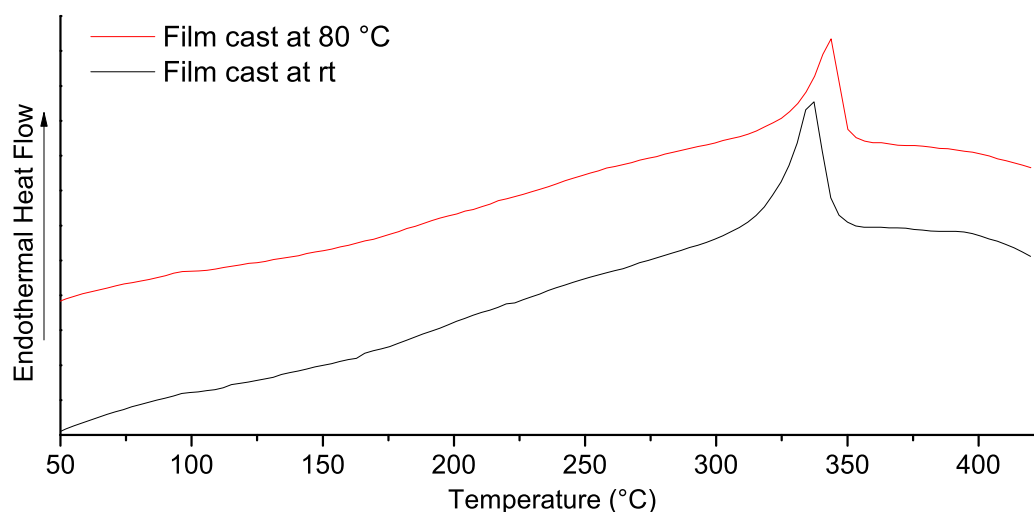


**Figure 6.5.** Thermograms of films of polymer **14c** prepared by solution casting from toluene solution at rt and at 80 °C. Both samples melt between 320 and 350 °C.

All in all, these results suggest that for polymer **14c** the nature of the solvent has a significant influence on the polymers morphology. Although the rate at which the polymer solidifies might also have a minor impact, such influence is only observed for the extreme

case, which is the immediate solidification by precipitation.

### 6.1.1 Aging

Finally, it was of interest whether over time an aging process occurs in which the predominantly amorphous films start to build up crystalline domains. Therefore, the previously used film which was solution cast from chloroform at 7 °C was studied by DSC after one week, five weeks and nine weeks of storage at rt. The resulting data (Figure 6.6) show that there is no change of the film within the observed time frame and sensitivity of DSC. Considering the high glass transition temperature and the low chain mobility at rt this reflects, this finding is not surprising.

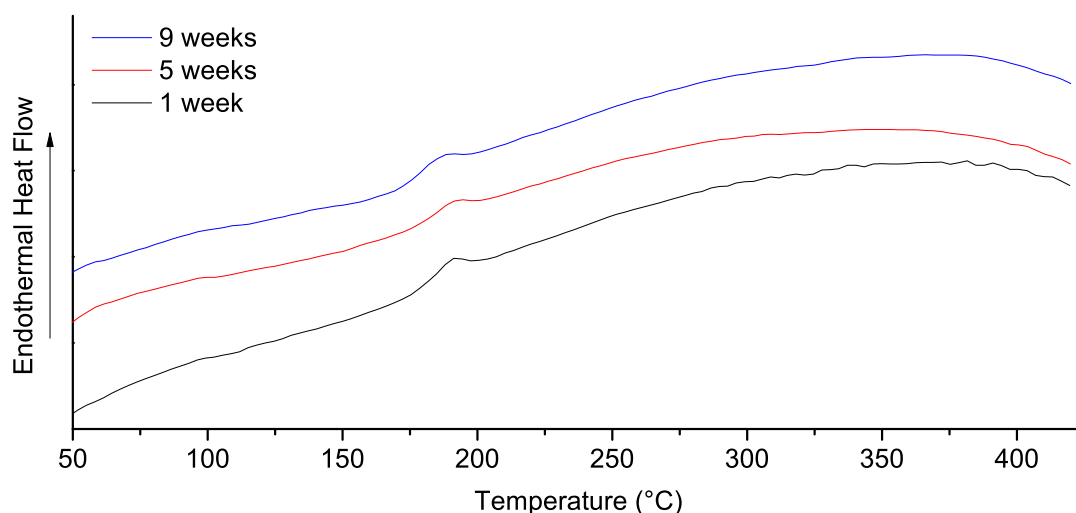


**Figure 6.6.** DSC curves of polymer **14c** cast at 7 °C and stored at rt for several weeks show no significant change in the observed time frame.

### 6.1.2 Glass transition and chain flexibility

In Chapter 5 we reported the synthesis of polyphenylenes **14c**, **32** and **33** with different rigidities due to a variation of the amount of kinks within the backbone. It is known that chain rigidity has an important influence on the thermal parameters of polymers like the  $T_g$  and melting point.<sup>[177]</sup> In our case, we focused on the investigation of the glass transition temperature, because the melting point for **32** lies beyond its degradation temperature. The polymers were subjected to DSC after precipitation from chloroform. The resulting thermograms of the three polymers **14c**, **32** and **33** are shown in Figure 6.7. They show

that the  $T_g$  rises from 125 °C over 180 °C to 250 °C with decreasing amount of kinks in the backbone. Therefore the density of *meta* substituted repeat units is a useful parameter in order to tune the  $T_g$  according to a desired application.

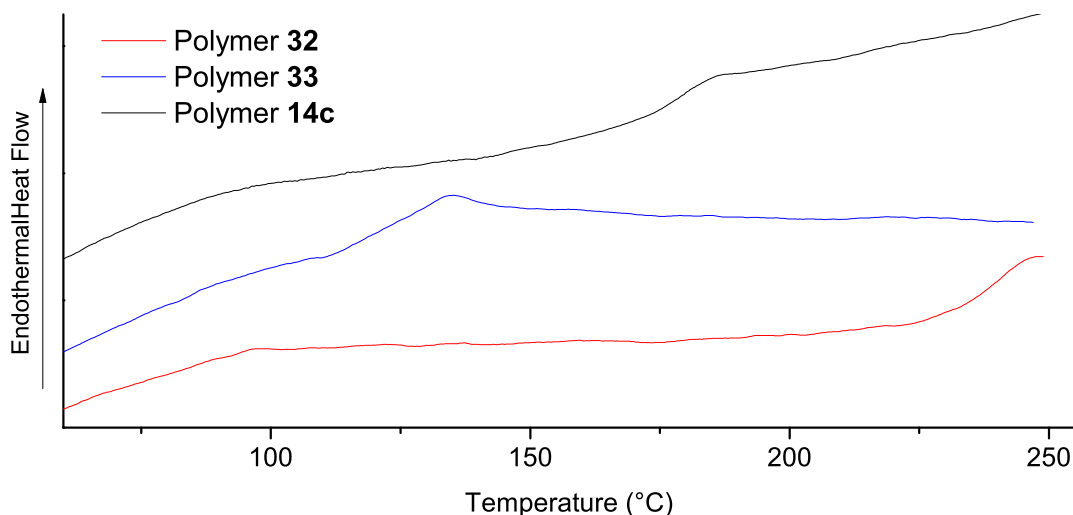


**Figure 6.7.** DSC thermograms of polymers **14c**, **32** and **33** showing an increasing glass transition with increasing chain stiffness.

### 6.2 Thermal stability

Thermal stability of polymers naturally is an important parameter for the choice of a polymer for a specific application. Thermogravimetric analysis (TGA) determines thermal stability by recording the mass loss of a compound upon heating. In order to get an insight in to the thermal stability of polymer **14c** TGA was performed in an air as well as in an nitrogen atmosphere. The resulting curves are shown in Figure 6.8. The black curve represents the polymer **14c** heated in a nitrogen atmosphere. The red curve represents polymer **14c** heated in the presence of air. The results imply that under nitrogen atmosphere the thermal degradation of the polymer starts at 425 °C. Upon further heating the decomposition continues to a total mass loss of 33.8 %. In the presence of oxygen the degradation already sets in at 300 °C and proceeds up to a mass loss of 78.7 %. Considering the structure of **14c**, in the presence of oxygen full oxidation of the material is expected, which would result in  $\text{SiO}_2$  as the only non-volatile residue. Therefore the expected mass loss is 77.6 %, which is in good agreement with the measured result, especially considering the accuracy of TGA, which lies in the range of  $\pm 3$  %.<sup>[178]</sup>

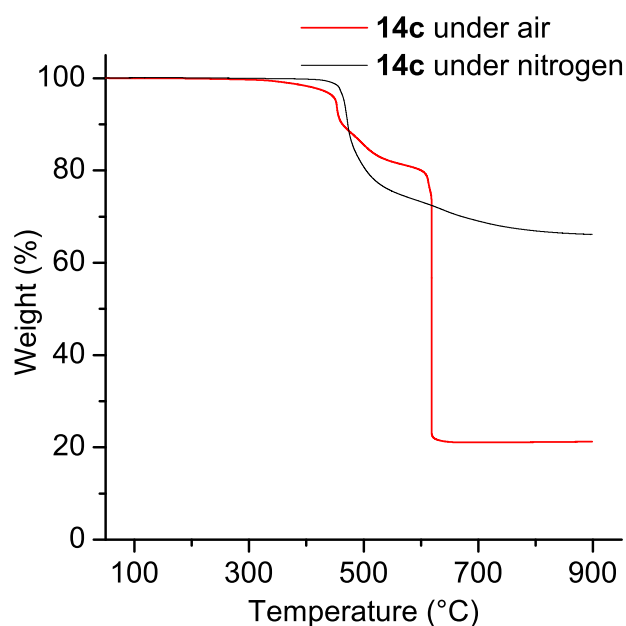


**Figure 6.8.** Thermogravimetric analysis data of polymer **14c** measured in a nitrogen atmosphere (black curve) and in air (red curve).

### 6.3 Mechanical properties

Above it was described that the polymers show the tendency to form films upon solution casting. As it was already reported that similar materials show very promising mechanical properties,<sup>[120]</sup> the films from the above reported polymers were also investigated concerning their mechanical properties. Exemplarily the results of polymer **14c** are presented here. The investigations concerning glass transition, melting point and crystallinity (Chapter 6.1) showed that there is an influence of the solvent from which the film is solution casted. Consequently, it was investigated if the found differences also reflect in the tensile behavior.

#### 6.3.1 Tensile behavior of films processed from toluene

As described above, the films of polymer **14c** from toluene showed a significant turbidity and no  $T_g$  in the DSC measurements. These findings also reflect in the tensile stress resistance at different temperatures. In Figure 6.9 the tensile stress curves of polymer films of **14c** at different temperatures as well as the development of the mechanical parameters with temperature are shown. Although it can be observed that with increasing temperature the yield strength decreases,

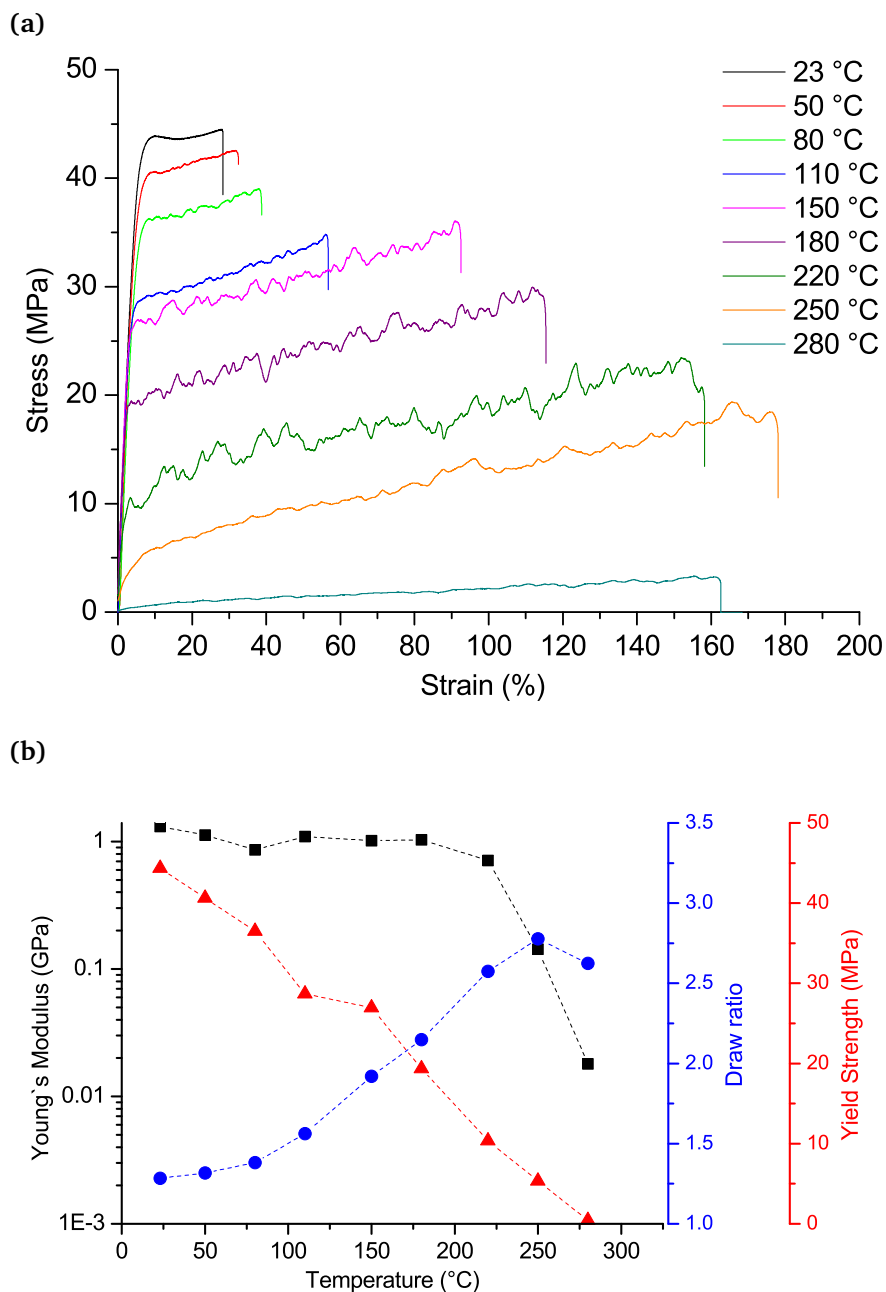


**Figure 6.9.** a) Stress-Strain behavior at different temperatures of poly(*m,p*-phenylene)films processed from toluene. b) Young's modulus, yield strength and maximum draw ratio as a function of temperature.

the Young's modulus stays more or less constant up to 250 °C. While this might be an interesting feature for high temperature applications, the polymer does not show an extended plasticity at any temperature below degradation under ambient conditions. This could become an issue if one wants to apply mold processing techniques.



## 6.3.2 Tensile behavior of films processed from chloroform

Like in the DSC and X-Ray studies above also concerning the stress-strain behavior the films of polymer **14c** processed from chloroform showed different results as compared to the toluene film. The tensile stress curves and the extracted parameters from a film cast from chloroform at rt are shown in Figure 6.10. They represent a brittle (glassy) behavior for temperatures below  $T_g$ , with similar moduli and strengths than the above tested toluene film. As soon as the glass transition is reached however, the material's behavior changes drastically.

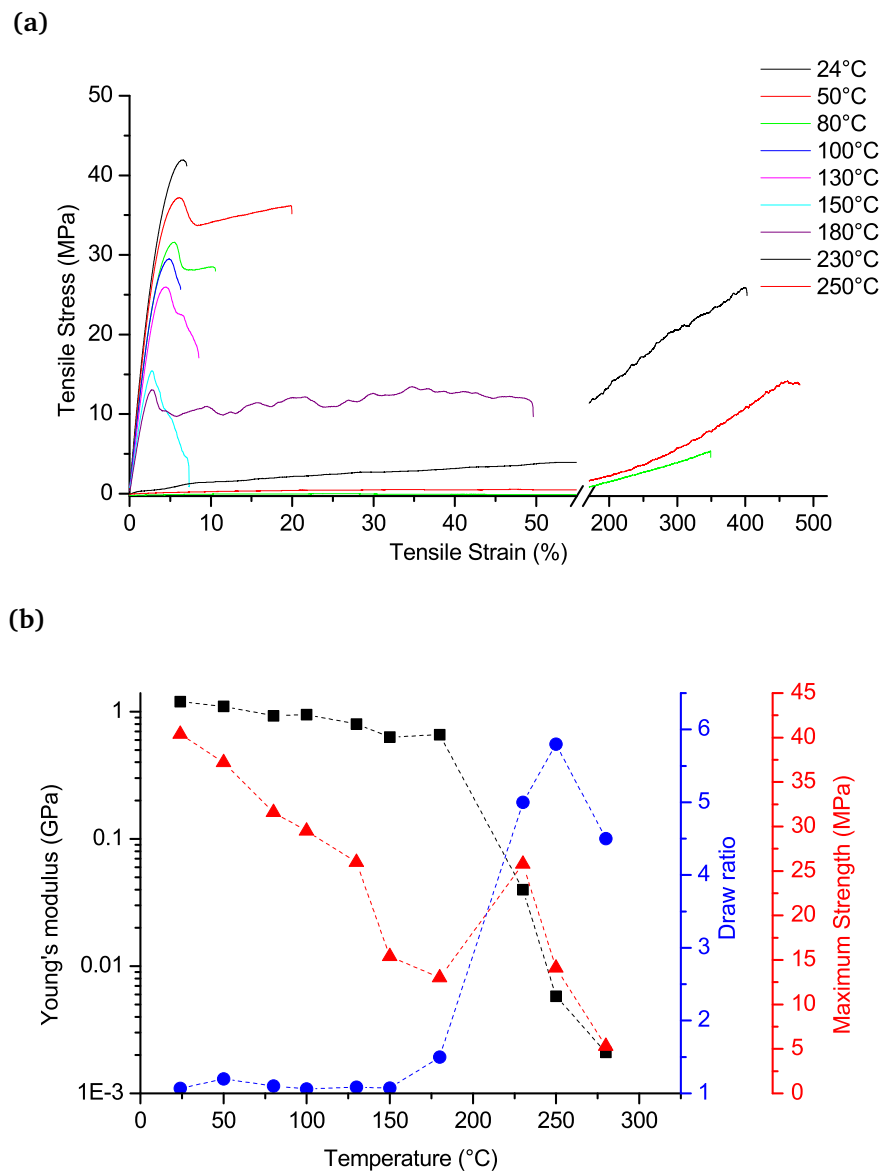


**Figure 6.10.** a) Stress-Strain behavior at different temperatures of poly(*m,p*-phenylene) films solution cast from chloroform. b) Young's modulus, yield strength and maximum draw ratio as a function of temperature.

The Young's modulus drops by three orders of magnitude and the maximum draw ratio raises significantly up to a value of 6. Further, it should be noted that above  $T_g$  no yield points are observed. Therefore, the maximum strengths in these cases occur at the material's point of failure.

### 6.3.3 Crystallization of elongated samples

In polymer fiber production, the elongation of polymer threads is a common method for increasing the strength of polymeric materials.<sup>[179]</sup> Therefore the extended ductility for the films prepared from chloroform above their glass transition temperature, was of great interest for improving their mechanical strength by orienting the polymer chains along a drawing direction. By stretching dog bone shaped samples of polymer **14c** at 220 °C and subsequent cooling to rt elongated threads of different draw ratios (1.5, 3 and 6) were prepared. These elongated samples were then subjected to XRD and DSC measurements before investigating their mechanical properties. The diffraction patterns in Figure 6.12 show that with increasing draw ratio, the amount of reflexes increases. Further, the width of the reflexes decreases, which indicates that the order within the elongated samples increases. In Figure 6.12d the decrease of the width of the meridional reflex is shown in dependence of the draw ratio. By stretching the samples crystallization of the polymer chains is induced. This crystal formation can again also be observed in DSC. The resulting curves in Figure 6.11 show a clear increase of the melting peak between 320 °C and 330 °C while the glass transition at 180 °C continuously vanishes.

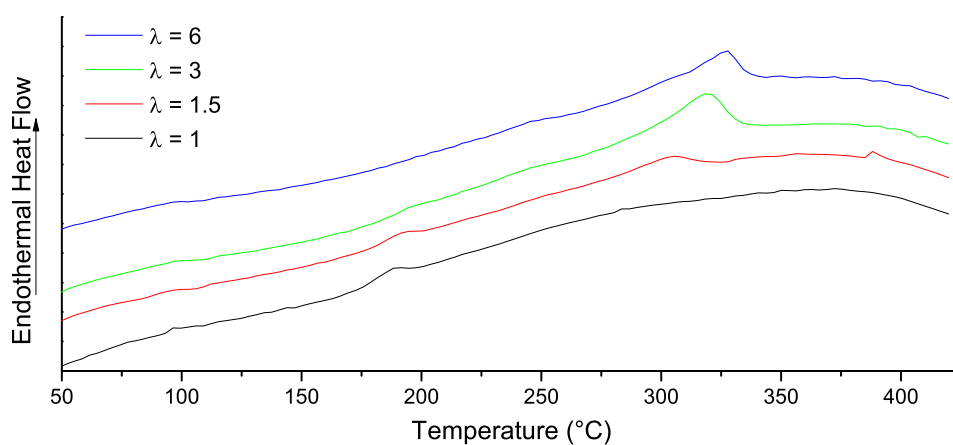


**Figure 6.11.** DSC curves of elongated samples of polymer **14c** at different draw ratios. The vanishing of the glass transition and the increase of the melting peak indicate an increase of crystallinity.

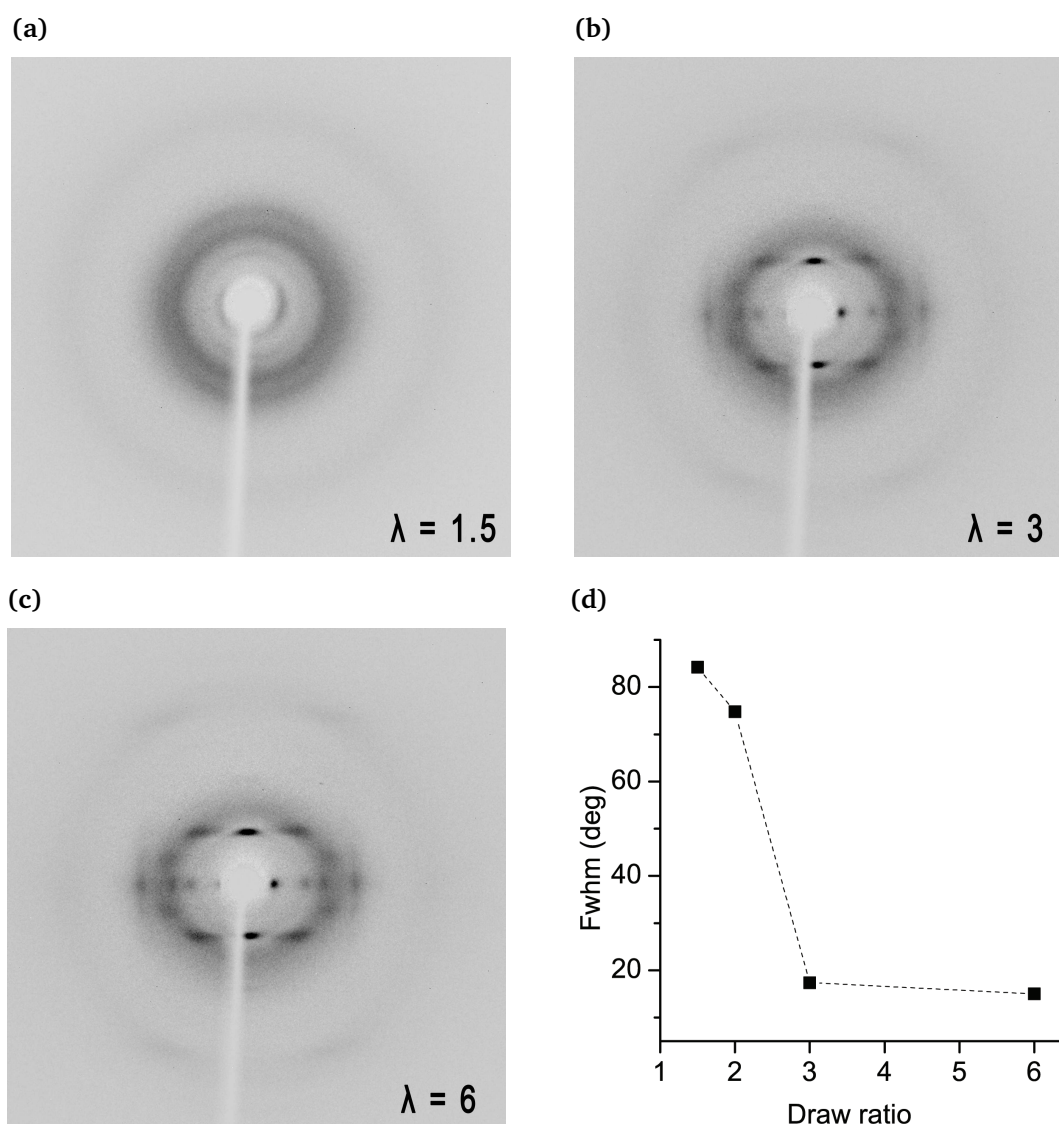


**Figure 6.12.** X-ray diffraction patterns of elongated films drawn at 220 °C to a draw ratio of  $\lambda = 1.5$  a),  $\lambda = 3$  b) and  $\lambda = 6$  c). d) Decrease of the meridional reflex with increasing draw ratio.

#### 6.3.4 Tensile behavior of elongated samples

The elongated samples were subsequently tested for their tensile behavior in the direction of elongation. The results presented in Figure 6.13 and Table 6.1 show that the alignment of the polymer chains leads to an increase of the Young's modulus as well as the tensile strength. This effect is known and commercially exploited for example in ultra high molecular weight polyethylene fibers.<sup>[180]</sup> With this in mind our findings show the great potential of polymer **14c** in the production for high performance materials. Because of their thermal stability and their high  $T_g$  they might be especially interesting for applica-

tions at elevated temperatures.

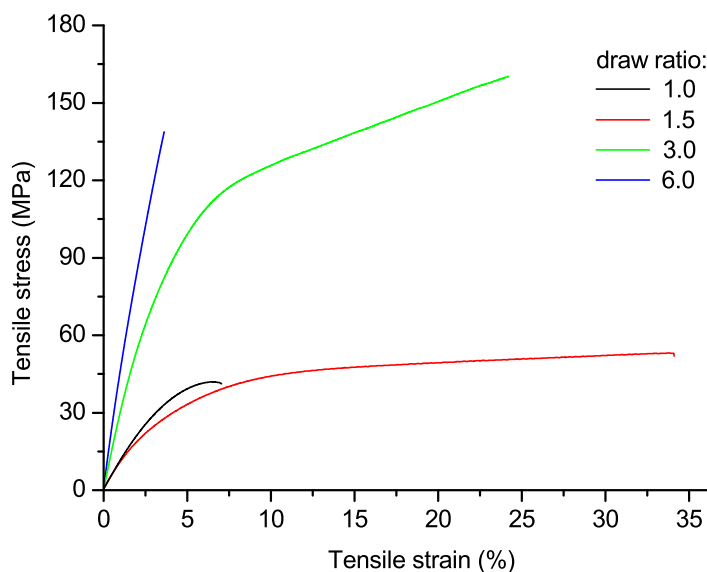


**Figure 6.13.** Tensile behavior of elongated threads of polymer **14c** at room temperature. With increasing orientation due to the drawing, the strength and stiffness of the samples increases.

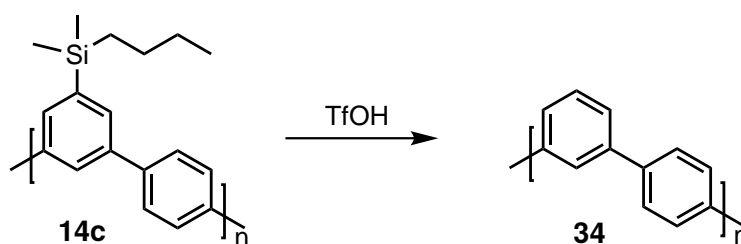
All samples tested in this chapter still bear the acid cleavable silyl side chains. As mentioned above, it has already been shown for other rigid polymers, that solubilizing side chains have a negative effect on their mechanical properties.<sup>[64,101]</sup> Therefore it is expected that the reported mechanical properties can be improved by their removal. Consequently, in the following chapter the side chain cleaving behavior upon acid treatment will be studied.

**Table 6.1:** Results of tensile stress tests for films of polymer **14c** processed from chloroform and hot drawn to different draw ratios.

Draw ratio	E [GPa]	$\sigma$ [MPa]	$\epsilon$ [%]
1.0	1.1	42	7
1.5	1.2	52	34
3.0	3.2	160	24
6.0	5.0	140	3.6

## 7 Removal of solubilizing side chains from bulk polymer

One of the goals of this project was to produce polymeric materials consisting exclusively of aromatic units made of carbon and hydrogen. After the complete synthesis and structural analysis of the polymers the attention consequently turned towards the removal of the solubilizing silyl side chains. Therefore, first the progress of the side chain cleavage of polymer **14c** towards polymer **34** was investigated (Scheme 7.1). Later in this chapter this approach will be extended towards polymer **32** and **33**.



**Scheme 7.1.** Side chain removal from polymer **14c** resulting in the parent polyphenylene.

It has been reported that the side chain removal works quantitatively for polymer **14a** by addition of trifluoromethanesulfonic acid (TfOH) to a toluene solution of the polymer.<sup>[107]</sup> Unfortunately, the resulting side chain free polymer precipitates as an insoluble and infusible powder which cannot be processed. Therefore, it was of interest to conduct the side chain cleavage from the bulk material (Scheme 7.1) after the processing of the polymer. In order to investigate whether this is a feasible approach, films from polymer **14c** of different thicknesses have been produced by solution casting from chloroform and subsequent hot compression moulding above  $T_g$ . A typical film of 0.1 mm thickness is shown in Figure 7.1. Subsequently, the polymer films of different thicknesses were exposed to TfOH and analyzed concerning the cleaving progress. For comparison, a cleaving experiment in solution, as described above, was also carried out. For that, polymer **14c** was dissolved in boiling toluene and then exposed to TfOH, which resulted in a brownish precipitate. Both experiments (cleaving from film and in solution) relied on the same analytical methods which were TGA after exhaustive oxidation of all Si content into  $\text{SiO}_2$ , IR-spectroscopy, and  $^{13}\text{C}$ -CP/MAS NMR spectroscopy. While the latter two methods are common practice, TGA had to be validated first. For this purpose, the starting polymer **14c** was subjected to TGA with full access to air.

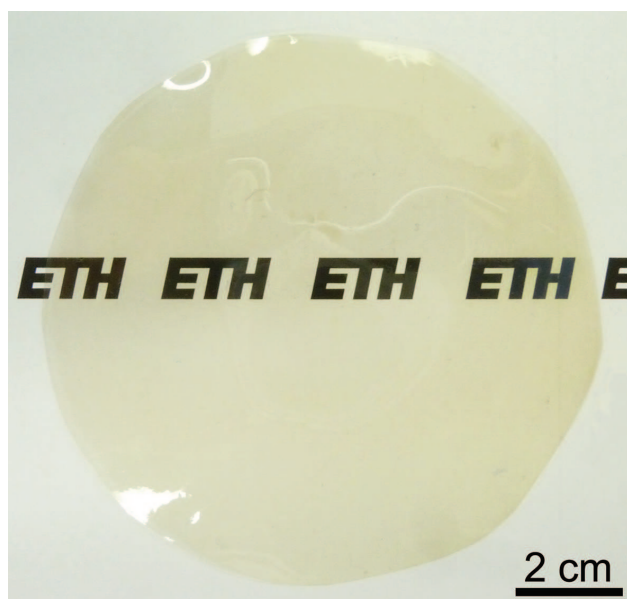


**Figure 7.1.** 0.1 mm thick film of polymer **14c**, solution cast from chloroform and hot compression moulded at 220 °C.

Assuming full oxidation of all Si-content to  $\text{SiO}_2$  takes place, the atomic ratio Si/C/H in polymer **14c** would suggest a residual mass of 22.5% solely due to  $\text{SiO}_2$ . The experimentally observed value was 21.3% (Figure 7.2a, black curve), which, taking into account the accuracy of TGA,<sup>[178]</sup> was considered good enough to apply the method. Additionally, it was confirmed by IR spectroscopy that the residue of the TGA experiments was in fact  $\text{SiO}_2$ . The IR spectrum in Figure 7.2b shows the typical Si-O-Si vibrations at  $1030\text{ cm}^{-1}$  and  $450\text{ cm}^{-1}$ .<sup>[181]</sup> The solution cleaving experiment was conducted to create a reference point because post-polymerization modifications in bulk are always confronted with a potentially hindered diffusion of reagents into the material. Upon addition of acid to a solution of polymer **14c**, immediate precipitation of a brownish material was observed. Quantitative removal of the side chains was confirmed by subjecting the material to TGA under ambient conditions: at 600 °C, a mass loss of approximately 98% was observed (Figure 7.2a, blue curve).

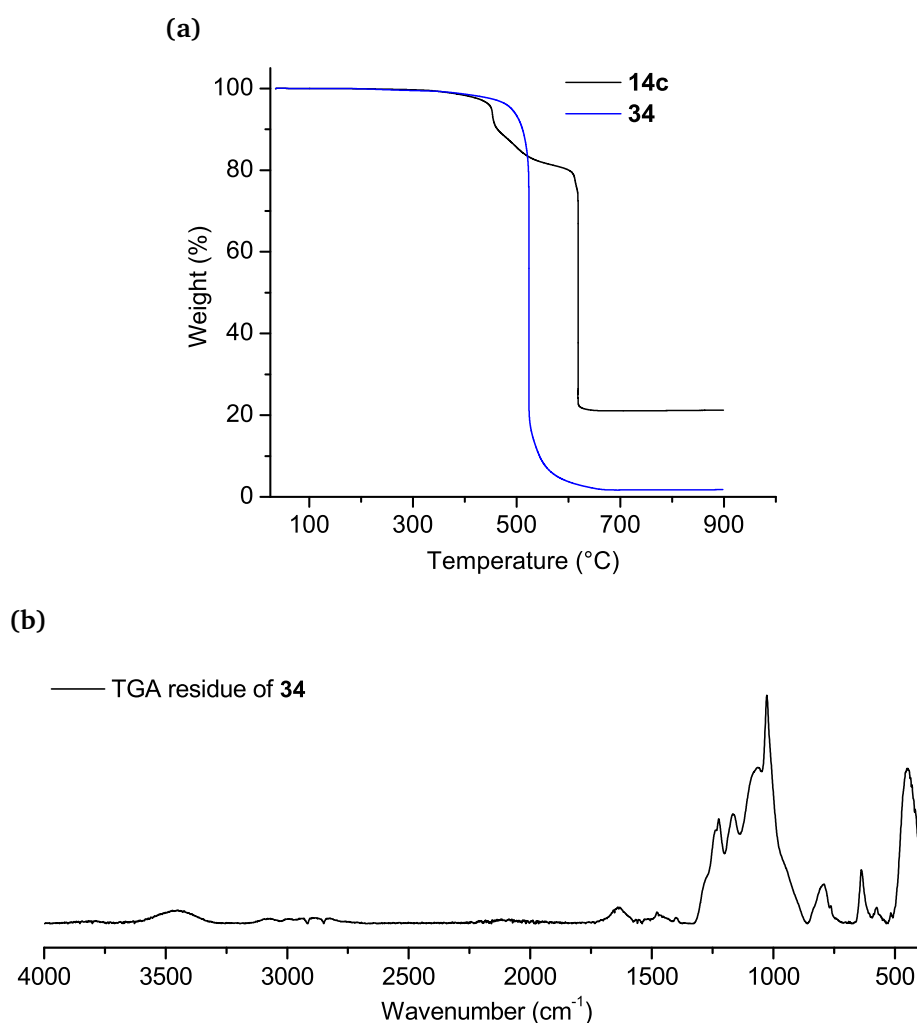


**Figure 7.2.** a) TGA curves of polymer **14c** before acid treatment (black curve) and after side chain cleavage from solution (**34**, blue curve). b) IR spectrum of residue from TGA showing the typical Si-O-Si vibrations of SiO<sub>2</sub> at 1030 cm<sup>-1</sup> and 450 cm<sup>-1</sup>.<sup>[181]</sup>

## 7.1 Influence of film thickness

Having the benchmark of the solution cleaved material, films of **14c** with thicknesses ranging from 0.1 to 0.6 mm were prepared by solution casting from chloroform and subsequent compression moulding at 220 °C. They were exposed in non-supported form to 10 wt% TfOH in toluene for periods ranging from 10 seconds to 60 minutes. Thereafter, the films were placed in a 10 wt% NEt<sub>3</sub> toluene solution for 12 hours, and then washed and dried at 75 °C under vacuum. A few general observations shall be mentioned: (a) with increasing exposure time to acid, the films appear darker; (b) while all films remain largely in their initial form, the treatment causes slight crumpling (Figure 7.6b); (c) thicker films

## 7 Removal of solubilizing side chains from bulk polymer

( $\geq 0.3$  mm) show pronounced swelling. The TGA results in Figure 7.3 refer to the series of films of different thicknesses, all exposed to acid for 60 minutes. The common feature is a dramatic mass loss at around 600 °C. Differences indicate the exact point at which the loss sets in and how exactly it proceeds. This series shows that differences in film thickness from 0.1 mm to 0.6 mm cause differences in residual mass on the order of 1-3%, with the 0.1 mm film furnishing the best result. Given the accuracy of the method, which was estimated to be on the order of  $\pm 3\%$ ,<sup>[178]</sup> it can be concluded, that the tested samples behave rather similar and that thicker samples might be somewhat inferior and might need longer exposure times.

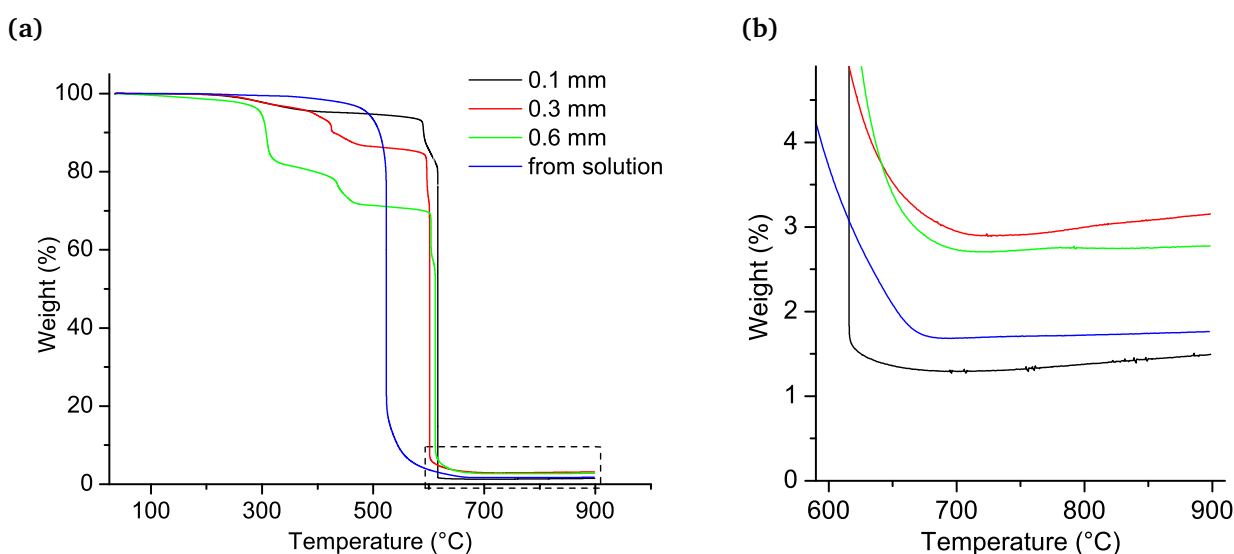


**Figure 7.3.** a) TGA curves of films from polymer **14c** of different thicknesses, after exposure to TfOH. b) Magnification of the area between 500 °C and 900 °C of the same TGA curves, showing small differences in residual mass.

### 7.2 Influence of acid exposure time

In a new experiment the dependence of the cleaving results on the exposure time was in the focus. Therefore 0.1 mm thick films of polymer **14c** were exposed to TfOH for different periods. After washing and drying the acid treated films were subjected to TGA. The results are shown in Figure 7.4 and indicate a dependence of residual mass on the acid exposure time for a constant film thickness. In particular it can be observed that the maximum effect is reached already within the first 10 minutes. More complete removal requires significantly increased exposure times. While there is an evident impact of the cleaving conditions, the effects are subtle and the overall behavior is similar: already after



10 seconds of exposure time most of the side chains are removed. Because of the relatively large error bar in TGA, IR- and NMR spectroscopy was chosen in order to corroborate the found results. Figure 7.5 shows the IR spectra of the reported time series as well as a magnification of the high-frequency range of the spectra. It can be observed that the alkyl-CH signals ( $2810\text{ cm}^{-1} < \tilde{\nu} < 2990\text{ cm}^{-1}$ ) as well as the Si-C signal ( $\tilde{\nu} = 1245\text{ cm}^{-1}$ )<sup>[182]</sup> disappear upon extended exposure to TfOH. Further, the change of the aromatic C-H signals ( $\tilde{\nu} > 3000\text{ cm}^{-1}$ ) reflects the change in substitution pattern. In agreement with the TGA results, the IR spectra also suggest a virtually quantitative removal of the side chains within 1 to 10 minutes.

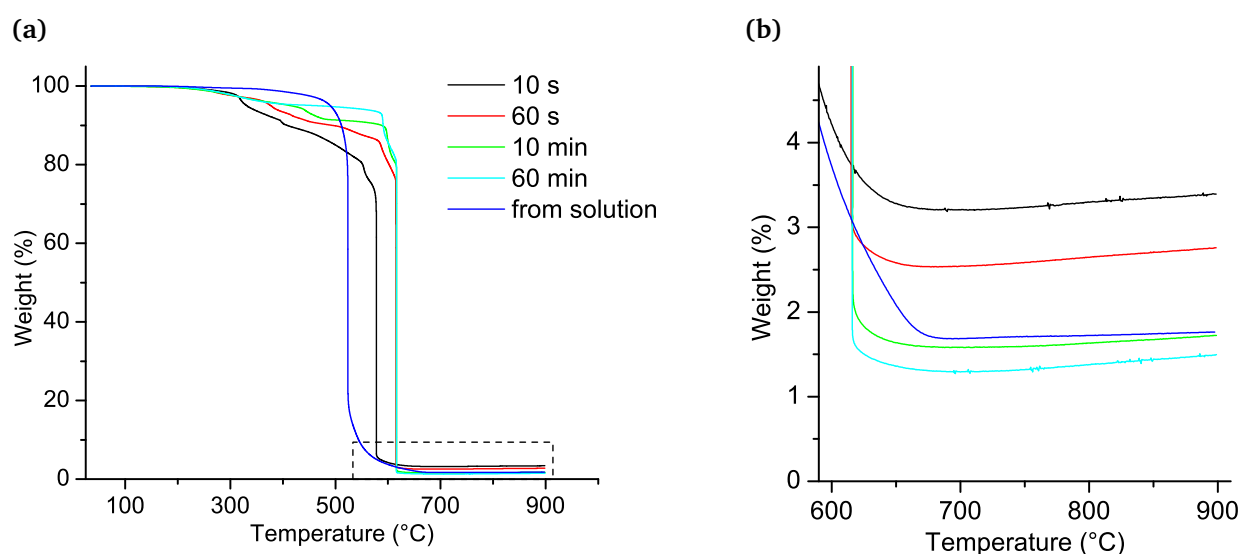


**Figure 7.4.** a) TGA curves of 0.1 mm thick films of polymer **14c** exposed to TfOH for different periods. b) Magnification of the area between 500 °C and 900 °C of the same TGA curves, showing the progress of the side chain removal over time.

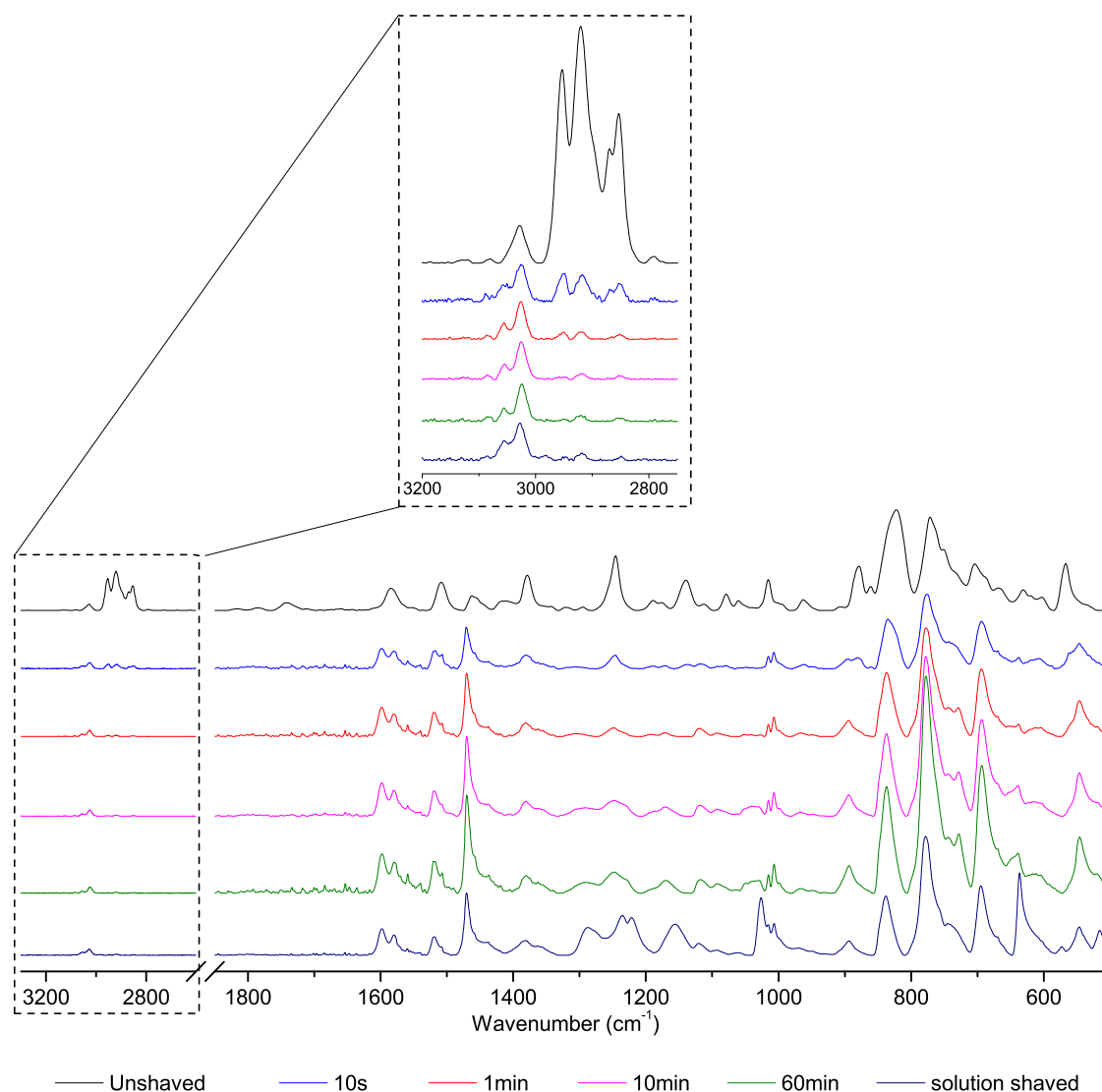


**Figure 7.5.** IR spectra with magnification into the area between 2700  $\text{cm}^{-1}$  and 3200  $\text{cm}^{-1}$  of 0.1 mm thick films of polymer **14c** exposed to TfOH for different periods. The vanishing of the alkyl C-H vibrations ( $2810 \text{ cm}^{-1} < \tilde{\nu} < 2990 \text{ cm}^{-1}$ ) and of the Si-C vibration ( $\tilde{\nu} = 1245 \text{ cm}^{-1}$ ) indicate the progress of the cleaving reaction.

In Figure 7.6a the  $^{13}\text{C}$ -CP/MAS NMR spectra of the starting material **14c** and the side chain free product **34** are compared. The two spectra show the disappearance of the aliphatic signals upon acid treatment. The blue curve corresponds to a 0.1 mm thick film which was exposed to diluted TfOH for 60 minutes. These findings additionally confirm the virtually quantitative cleavage of the stabilizing side chain. Figure 7.6b refers to a 0.6 mm thick film before (left) and after (right) side chain cleavage. After drying the acid-treated film, shrinkage is observed besides the vanished transparency. Mechanically, this

film appears somewhat stiffer but still intact. That the film is still mechanical stable does not go without saying considering the significant mass loss of 43 % due to the side chain removal. A detailed investigation concerning the mechanical properties of the side chain free films is described in chapter 8.

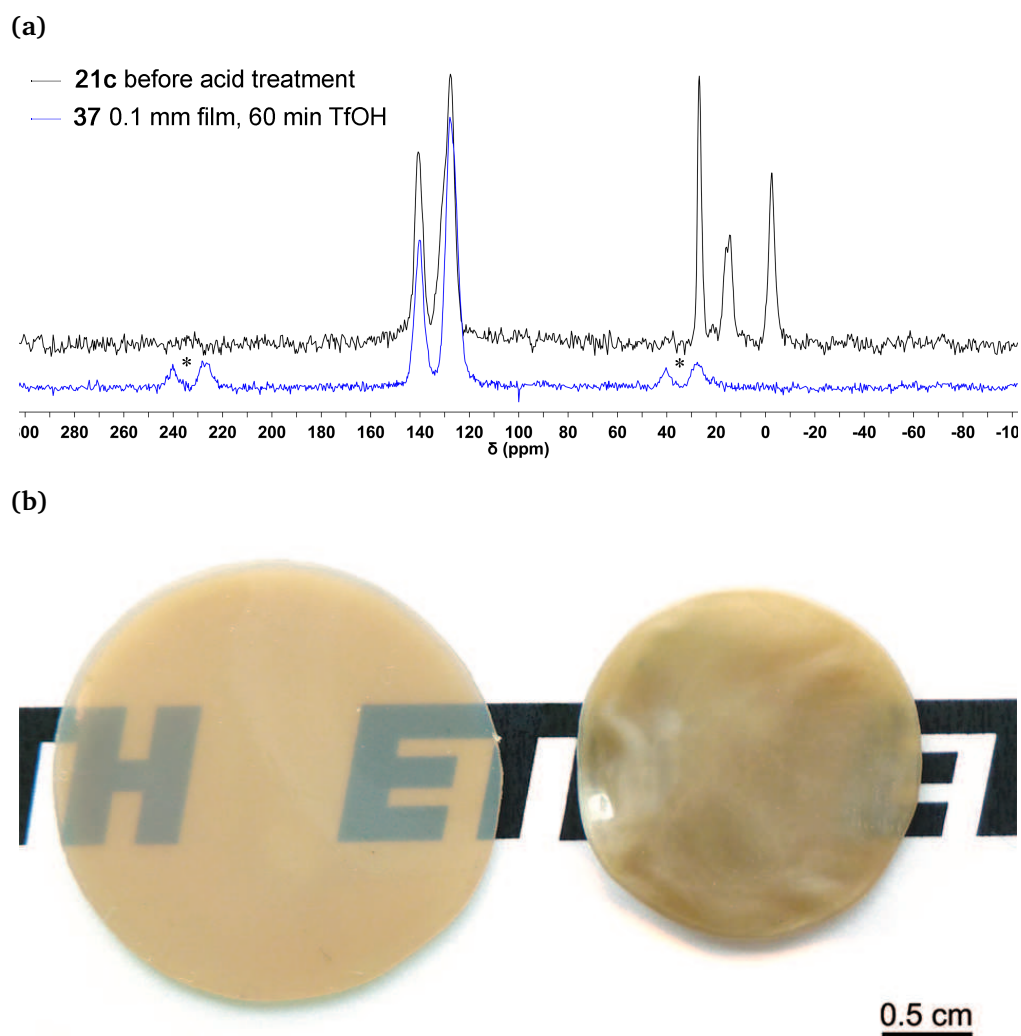
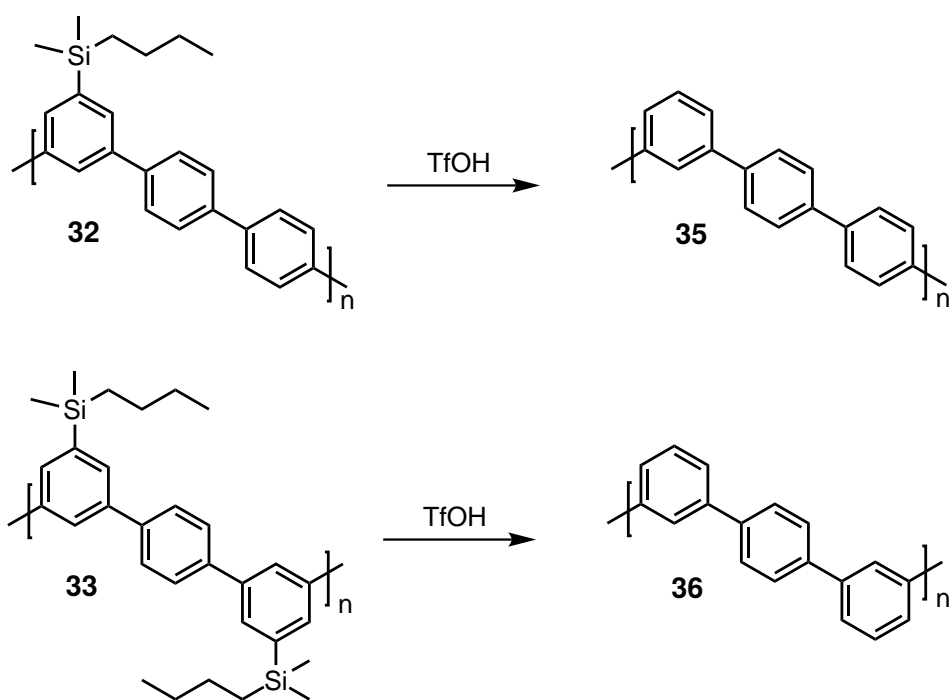


**Figure 7.6.** a)  $^{13}\text{C}$ -CP/MAS NMR spectra of polymer **14c** at 25 °C with a spinning speed of 20 kHz (black) and of polymer **14** at a spinning speed of 11 kHz (blue). The spinning side bands marked with \* are not visible in the black spectrum because of the higher spinning speed. b) 0.6 mm thick film of polymer **14c** before (left) and after acid treatment (right).

7.3 Side chain cleavage of films from polymers **32** and **33**

In order to broaden the scope of the method, the above mentioned procedure for side chain removal was also applied to 0.1 mm thick films of polymers **32** and **33**. By TGA, the progress of side chain removal over time of acid exposure was again investigated. The resulting curves are shown in Figure 7.7. The first observation is that the TGA curves of the untreated polymers **32** and **33** result in a residual mass of 16.8 % and 24.0 % respectively. These values are in good agreement with the theoretical values of 17.5 % for **32** and 26.3 % for **33**. The results confirm the validity of this fast and easy method.



**Scheme 7.2.** Side chain removal from polymer **32** and **33** resulting in the parent polyphenylenes **35** and **36**.

For both polymers we observe a similar behavior concerning the dependence of cleaving progress on acid exposure time. Within one minute most of the side chains are already cleaved and after 10 minutes of acid exposure virtually no further progress can be observed. Note that in case of polymer **33** the relative mass loss due to the side chain removal is 50%, whereas for polymer **32** its only 33.4 %. The strong variations of the TGA curves of polymer **33** might be an artifact of the high mass loss. It could be that the increased amount of leaving groups would require longer washing times in order to diffuse out of the polymer. It thus supports the initial assumption that keeping the amount of side chains

as small as possible is beneficial.

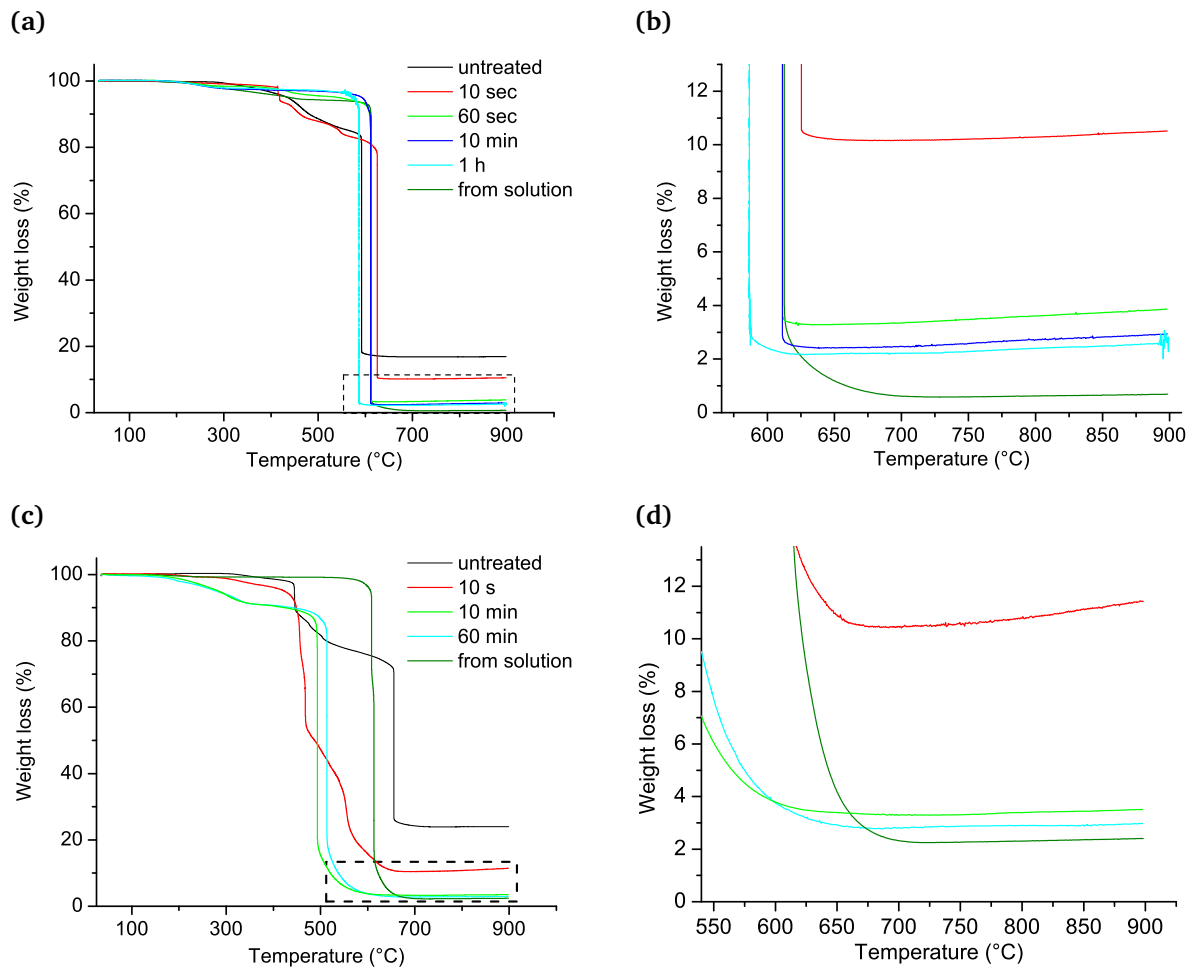


**Figure 7.7.** TGA results of 0.1 mm thick films from polymer **32** a) and **33** c) cast from chloroform, hot compression molded and exposed to diluted TfOH for various periods. Magnifications of the area between 500 °C and 900 °C (**32** b) and **33** d)) of the same TGA curves showing the progress of the side chain removal over acid exposure time.

### 8 Properties of unsubstituted polyphenylene

One initial goal of this thesis was to obtain materials of side chain free polyphenylenes and investigate whether they are superior concerning mechanical stress resistance as compared to polyphenylenes still bearing the solubilizing side chain. After the previous studies which showed that a quantitative removal of the solubilizing side chains from the bulk material is possible, several samples of polymer **34** were prepared and studied for their stress-strain behavior as well as their thermal stability. To our knowledge, no stress resistance data have been reported so far for unsubstituted polyphenylenes. In order to reproducibly obtain measurable samples for the tensile tests, some experimental precautions had to be taken.

In order to avoid a crumbling of the dogbone shaped specimens, a device from stainless steel was built, which holds the samples straight during the cleaving process (Figure 8.1). By turning the thread bar, the sample could be stretched by applying a strain through the spring. It was taken care of that the applied strain is as small as possible such that no elongation can occur during acid treatment of the sample.

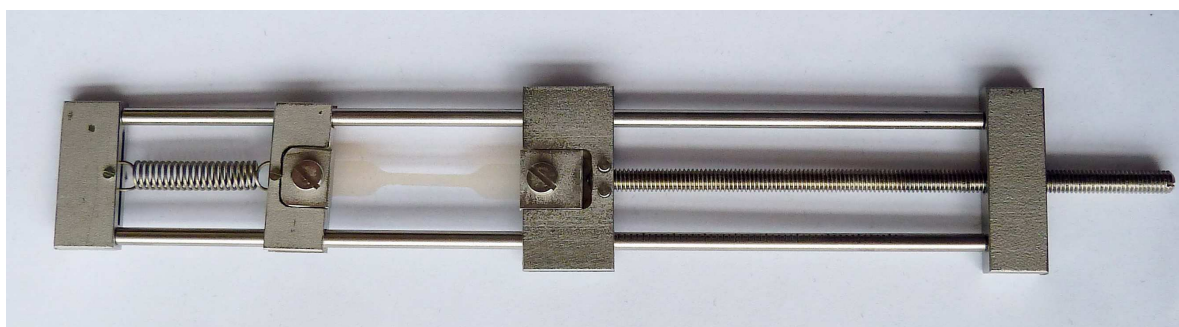


**Figure 8.1.** Sample holder which prevents crumbling of dogbone shaped samples during the treatment with TfOH.

Additionally it was found that it is favorable for the given setup to use pure TfOH for the side chain removal instead of the 10% toluene solution as described above. The softening, which occurs if the toluene solution is used, led to an elongation during the cleaving process only due to the weight of the sample itself. While the simultaneous elongation during the cleaving process could be a desired process in the future, for now this additional parameter should be excluded and therefore pure TfOH was used. The residual mass in TGA (Figure 8.2) shows that for the tested samples the treatment with pure acid also leads to satisfying cleaving results and thus the samples qualify as side chain free polymer **34**.

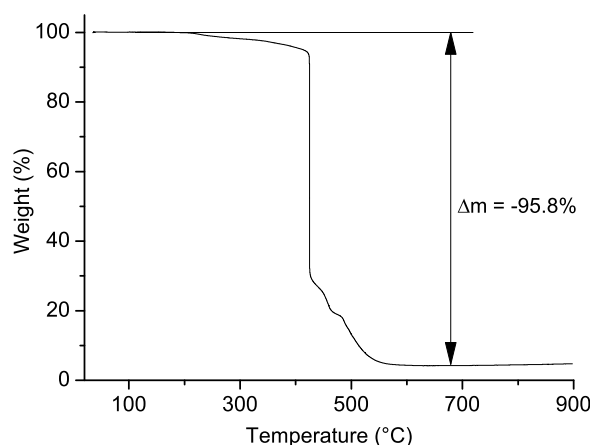


**Figure 8.2.** TGA curves of film from polymer **34** cleaved with pure TfOH. The TGA mass loss under ambient conditions shows that side chain removal proceeds to high conversions.

### 8.1 Thermal stability

As has already been shown in Chapter 7 Figure 7.2a the thermal stability under ambient conditions somewhat increases upon side chain removal. While the side chain bearing polymer **14c** starts to degrade at around 300 °C, the side chain free material **34** appears to be stable up to 425 °C. The same trend can be observed in a nitrogen atmosphere. As shown in Figure 8.3 the side chain free polymer **34** is stable up to 570 °C while the polymer **14c** already degrades at 425 °C. It should be noted, that the exact temperature at which the degradation sets in also appeared to be dependent on the type of the sample.

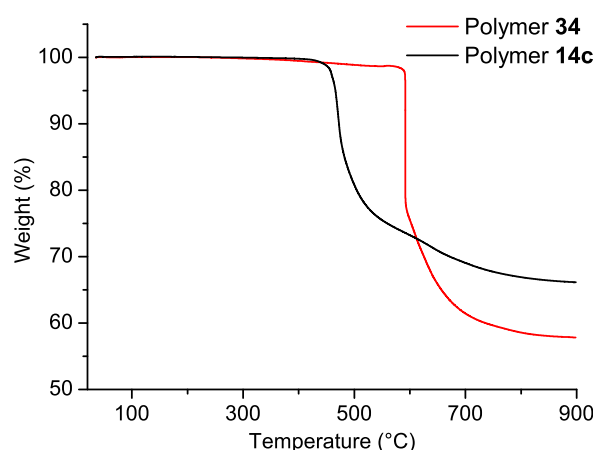


**Figure 8.3.** TGA curve of films from polymer **14c** and **34** in N<sub>2</sub> atmosphere showing the increase in thermal stability due to the side chain removal.

Thus polymer films in general exhibited a higher thermal stability as samples used in powder form.

## 8.2 Mechanical Properties

Finally the samples of side chain free polymer **34** were investigated concerning their tensile strain behavior. For that several samples were used. One was a film which was subjected to the cleaving procedure directly after solution casting from chloroform and subsequent hot compression molding ( $\lambda = 1$ ). And three others which were drawn at 220 °C to different draw ratios prior to the side chain removal (see Chapter 6.3.4) The stress-strain curves of these samples are depicted in Figure 8.4 (solid lines). For comparison the results of the samples still carrying the side chains are also displayed in dashed lines. The stress-strain curves as well as the summarized results in Table 8.1 show that in all samples the Young's modulus  $E$  as well as the strength  $\sigma$  increases upon side chain removal. Thereby it was shown that the chosen cleavable side chain approach for achieving materials from purely aromatic polymers is successful and that there is in fact a potential for producing strong, chemical and thermal resistant materials following this approach.

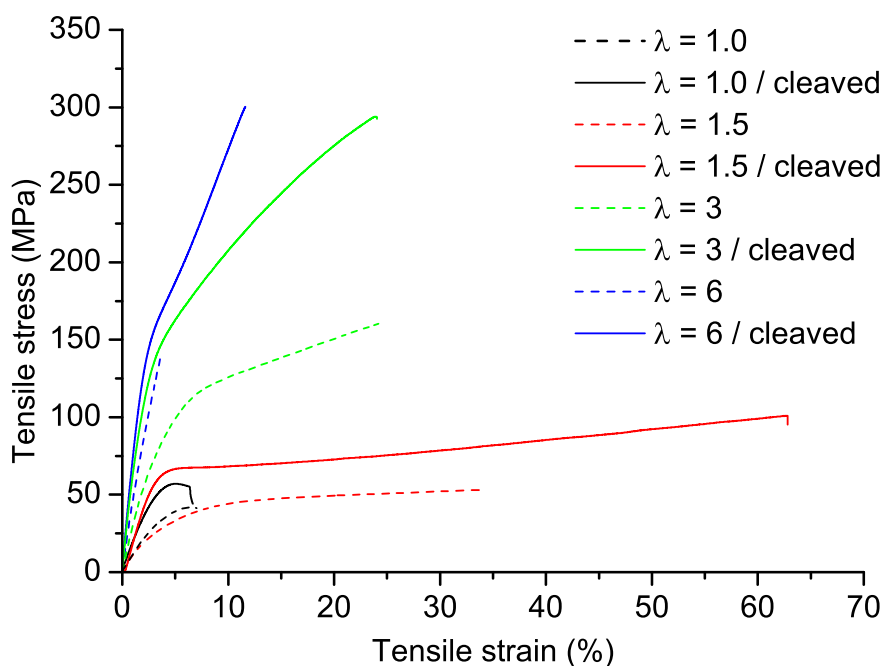


**Figure 8.4.** Stress-Strain curves of samples from side chain free polymer **34** (solid lines). For comparison the results from the above tested polymer **14c** still bearing the solubilizing side chains are displayed as well (dashed lines).



Additionally, the initial concerns of destroying the samples by the removal of the side chain could be ruled out.

**Table 8.1:** Results of tensile stress tests for films of polymer **14c** processed from chloroform and of polymer **14** still bearing the solubilizing side chains.

Draw ratio	<b>14c</b>			<b>34</b>		
	E [GPa]	$\sigma$ [MPa]	$\epsilon$ [%]	E [GPa]	$\sigma$ [MPa]	$\epsilon$ [%]
1.0	1.1	42	7	1.5	60	6.0
1.5	1.2	52	34	2.6	101	63
3.0	3.2	160	24	6.4	293	24
6.0	5.0	140	3.6	7.5	300	12



## 9 Summary and conclusions

The present thesis describes significant progress in polymer synthesis based on Suzuki polycondensation (SPC) and how this relatively novel polymerization technique can be used as route towards high performance materials for film and fiber applications.

During the course this thesis new aromatic AA- and BB-type monomers for SPC were designed and synthesized. More specifically, fast and scalable procedures leading to monomers with purities exceeding 99.5% were established. Because the monomer purity is crucial for SPC it was confirmed by means of NMR spectroscopy and gas chromatography. The monomers were designed in order to enable access to polyphenylenes containing *meta*-connected repeating units and bearing acid cleavable silyl side groups.

Subsequently these monomers were used in order to develop a robust procedure for the synthesis of novel polyphenylenes with molecular weights above 100 kDa. This was achieved by optimization of the reaction in terms of concentration, catalyst, stoichiometry and scale. The found conditions enabled a soluble poly(*m,p*-phenylene) with a molecular weight of 150 kDa on a scale of 14 g.

By GPC and MALDI-TOF analysis it was found that the obtained polymer contains considerable amounts of macrocyclic byproducts, which is a known phenomena for polyphenylenes containing *meta* connected repeating units. It was discovered that by Soxhlet extraction and subsequent precipitation these side products could be removed selectively to a large degree. Thus the developed synthesis and purification procedures results in poly(*m,p*-phenylene)s with up to 300 kDa on a 9 g scale.

As it is common standard, molecular weight determination relied on GPC using a conventional polystyrene calibration. Because it has been shown that for some rigid polymers this GPC method tends to overestimate the molecular weight, static light scattering was selected as an independent method in order to evaluate the reliability of the GPC obtained molar masses. It was found that in case of poly(*m,p*-phenylene)s the molecular weights determined by GPC are not overestimated, which confirmed the outstanding DP's obtained. The high molecular weights could be reproduced using different monomers. Thus polyphenylenes comprising different amounts of *meta*-connected repeating units were obtained. Depending on the number of such kinks two observations were made. First, with an increasing number of *meta*-connected phenylenes inside the backbone, the amount of formed

macrocycles increases. This results from the higher number of conformations which allow cycle formation. Second, the increased flexibility, which comes by the incorporation of kinks, leads to a decrease of the glass transition temperature of the polymers.

The synthesized poly(*m,p*-phenylene)s were used for the production of films by solution casting and subsequent hot compression molding. It was found that depending on the solvent (chloroform or toluene) used for solution casting, the morphology of the film can be tuned from predominantly amorphous to semicrystalline. This is also reflected in the tensile behavior of the films and only the amorphous material showed an extended plasticity above its glass transition temperature. This ductility was used for producing elongated threads of poly(*m,p*-phenylene) with a draw ratio of up to 6. It was shown by XRD that upon elongation, the orientation of the polymer chains within the sample increases, which brings about an increase in tensile strength and modulus.

Finally, the cleaving reaction of the solubilizing side chain from the bulk material was under investigation. Therefore films of thicknesses between 0.1 and 0.6 mm were produced. These films were then subjected to an acid treatment and the degree of side chain cleavage was determined by TGA, IR- and <sup>13</sup>C-CP/MAS solid state NMR spectroscopy. The removal occurs on a time scale of seconds and virtually complete removal was observed after maximally 60 minutes. Despite the mass loss associated with the side chain removal, films subjected to this process remained largely in shape.

Motivated by those findings the elongated samples were also subjected to the cleaving procedure and tested for their tensile behavior. It was found that the removal of the side groups improves the strength as well as the stiffness of the material. The results are therefore in line with earlier findings about the weakening effect of side groups on the mechanical properties of rigid chain polymers. To the best of our knowledge, this is the first time an unsubstituted polyphenylene was obtained in film form and investigated for its mechanical properties. Thus, we see considerable potential to carry this research on towards promising high performance materials.

# Experimental



## 10 Materials and methods

### Chemicals

1,3,5-Tribromobenzene **22** was purchased from TCI and recrystallized either from ethanol or acidic acid prior to usage. All other reagents were purchased from ABCR, Acros, Aldrich or TCI, and used without further purification.

Dry solvents were distilled using a solvent drying system from LC Technology Solutions Inc. SP-105 under nitrogen atmosphere (H<sub>2</sub>O content < 10 ppm as determined by Karl-Fischer titration).

All reaction vessels were dried in an oven at 82 °C over night. For moisture sensitive reactions the flasks were additionally dried under vacuum with a heat gun.

Tetrakis(triphenylphosphane)palladium(0) (Pd(PPh<sub>3</sub>)<sub>4</sub>) catalyst was prepared following literature procedure.<sup>[183]</sup>

Tris(tri-*p*-tolylphosphine)palladium (Pd[P(*p*-tol)<sub>3</sub>]<sub>3</sub>) was synthesized according to the procedure reported by Tolman et al.<sup>[184]</sup> After synthesis all catalysts were stored in a glovebox and used within one week.

### Chromatography

Reactions were monitored by TLC, using a silica gel 60 F254 on aluminum foil from Merck (particle size: 5-20 μm). Detection was done by UV light (λ = 254 nm and/or 366 nm) for fluorescent / phosphorescent compounds.

Column chromatography for purification of products was performed by using Fluka silica gel (pore size 60 Å, particle size 40-63 μm) as a stationary phase. The mobile phase depended on the reaction and was carefully chosen and the process was monitored by TLC.

GC analyses were carried out on an Agilent 7820A GC equipped with an HP-5 MS column (30 m *N* × *N* 0.25 mm *N* × *N* 0.5 μm, 5% phenyl methyl-siloxane), FID detector, and helium as the carrier gas. All runs were performed with an initial temperature of 150°C and a gradient of 10°C/min after 8 minutes with a final temperature of 250°C.

Analytical GPC measurements were performed using a Viscotek GPC-system with chloroform as eluent, equipped with a pump and a degasser (GPCmax VE2001, flow rate 1.0 ml min<sup>-1</sup>), a detector module (Viscotek 302 TDA), a UV detector (Viscotek 2500, λ = 254

nm) and two columns (1 × PLGel Mix-B and 1 × PLGel Mix-C, 7.5×300 mm for each). Conventional calibration was performed with polystyrene standards (Polymer Laboratories) in the range of  $M_p$  1480 to 4340000  $g\ mol^{-1}$ . Prior to injection, the sample solution was filtered through a sintered stainless steel filter (pore size 2  $\mu m$ ).

Preparative recycling GPC was performed on a LC-9101 system from Japan Analytical Industry Co., Ltd. (JAI) equipped with a pump (Hitachi L-7110, flow rate 4.0 mL/min), a RI detector (Jai RI-7), a UV detector set at  $\lambda = 335\ nm$  (Jai UV-3702) and two columns (1 x JAIGEL-2H and 1 x JAIGEL-2.5H, 20 x 600 mm each), using chloroform as eluent at room temperature.

### NMR spectroscopy

Solution NMR measurements were performed on Bruker AM ( $^1H$ : 300 MHz,  $^{13}C$ : 75 MHz) spectrometers at room temperature using deuterated chloroform( $CDCl_3$ ) or dimethyl sulfoxide (DMSO- $d_6$ ) as solvents. The solvent signal was used as an internal standard for the chemical shift ( $^1H$ :  $\delta = 7.26\ ppm$ ,  $^{13}C$ :  $\delta = 77.00\ ppm$  for chloroform,  $^1H$ :  $\delta = 2.50\ ppm$ ,  $^{13}C$ :  $\delta = 39.5\ ppm$  for dimethyl sulfoxide).

Solid state  $^{13}C$  CP/MAS NMR measurements were carried out on a Bruker AVANCE 400 spectrometer operating at 100.5 MHz for  $^{13}C$  under MAS conditions with 2.5 mm rotors and a sample rotation frequency of 11 or 20 kHz and cross-polarization employing a contact time of 1 ms and  $^1H$  high-power decoupling.

### Mass spectrometry

High resolution mass spectroscopy analysis were performed by the MS-service of the laboratory for organic chemistry at ETH Zürich using ESI- and MALDI-ICR-FTMS: IonSpec Ultima Instrument spectrometers. Either 3-hydroxypicolinic acid (3-HPA) or trans-2-[3-(4-tert-butylphenyl)-2-methyl-2-propenylidene] malononitrile (DCTB) were used as matrix in the presence of silver triflate for the latter.

### Thermal analysis

Differential scanning calorimetry (DSC) measurements were carried out using a DSC Q1000 differential scanning calorimeter from TA Instruments in a temperature range of 25 to



250°C with a heating and cooling rate of 10°C/min. Samples of a total weight ranging between 1 and 2 mg were closed into aluminum pans of 40 $\mu$ L, covered by a holed cap, and analysed under a nitrogen atmosphere.

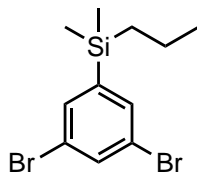
TGA analyses were performed under air with a TA Instruments Q500 thermogravimetric analyser (heating rate: 20 °C min<sup>-1</sup>).

### **X-ray diffraction**

Powder XRD measurements were carried out on a XCalibur single-crystal X-ray diffractometer (Oxford Diffraction, UK) using an Onyx CCD detector. The wavelength used was Mo-K $\alpha$  ( $\lambda = 0.71073 \text{ \AA}$ ) using a graphite monochromator. Data evaluation was done with FIT2D.<sup>[185]</sup>

## 11 Synthesis

### (3,5-dibromophenyl)dimethyl(propyl)silane<sup>[107]</sup> (21a)

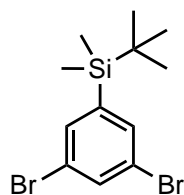


In a dry 1 L three-neck flask 1,3,5-tribromobenzene (**22**) (10.0 g, 33.8 mmol) was dissolved in 400 mL of dry diethyl ether. The mixture was cooled to  $-78\text{ }^{\circ}\text{C}$  with an acetone dry ice bath and a 1.6 M hexane solution of n-butyl lithium (20.5 mL, 32.7 mmol) was added dropwise during 1 h. The reaction was stirred for 2 h at  $-78\text{ }^{\circ}\text{C}$  and then dimethylpropylsilyl chloride (4.78 g, 34.9 mmol) was added slowly. The mixture was heated to room temperature overnight, quenched with water (100 mL) and diluted with diethyl ether (100 mL). The organic phase was separated and washed with water (100 mL) and brine (100 mL). The combined aqueous phases were extracted with diethyl ether and the combined organic phases were dried over magnesium sulphate, followed by solvent removal. The residual brown liquid was pre-purified by a short silica column which led to a bright yellow liquid. Distillation at  $155\text{ }^{\circ}\text{C}$  and 0.1 mbar gave the product as colourless viscous oil. In order to achieve the desired purity the distillation was repeated twice (7.20 g, 67.4%).

$^1\text{H NMR}$  (300 MHz,  $\text{CDCl}_3$ ,  $\delta$ ): 7.65 (t,  $J = 1.8\text{ Hz}$ , 1H), 7.52 (d,  $J = 1.8\text{ Hz}$ , 2H), 1.35 (m, 2H), 0.97 (t,  $J = 7.2\text{ Hz}$ , 3H), 0.75 (m, 2H), 0.27 (s, 6H) ppm.

$^{13}\text{C NMR}$  (75 MHz,  $\text{CDCl}_3$ ,  $\delta$ ): 145.35, 134.62, 134.12, 123.15, 18.18, 17.95, 17.23, -3.17 ppm.

**HRMS** (EI)  $m/z$ : calculated for  $\text{C}_{11}\text{H}_{16}\text{Br}_2\text{Si}$   $[\text{M}]^+$  333.9383, found 333.9385; calculated for  $\text{C}_8\text{H}_9\text{Br}_2\text{Si}$   $[\text{M}-\text{C}_3\text{H}_7]^+$  290.8840, found 290.8835.

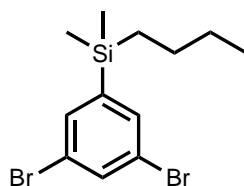
**(3,5-dibromophenyl)tert-butyl(dimethyl)silane (21b)**

In a dry 1 L three-neck flask 1,3,5-tribromobenzene (**22**) (10.0 g, 33.8 mmol) was dissolved in 400 mL of dry diethyl ether. The mixture was cooled to -78 °C with an acetone dry ice bath and a 1.6 M hexane solution of n-butyl lithium (20.5 mL, 32.7 mmol) was added dropwise during 1 h. The reaction was stirred for 2 h at -78 °C and then tert-Butyldimethylsilyl chloride (5.27 g, 34.9 mmol) was added slowly. The mixture was heated to room temperature overnight, quenched with water (100 mL) and diluted with diethyl ether (100 mL). The organic phase was separated and washed with water (100 mL) and brine (100 mL). The combined aqueous phases were extracted with diethyl ether and the combined organic phases were dried over magnesium sulphate, followed by solvent removal. The residual brown liquid was pre-purified by a short silica column which led to a bright yellow liquid. Distillation at 170 °C and 0.2 mbar gave the product as colourless viscous oil. (0.620 g, 5.6%).

$^1\text{H NMR}$  (300 MHz,  $\text{CDCl}_3$ ,  $\delta$ ): 7.66 (t,  $J = 1.8$  Hz, 1H), 7.50 (d,  $J = 1.8$  Hz, 2H), 0.88 (s, 9H), 0.27 (s, 6H) ppm.

$^{13}\text{C NMR}$  (75 MHz,  $\text{CDCl}_3$ ,  $\delta$ ): 143.55, 135.42, 134.19, 122.97, 26.35, 16.90, -6.26 ppm.

**HRMS** (EI) m/z: calculated for  $\text{C}_{12}\text{H}_{18}\text{Br}_2\text{Si}$   $[\text{M}]^+$  347.9539, found 347.9542; calculated for  $\text{C}_8\text{H}_9\text{Br}_2\text{Si}$   $[\text{M}-\text{C}_4\text{H}_9]^+$  290.8835, found 290.8829.

**(3,5-dibromophenyl)butyl(dimethyl)silane (21c)**

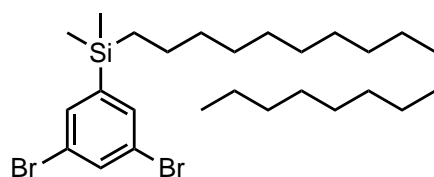
In a dry 6 L three-neck flask 1,3,5-tribromobenzene (**22**) (44.5 g, 0.141 mol) was dissolved in 3 L of dry diethyl ether. The mixture was cooled to  $-78\text{ }^{\circ}\text{C}$  with an acetone dry ice bath and a 1.6 M hexane solution of *n*-butyl lithium (88.9 mL, 0.141 mol) was added dropwise. The reaction was stirred for 2 h at  $-78\text{ }^{\circ}\text{C}$  and then *n*-Butyldimethylsilyl chloride (21.32 g, 0.141 mol) was slowly added. The mixture was heated to room temperature overnight, quenched with water (300 mL) and diluted with diethyl ether (300 mL). The organic phase was separated and washed with water (300 mL) and brine (300 mL). The combined aqueous phases were extracted with diethyl ether and the combined organic phases were dried over magnesium sulphate, followed by solvent removal. The residual brown liquid was pre-purified by a short silica column which led to a bright yellow liquid. Distillation at  $110\text{ }^{\circ}\text{C}$  and 0.05 mbar gave the product as colourless viscous oil. In order to achieve the desired purity the distillation was repeated twice (40.2 g, 81.2%).

$^1\text{H NMR}$  (300 MHz,  $\text{CDCl}_3$ ,  $\delta$ ): 7.64 (t,  $J = 1.8\text{ Hz}$ , 1H), 7.49 (d,  $J = 1.8\text{ Hz}$ , 2H), 1.32 (m, 4H), 0.90 (t,  $J = 6.9\text{ Hz}$ , 3H), 0.75 (m, 2H), 0.28 (s, 6H) ppm.

$^{13}\text{C NMR}$  (75 MHz,  $\text{CDCl}_3$ ,  $\delta$ ): 145.32, 134.62, 134.11, 123.16, 26.41, 25.83, 15.02, 13.72,  $-3.22$  ppm.

**HRMS** (EI)  $m/z$ : calculated for  $\text{C}_{12}\text{H}_{18}\text{Br}_2\text{Si}$   $[\text{M}]^+$  347.9539, found 347.9539; calculated for  $\text{C}_8\text{H}_9\text{Br}_2\text{Si}$   $[\text{M}-\text{C}_4\text{H}_9]^+$  290.8840, found 290.8841.

**Elemental analysis**: calculated for  $\text{C}_{12}\text{H}_{18}\text{Br}_2\text{Si}$ : C, 41.16; H, 5.18; Si, 8.02; Br, 45.64, found: C, 40.97; H, 5.38; Br, 45.85

**(3,5-dibromophenyl)dimethyl(octadecyl)silane (21d)**

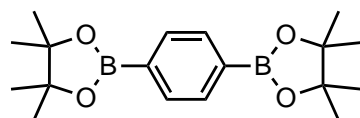
In a dry 1 L three-neck flask 1,3,5-tribromobenzene (**22**) (7.50 g, 23.8 mmol) was dissolved in 300 mL of dry diethyl ether. The mixture was cooled to  $-78\text{ }^{\circ}\text{C}$  with an acetone dry ice bath and a 1.6 M hexane solution of n-butyl lithium (14.9 mL, 23.8 mmol) was added dropwise during 30 minutes. The reaction was stirred for 2 h at  $-78\text{ }^{\circ}\text{C}$  and then dimethyloctadecylsilyl chloride (9.10 g, 26.2 mmol) was added slowly. The mixture was heated to room temperature overnight, quenched with water (100 mL) and diluted with diethyl ether (100 mL). The organic phase was separated and washed with water (100 mL) and brine (100 mL). The combined aqueous phases were extracted with diethyl ether and the combined organic phases were dried over magnesium sulphate, followed by solvent removal. The residual brown solid was distilled at  $150\text{ }^{\circ}\text{C}$  and 0.1 mbar to give the product as colourless wax. (11.0 g, 84.5%).

$^1\text{H NMR}$  (300 MHz,  $\text{CDCl}_3$ ,  $\delta$ ): 7.64 (t,  $J = 1.8\text{ Hz}$ , 1H), 7.49 (d,  $J = 1.8\text{ Hz}$ , 2H), 1.26 (m, 32H), 0.88 (m, 3H), 0.72 (m, 2H), 0.27 (s, 6H) ppm.

$^{13}\text{C NMR}$  (75 MHz,  $\text{CDCl}_3$ ,  $\delta$ ): 145.48, 134.66, 134.12, 123.15, 33.41, 31.93, 29.67, 29.55, 29.36, 29.22, 23.62, 22.70, 15.29, 14.12, -3.19 ppm.

**1,4-bis(4,4,5,5-tetramethyl-1,3,2-dioxaborolan-2-yl)benzene (27)**

[165]



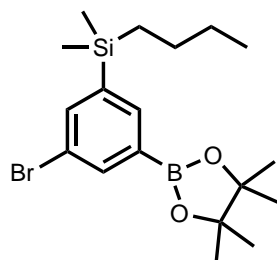
A 3 L round bottom flask was charged with Phenylenedibornic acid (50.0 g, 0.302 mol), pinacol (73.1 g, 0.618 mol) and 1.50 L of toluene. The flask was equipped with a Dean-Stark apparatus and the suspension was heated to reflux overnight, which led to the formation of a clear solution. The mixture was cooled to room temperature and the solvent was removed under vacuum. The resulting crude product was recrystallized twice from diethyl ether to obtain the pure product as colorless crystals. The crystals were pestled and dried under vacuum (51.2 g, 51.4%).

$^1\text{H NMR}$  (300 MHz,  $\text{CDCl}_3$ ,  $\delta$ ): 7.80 (s, 4H), 1.35 (s, 24H) ppm.

$^{13}\text{C NMR}$  (75 MHz,  $\text{CDCl}_3$ ,  $\delta$ ): 133.87, 83.83, 24.87 ppm (Carbon attached to boron was not observed due to quadrupolar relaxations).

**HRMS** (ESI)  $m/z$ : calculated for  $\text{C}_{18}\text{H}_{29}\text{B}_2\text{O}_4$   $[\text{M}+\text{H}]^+$  331.2253, found 331.2258.

**Elemental analysis** calculated for  $\text{C}_{18}\text{H}_{28}\text{B}_2\text{O}_4$ : C, 65.51; H, 8.55; O, 19.39; B, 6.55, found: C, 65.36; H, 8.50

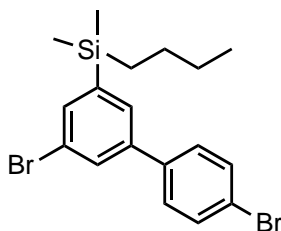
**3-bromo-5-boropinacol-1-(dimethylbutylsilyl)-benzene (25)**

In a 2 L three-necked flask **21c** (40.0 g, 0.114 mol) was dissolved in dry diethyl ether (1 L). The solution was cooled to  $-78\text{ }^{\circ}\text{C}$  with an acetone dry ice bath and a 1.6 M solution of n-butyl lithium in hexane (75.0 mL, 0.120 mol) was added dropwise over 40 minutes. The reaction was stirred for 3h at  $-78\text{ }^{\circ}\text{C}$  and then Isopropoxyboronic acid pinacol ester (30.0 mL, 0.147 mol) was added slowly. The mixture was heated to room temperature overnight and quenched with saturated  $\text{NH}_4\text{Cl}$  aq. (200 mL) and water (100 mL). The aqueous phases was separated and extract twice with diethyl ether (100 mL). The organic layers were combined and dried over  $\text{MgSO}_4$  followed by solvent removal under vacuum. The resulting colorless oil crystallized in the fridge. The solid was pestled and then washed with cold MeOH to give the product as colorless crystals (35.0 g, 77.1%).

$^1\text{H NMR}$  (300 MHz,  $\text{CDCl}_3$ ,  $\delta$ ): 7.90 (s, 1H), 7.80 (s, 1H), 7.67 (s, 1H), 1.34 (s, 12H), 1.31-1.27 (m, 4H), 0.87 (t,  $J = 6.8$  Hz), 0.79-0.70 (m, 2H), 0.26 (s, 6H) ppm.

$^{13}\text{C NMR}$  (75 MHz,  $\text{CDCl}_3$ ,  $\delta$ ): 142.35, 138.86, 138.01, 137.76, 122.83, 84.06, 26.45, 25.96, 24.84, 15.20, 13.73, -3.06 ppm. (Carbon attached to boron was not observed due to quadrupolar relaxations);

**HRMS** (EI) m/z: calculated for  $\text{C}_{18}\text{H}_{30}\text{BBr}_2\text{O}_2\text{Si}$   $[\text{M}]^+$  396.1291, found: 396.1293; calculated for  $\text{C}_{17}\text{H}_{27}\text{BBrO}_2\text{Si}$   $[\text{M}-\text{CH}_3]^+$  381.1057, found 381.1062; calculated for  $\text{C}_{14}\text{H}_{21}\text{BBrO}_2\text{Si}$   $[\text{M}-\text{C}_4\text{H}_9]^+$  339.0587, found 339.0592.

**5,4'-dibromo-3-(dimethylbutylsilyl)-diphenyl (24)**

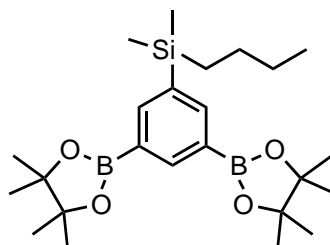
A 500 mL-Schlenk-flask was charged with **25** (10.0 g, 25.2 mmol), p-iodobromobenzene (8.50 g, 30,0 mmol), THF (100 mL), Na<sub>2</sub>CO<sub>3</sub> (15.0 g, 142 mmol) and water (35 mL). A reflux condenser was attached and the mixture was degassed by 6 cycles of vacuum and nitrogen backfilling. In a Schlenk-tube Pd(PPh<sub>3</sub>)<sub>4</sub> (130 mg, 0.112 mmol) was dissolved in degassed THF (10 mL) and transferred into the reaction mixture with a syringe. The resulting yellow solution was heated at 80 °C overnight. After cooling to room temperature the reaction was quenched with saturated NH<sub>4</sub>Cl aq. (50 mL) and the phases were separated. The aqueous layer was extracted twice with diethyl ether (50 mL). The combined organic phases were dried over MgSO<sub>4</sub>, filtered and concentrated under vacuum to yield a yellow crude product. For purification the excess of p-iodobromobenzene was distilled off under vacuum (170 °C, 0.30 mbar). The remaining distillation bottom was then purified by column chromatography with hexane to yield the product as a colorless (6.55 g, 61.0%).

<sup>1</sup>H NMR (300 MHz, CDCl<sub>3</sub>, δ): 7.67 (t, *J* = 1.8 Hz, 1H), 7.61-7.52 (m, 4H), 7.43 (d, *J* = 8.5 Hz, 2H), 1.37-1.24 (m, 4H), 0.90 (t, *J* = 6.9 Hz, 3H), 0.81-0.73 (m, 2H), 0.31 (s, 6H) ppm.

<sup>13</sup>C NMR (75 MHz, CDCl<sub>3</sub>, δ): 143.68, 141.50, 138.99, 135.23, 131.96, 130.44, 130.25, 128.79, 123.30, 122.10, 26.45, 25.96, 15.19, 13.74, -3.07 ppm.

HRMS (EI) *m/z*: calculated for C<sub>18</sub>H<sub>22</sub>Br<sub>2</sub>Si [M]<sup>+</sup> 423.9858, found 423.9861 calculated for C<sub>14</sub>H<sub>13</sub>Br<sub>2</sub>Si [M-C<sub>4</sub>H<sub>9</sub>]<sup>+</sup> 366.9153, found 366.9162.



**(3,5-bis(4,4,5,5-tetramethyl-1,3,2-dioxaborolan-2-yl)phenyl(butyl)dimethylsilane (28)**

A 1 L Schlenk-flask was charged with **21c** (10.0 g, 28.6 mmol), bis(pinacolato)diboron (16.0 g, 63.0 mmol), KOAc (11.5 g, 117 mmol) and DMF (300 mL). This suspension was degassed by 7 cycles of vacuum and nitrogen backfilling. Pd(dppf)Cl<sub>2</sub> (63.0 mg, 86.1 μmol) was dissolved in degassed DMF (10 mL) and added to the mixture with a syringe. The suspension was stirred at 130 °C for 3 hours until no starting material was observed by TLC in hexane. After cooling to room temperature water (200mL) and diethyl ether (300 mL) was added. The phases were separated and the aqueous phase was extracted twice with diethyl ether (150 mL). The organic phases were combined, dried over MgSO<sub>4</sub> and filtered. After solvent removal under vacuum, the remaining yellow oil crystallized in the fridge within 4 days. After recrystallization in MeOH the product was obtained as a colorless powder (8.20 g, 64.6 %).

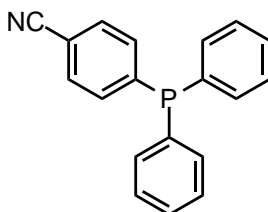
<sup>1</sup>H NMR (300 MHz, CDCl<sub>3</sub>, δ): 8.27 (t, *J* = 1.5 Hz, 1H), 8.03 (t, *J* = 1.5 Hz, 2H), 1.34 (s, 24H), 1.32-1.25 (m, 4H), 0.87 (t, *J* = 6.8 Hz, 3H), 0.81-0.74 (m, 2H), 0.28 (s, 6H) ppm.

<sup>13</sup>C NMR (75 MHz, CDCl<sub>3</sub>, δ): 142.79, 141.88, 137.81, 83.64, 26.49, 26.10, 24.84, 15.35, 13.77, -2.90 ppm.

HRMS (ESI) *m/z*: calculated for C<sub>24</sub>H<sub>43</sub>B<sub>2</sub>O<sub>4</sub>Si [M+H]<sup>+</sup> 445.3120, found 445.3114.

**4-(diphenylphosphino)benzonitrile (37)**

[169]



In a 500 mL Schlenk flask KOH (5.22 g, 93.0 mmol) was suspended in dry DMSO (260 mL) under nitrogen atmosphere for 30 minutes. Diphenylphosphane (9.63 g, 51.7 mmol) was added and the mixture was stirred at room temperature for 2 hours. After the addition of 4-Fluorobenzonitrile (6.26 g, 51.7 mmol) the reaction turned orange and was stirred for additional 30 minutes. The mixture was poured into ice water (250 mL) and the precipitated solid was filtered off. After recrystallization from MeOH the product was obtained as colorless crystals (8.50 g, 57.2 %).

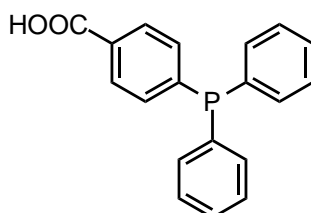
$^1\text{H NMR}$  (300 MHz,  $\text{CDCl}_3$ ,  $\delta$ ): 7.58 (dd,  $J_1 = 8.3$  Hz,  $J_2 = 1.5$  Hz, 2H), 7.35 (m, 10H) ppm.

$^{13}\text{C NMR}$  (75 MHz,  $\text{CDCl}_3$ ,  $\delta$ ): 145.10 (d,  $J_{\text{C-P}} = 16.8$  Hz), 135.35 (d,  $J_{\text{C-P}} = 10.5$  Hz), 134.00 (d,  $J_{\text{C-P}} = 20.3$  Hz), 133.46 (d,  $J_{\text{C-P}} = 18.5$  Hz), 131.67 (d,  $J_{\text{C-P}} = 6.0$  Hz), 129.49, 128.83 (d,  $J_{\text{C-P}} = 7.4$  Hz), 118.69, 111.89 ppm.

**HRMS** (EI)  $m/z$ : calculated for  $\text{C}_{19}\text{H}_{14}\text{NP}$   $[\text{M}]^+$  287.0864, found 287.0859 calculated for  $\text{C}_{12}\text{H}_{10}\text{P}$   $[\text{M-C}_7\text{H}_4\text{N}]^+$  185.0520, found 185.0518.

**4-(diphenylphosphino)benzoic acid (L-AC)**

[169]



In an 250 mL round bottom flask **37** (8.50 g, 29.59 mmol) was suspended in concentrated HCl(aq.) (100 mL). The mixture was stirred under reflux for 1 hour in a nitrogen atmosphere, which resulted in a clear solution. The crude product was precipitated in ice water (500 mL), filtered and recrystallized from Methanol (6.50 g, 71.7%).

$^1\text{H NMR}$  (300 MHz,  $\text{CDCl}_3$ ,  $\delta$ ): 8.03 (dd,  $J_1 = 8.3$  Hz,  $J_2 = 1.6$  Hz, 2H), 7.36 (m, 10H) ppm.

$^{13}\text{C NMR}$  (75 MHz,  $\text{CDCl}_3$ ,  $\delta$ ): 171.26, 145.40 (d,  $J_{\text{C-P}} = 14.8$  Hz), 135.97 (d,  $J_{\text{C-P}} = 10.4$  Hz), 134.01 (d,  $J_{\text{C-P}} = 20.1$  Hz), 133.16 (d,  $J_{\text{C-P}} = 18.6$  Hz), 129.84 (d,  $J_{\text{C-P}} = 6.3$  Hz), 129.22, 128.98, 128.72 (d,  $J_{\text{C-P}} = 7.4$  Hz) ppm.

**HRMS** (EI)  $m/z$ : calculated for  $\text{C}_{19}\text{H}_{14}\text{NP}$   $[\text{M}]^+$  306.0810, found 306.0811 calculated for  $\text{C}_{12}\text{H}_{10}\text{P}$   $[\text{M-C}_7\text{H}_5\text{O}_2]^+$  185.0520, found 185.0518.

**Catalyst Pd(L-AC)<sub>3</sub>**

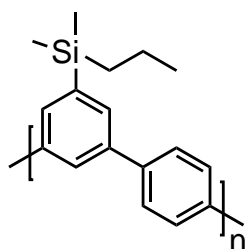
In a 50 mL Schlenk flask  $\text{PdCl}_2$  (56 mg, 0.318 mmol) and **L-AC** (487 mg, 1.59 mmol) were dissolved in 2.8 mL of DMSO. The suspension was degassed by 5 cycles of vacuum and nitrogen back-filling. During heating to 150 °C a red solution formed, which after 10 minutes at this temperature was allowed to cool down to 120 °C. After the addition of hydrazine hydrate (62  $\mu\text{L}$ , 1.27 mmol) the mixture was allowed to cool to room temperature. Upon addition of 25 mL degassed THF, the catalyst precipitated as yellow crystalline solid. The crystals were filtered through a Schlenk frit and washed twice with THF. The catalyst was dried overnight and finally stored in a glovebox.

$^1\text{H NMR}$  (300 MHz,  $\text{CDCl}_3$ ,  $\delta$ ): 7.56 (d,  $J = 7.9$  Hz, 6H), 7.22 (t,  $J = 6.8$  Hz, 6H), 7.02-7.13 (m, 30H).

### Typical procedure for Suzuki Polycondensation

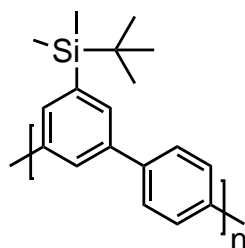
In a 1 L Schlenk flask, a precise amount of **21c** (10.028 g, 28.639 mmol) and 1.005 eq. of **27** (9.499 g, 28.782 mmol) were dissolved in a mixture of THF (600 mL) and water (200 mL). 25 mL of saturated  $K_2CO_3$  (aq.) were added and the biphasic system was degassed by applying five vacuum and nitrogen back-filling cycles. The catalyst  $Pd(L2)_3$  (88.10 mg, 85.93  $\mu$ mol) was dissolved in THF, which had previously been degassed by three freeze–pump–thaw cycles. The catalyst suspension was added under nitrogen counter flow and the resulting mixture was heated to 85 °C for 48 h, during which time a colourless precipitate was formed. The reaction was quenched with 150 mL toluene and 100 mL water. As soon as the solid was dissolved, the phases were separated and the organic phase was washed with 200 mL of saturated  $NaHCO_3$  (aq.). To remove the residual Pd, the organic phase was washed with a solution of 40 mg NaCN dissolved in 100 mL water by vigorous stirring of the biphasic mixture for 3 h. The phases were again separated and the organic phase was washed twice with 100 mL of saturate  $NaHCO_3$  (aq.) followed by solvent removal. The residue was dissolved in 70 mL of toluene and the product was precipitated by dropping this solution in 700 mL of methanol. After filtration the colourless polymer was dried in a vacuum at 75 °C (7.30 g, 95.7%).

### Poly[3-(dimethyl(propyl)silyl)-4',5 biphenylene] **14a**



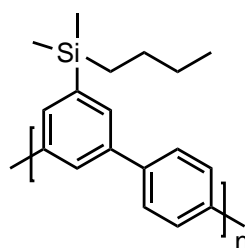
$^1H$  NMR (300 MHz,  $CDCl_3$ ,  $\delta$ ): 7.92 (s, 1H), 7.82 (m, 6H), 1.47 (m, 2H), 1.03 (t,  $J = 6.8$  Hz, 3H), 0.89 (s, 2H), 0.40 (s, 6H) ppm.

$^{13}C$  NMR (75 MHz,  $CDCl_3$ ,  $\delta$ ): 141.21, 140.66, 140.62, 131.48, 127.84, 126.65, 18.46, 18.37, 17.52, -2.80 ppm.

Poly[3-(*t*-butyl(dimethyl)silyl)-4',5 biphenylene] 14b

$^1\text{H NMR}$  (300 MHz,  $\text{CDCl}_3$ ,  $\delta$ ): 7.93 (s, 1H), 7.81 (m, 6H), 1.01 (s, 9H), 0.42 (s, 6H) ppm.

$^{13}\text{C NMR}$  (75 MHz,  $\text{CDCl}_3$ ,  $\delta$ ): 140.64, 140.38, 135.31, 132.38, 127.86, 126.66, 26.60, 16.99, -6.01 ppm.

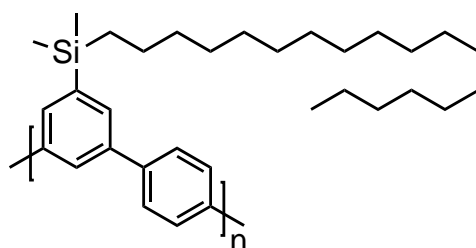
Poly[3-(*n*-butyl(dimethyl)silyl)-4',5 biphenylene] 14c

$^1\text{H NMR}$  (300 MHz,  $\text{CDCl}_3$ ,  $\delta$ ): 7.92 (s, 1H), 7.82 (m, 6H), 1.41 (m, 4H), 0.92 (m, 5H), 0.39 (s, 6H) ppm.

$^{13}\text{C NMR}$  (75 MHz,  $\text{CDCl}_3$ ,  $\delta$ ): 141.22, 140.65, 140.63, 131.48, 127.84, 126.65, 26.57, 26.16, 15.47, 13.81, -2.84 ppm.

**Elemental analysis:** calculated for  $(\text{C}_{18}\text{H}_{22}\text{Si})_n$ : C, 81.14; H, 8.32; Si, 10.54, found: C, 81.31; H, 8.27

## Poly[3-dimethyl(octadecyl)silyl)-4',5 biphenylene] 14d



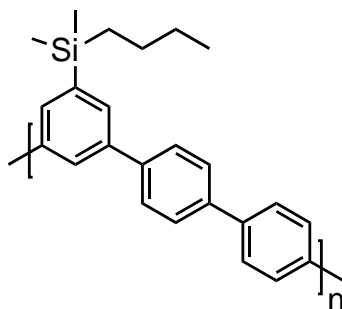
## 11 Synthesis

---

$^1\text{H NMR}$  (300 MHz,  $\text{CDCl}_3$ ,  $\delta$ ): 7.96 (s, 1H), 7.85 (m, 6H), 1.28 (br-s, 32H), 0.92 (m, 5H), 0.43 (s, 6H) ppm.

$^{13}\text{C NMR}$  (75 MHz,  $\text{CDCl}_3$ ,  $\delta$ ): 141.23, 140.68, 140.64, 131.51, 127.84, 126.63, 33.64, 31.94, 29.72, 29.67, 29.37, 23.97, 22.70, 15.77, 14.13, -2.82 ppm.

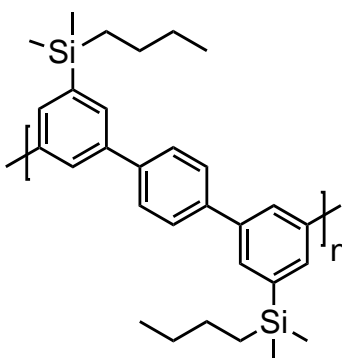
### Poly[(1,1':4',1''-terphenyl)-3-yl(butyl)dimethylsilane] 32



$^1\text{H NMR}$  (300 MHz,  $\text{CDCl}_3$ ,  $\delta$ ): 7.92 (s, 1H), 7.81 (s, 10H), 1.41 (m, 4H), 0.93 (m, 5H), 0.40 (s, 6H) ppm.

$^{13}\text{C NMR}$  (75 MHz,  $\text{CDCl}_3$ ,  $\delta$ ): 141.22, 140.60, 139.74, 131.43, 127.85, 127.48, 126.61, 26.58, 26.17, 15.48, 13.81, -2.84 ppm.

### Poly[3,3''-bis(butyldimethylsilyl)-1,1':4',1''-terphenylene] 33



$^1\text{H NMR}$  (300 MHz,  $\text{CDCl}_3$ ,  $\delta$ ): 7.89 (s, 1H), 7.79 (m, 8H), 1.39 (s, 8H), 0.91 (m, 10H), 0.37 (s, 12H) ppm.

$^{13}\text{C NMR}$  (75 MHz,  $\text{CDCl}_3$ ,  $\delta$ ): 141.62, 141.20, 140.64, 131.84, 131.48, 127.87, 126.99, 26.58, 26.18, 15.46, 13.81, -2.84 ppm.

## 12 Polymer processing

### Removal of cyclic byproducts

The raw polymer **1c** was placed in a Soxhlet apparatus and extracted with hot acetone for 5 d. During the extraction, the partially soluble macrocycles precipitated in the solvent reservoir. The polymeric material was dried and re-dissolved in toluene ( $0.1 \text{ g mL}^{-1}$ ). By dropwise addition of this solution into acetone (10-fold volume) the linear polymer was precipitated as a colourless solid. After filtration the material was dried in a vacuum for 3 d at  $75 \text{ }^\circ\text{C}$ .

### Film preparation

800 mg of the purified and fractionated polymer were dissolved in 7.20 g of chloroform (10 % w/w). The viscous solution was filtered into a petri dish ( $\varnothing 9 \text{ cm}$ ) through a plug of glass wool inside a pipette. The dish was covered and the solution was dried at room temperature over 4 d. Thereafter, water was added, which helped lifting the film from the glass dish. The film was removed from the water surface and dried under vacuum at  $75 \text{ }^\circ\text{C}$  for 5 d and subsequently hot compression moulded at  $220 \text{ }^\circ\text{C}$  and 0.6 MPa pressure. The resulting films were approximately  $100 \mu\text{m}$  thick. For thicker films, either the amount of polymer or the diameter of the petri dish was adjusted.

### Side chain cleavage from solution

Polymer **14c** (100 mg) was dissolved in 15 mL of toluene and heated to  $110 \text{ }^\circ\text{C}$ . After 2 h, TfOH (2 mL) was added dropwise, which led to the precipitation of a brownish powder. The mixture was kept at  $110 \text{ }^\circ\text{C}$  for 1 h, and then cooled to room temperature, followed by the addition of  $\text{NEt}_3$  (2 mL). Upon addition of methanol (10 mL), the solid was filtered off and washed with toluene. Polymer **34** was yielded as a brownish solid (30 mg, 52.8%).

### Side from polymer films

A 10 wt% solution of TfOH in toluene was prepared in a glass vial and the polymer film was immersed within. After the desired time (1, 10, 60 min), the film was transferred into another glass vial containing a 10 wt%  $\text{NEt}_3$  solution in toluene. After 12 h, the film

## 12 Polymer processing

---

was transferred into another vial with pure toluene, where it was kept for 2 h to remove residual  $\text{NEt}_3$ . Finally, the sample was placed in a glass dish and dried first at 75 °C and ambient pressure for 12 h, followed by drying for 5 d at 75 °C under vacuum.



# Appendix



## 13 List of abbreviations

$\delta$	= chemical shift (in ppm) used in NMR spectroscopy
$\lambda$	= wavelength
$\tilde{\nu}$	= wavenumber
Ar	= aryl
aq.	= aqueous
CCD	= charge-coupled device
CP/MAS	= cross-polarization / magic angle spinning
Da	= dalton
DCM	= dichloromethane
DSC	= differential scanning calorimetry
DIBAL	= diisobutylaluminum hydride
DMF	= N,N-dimethylformamide
DMSO	= dimethyl sulfoxide
DP	= Degree of polymerization
eq.	= equivalents
EI	= electron impact
ESI	= electrospray ionization
EtOAc	= ethyl acetate
et al.	= et alii (=Latin for and others)
FID	= flame ionization detector
FT	= fourier transform
d	= doublet
dd	= doublet of doublets
GPC	= gel permeation chromatography
IR	= infrared
$J$	= spin-spin coupling constant
KOAc	= potassium acetate
m	= multiplet
M	= mol/L
m/z	= mass-to-charge ratio

### 13 List of abbreviations

---

MALDI	= matrix-assisted laser desorption ionization
MAS	= magic angle spinning
MS	= mass spectrometry
n-BuLi	= n-butyllithium
nm	= nanometer
NMR	= nuclear magnetic resonance
Pd(dppf)Cl <sub>2</sub>	= [1,1'-bis(diphenylphosphino)ferrocene]dichloropalladium(II)
PMMA	= polymethylmethacrylat
PmpP	= poly( <i>m,p</i> -phenylene)
ppm	= parts per million
PS	= polystyrene
rt	= room temperature
s	= singlet
sat.	= saturated
SLS	= static light scattering
SMCC	= Suzuki-Miyaura cross-coupling
SPC	= Suzuki polycondensation
t	= triplet
TfOH	= trifluoromethanesulfonic acid
T <sub>g</sub>	= glass transition temperature
TGA	= thermogravimetric analysis
THF	= tetrahydrofuran
TLC	= thin layer chromatography
TOF	= time of flight
XRD	= X-ray diffraction

---

## 14 References

- [1] H. Staudinger, *Ber. Dtsch. Chem. Ges.* **1920**, *53*, 1073–1085.
- [2] Plastics – the Facts 2015, [http://www.plasticseurope.org/documents/document/20151216062602-plastics\\_the\\_facts\\_2015\\_final\\_30pages\\_14122015.pdf](http://www.plasticseurope.org/documents/document/20151216062602-plastics_the_facts_2015_final_30pages_14122015.pdf), **2015**, online; accessed May 23, 2016.
- [3] G. V. Korolev, M. M. Mogilevich, *Three-Dimensional Free-Radical Polymerization*, Springer-Verlag, Berlin, Heidelberg, **2006**.
- [4] F. Fischer, U. Beier, F. Wolff-Fabris, V. Altstädt, *Sci. Eng. Compos. Mater.* **2011**, *18*, 209–215.
- [5] Plastics – the Facts 2015, <http://www.epoxy-europe.eu/25>, **2016**, online; accessed June 22, 2016.
- [6] F. R. Mayo, F. M. Lewis, *J. Am. Chem. Soc.* **1944**, *66*, 1594–1601.
- [7] I. W. Hamley, *Developments in Block Copolymer Science and Technology*, John Wiley & Sons, Ltd, Chichester, UK, **2004**.
- [8] I. W. Hamley, *The Physics of Block Copolymers*, 1st ed. Ed., Oxford University Press, **1999**.
- [9] K. A. Parker, N. S. Sampson, *Acc. Chem. Res.* **2016**, *49*, 408–417.
- [10] B. Heuer, W. Kaminsky, *Macromolecules* **2005**, *38*, 3054–3059.
- [11] K. Matyjaszewski, K. A. Davis, *Statistical, Gradient, Block and Graft Copolymers by Controlled/Living Radical Polymerizations*, vol. 159 of *Advances in Polymer Science*, Springer Berlin Heidelberg, Berlin, Heidelberg, **2002**.
- [12] H. Künstle, T. Melchin, R. Tangelder, *Aqueous, polyvinyl alcohol stabilized vinyl acetate-ethylene-copolymer dispersion having high filler compatibility for carpet coating compositions*, **2016**, WO2016012209.
- [13] M. Dupont, M. Stol, *Adhesive compositions containing a block copolymer with polymyrcene*, **2015**, WO2015153736.

## 14 References

---

- [14] O. G. Piringer, A. L. Baner, *Plastic Packaging: Interactions with Food and Pharmaceuticals*, 2nd Ed., Wiley-VCH Verlag GmbH & Co. KGaA, Weinheim, Germany, **2008**, p. 32–33.
- [15] S. Hilf, A. F. M. Kilbinger, *Nat. Chem.* **2009**, *1*, 537–546.
- [16] H. Willcock, R. K. O'Reilly, *Polym. Chem.* **2010**, *1*, 149–157.
- [17] A. Bousquet, H. Awada, R. C. Hiorns, C. Dagron-Lartigau, L. Billon, *Prog. Polym. Sci.* **2014**, *39*, 1847–1877.
- [18] L. Charles, *Mass Spectrom. Rev.* **2014**, *33*, 523–543.
- [19] K. Müllen, G. Wegner, *Electronic Materials: The Oligomer Approach*, Wiley-VCH Verlag GmbH, Weinheim, Germany, **1998**.
- [20] G. Moad, D. H. Solomon, *The Chemistry of Radical Polymerization*, 2nd Ed., Elsevier Science Ltd, Amsterdam, **2005**.
- [21] L. J. Fetters, J. Lustoň, R. P. Quirk, F. Vašš, R. N. Young, *Anionic Polymerization*, vol. 56 of *Advances in Polymer Science*, Springer Berlin Heidelberg, Berlin, Heidelberg, **1984**.
- [22] K. Matyjaszewski, *Cationic Polymerizations: Mechanisms, Synthesis & Applications*, Marcel Dekker, Inc., New York, **1996**.
- [23] R. H. Grubbs, W. Tumas, *Science* **1989**, *243*, 907–915.
- [24] J. Boor, *Ziegler–Natta Catalysts Polymerizations*, Academic Press, Inc., New York, **1979**.
- [25] M. E. Rogers, T. E. Long, *Synthetic Methods in Step-Growth Polymers*, John Wiley & Sons, Inc., Hoboken, **2003**.
- [26] C. Gao, D. Yan, *Prog. Polym. Sci.* **2004**, *29*, 183–275.
- [27] W. H. Carothers, *Trans. Faraday Soc.* **1936**, *32*, 39–49.
- [28] A. Rudin, *J. Chem. Educ.* **1969**, *46*, 595.

- 
- [29] A. R. Cooper, *Determination of Molecular Weight*, Wiley, New York, **1989**.
- [30] F. W. Billmeyer, *J. Polym. Sci. Part C Polym. Symp.* **2007**, *8*, 161–178.
- [31] F. B. Rolfson, H. Coll, *Anal. Chem.* **1964**, *36*, 888–894.
- [32] C. A. Glover, *Advances in Chemistry* **1973**, *125*, 1–8.
- [33] G. C. Berry, P. R. Eisaman, *J. Polym. Sci. Polym. Phys. Ed.* **1974**, *12*, 2253–2266.
- [34] P. J. Flory, T. G. Fox, *J. Polym. Sci.* **1950**, *5*, 745–747.
- [35] P. Debye, *J. Phys. Colloid Chem.* **1947**, *51*, 18–32.
- [36] B. H. Zimm, *J. Chem. Phys.* **1948**, *16*, 1093–1099.
- [37] W. Schärtel, *Light Scattering from Polymer Solutions and Nanoparticle Dispersions*, Springer-Verlag, Berlin, Heidelberg, **2007**.
- [38] T. Williams, *J. Mater. Sci.* **1970**, *5*, 811–820.
- [39] J. C. Moore, *J. Polym. Sci. Part A Gen. Pap.* **1964**, *2*, 835–843.
- [40] V. G. Meyerhoff, *Die Makromol. Chemie* **1968**, *118*, 265–271.
- [41] Z. Grubisic, P. Rempp, H. Benoit, *J. Polym. Sci. Part B Polym. Phys.* **1996**, *34*, 1707–1713.
- [42] H. G. Barth, *J. Polym. Sci. Part B Polym. Phys.* **1996**, *34*, 1705–1706.
- [43] L. H. Sperling, *Introduction to Physical Polymer Science*, John Wiley & Sons, Inc., Hoboken, Chap. The crystalline state, 4th Ed., **2006**, p. 239–323.
- [44] Y. Long, R. A. Shanks, Z. H. Stachurski, *Prog. Polym. Sci.* **1995**, *20*, 651–701.
- [45] M. Eder, A. Wlochowicz, *Polymer* **1983**, *24*, 1593–1595.
- [46] L. H. Sperling, *Introduction to Physical Polymer Science*, John Wiley & Sons, Inc., Hoboken, Chap. Glass–Rubber transition behavior, 4th Ed., **2006**, p. 349–425.
- [47] Y. Kong, J. Hay, *Polymer* **2002**, *43*, 3873–3878.

## 14 References

---

- [48] I. M. Ward, J. Sweeney, *Mechanical Properties of Solid Polymers*, John Wiley & Sons, Ltd, Chichester, UK, **2012**.
- [49] L. H. Sperling, *Introduction To Physical Polymer*, 4th ed. Ed., John Wiley & Sons, Inc., Hoboken, **2006**.
- [50] U. Scherf, *Top. Curr. Chem.* **1999**, *201*, 163–222.
- [51] M. Leclerc, J.-F. Morin, *Design and Synthesis of Conjugated Polymers*, Wiley-VCH Verlag GmbH & Co. KGaA, Weinheim, Germany, **2010**.
- [52] C. K. Chiang, C. R. Fincher, Y. W. Park, A. J. Heeger, H. Shirakawa, E. J. Louis, S. C. Gau, A. G. MacDiarmid, *Phys. Rev. Lett.* **1977**, *39*, 1098–1101.
- [53] A. C. Grimsdale, K. Müllen, *Angew. Chemie Int. Ed.* **2005**, *44*, 5592–5629.
- [54] M. Inbasekaran, W. Wu, E. P. Woo, *Process for preparing conjugated polymers*, **1997**, US 5777070 A.
- [55] A. Kraft, A. C. Grimsdale, A. B. Holmes, *Angew. Chemie Int. Ed.* **1998**, *37*, 402–428.
- [56] G. Strobl, *Conjugated Polymers*, Springer Berlin Heidelberg, Berlin, Heidelberg, Chap. Conjugated, **2007**, p. 287–312.
- [57] J. Brédas, R. Silbey, *Conjugated polymers: The novel science and technology of highly conducting and nonlinear optically active materials*, Kluwer Academic Publishers, Dordrecht, **1991**.
- [58] T. A. . Skotheim, J. R. . Reynolds, *Conjugated Polymers*, 3rd Ed., Handbook of Conducting Polymers, CRC Press, Boca Raton, **2006**.
- [59] T. Vahlenkamp, G. Wegner, *Macromol. Chem. Phys.* **1994**, *195*, 1933–1952.
- [60] M. Kobayashi, J. Chen, T.-C. Chung, F. Moraes, A. Heeger, F. Wudl, *Synthetic Metals* **1984**, *9*, 77 – 86.
- [61] D. Neher, *Macromol. Rapid Commun.* **2001**, *22*, 1365–1385.
- [62] J. H. Burroughes, D. D. C. Bradley, A. R. Brown, R. N. Marks, K. Mackay, R. H. Friend, P. L. Burns, A. B. Holmes, *Nature* **1990**, *347*, 539–541.



- [63] G. W. Smith, *Mol. Cryst. Liq. Cryst.* **1979**, *49*, 207–209.
- [64] J. Moulton, P. Smith, *Polymer* **1992**, *33*, 2340–2347.
- [65] S. Tokito, P. Smith, A. J. Heeger, *Polymer* **1991**, *32*, 464–470.
- [66] H. Gaspar, L. Fernandes, L. Brandão, G. Bernardo, *Polym. Test.* **2014**, *34*, 183–191.
- [67] T. Ito, H. Shirakawa, S. Ikeda, *J. Polym. Sci. Polym. Chem. Ed.* **1974**, *12*, 11–20.
- [68] P. Kovacic, M. B. Jones, *Chem. Rev.* **1987**, *87*, 357–379.
- [69] G. K. Noren, J. K. Stille, *J. Polym. Sci. Macromol. Rev.* **1971**, *5*, 385–430.
- [70] K. Tamao, K. Sumitani, M. Kumada, *J. Am. Chem. Soc.* **1972**, *94*, 4374–4376.
- [71] T. Yamamoto, Y. Hayashi, A. Yamamoto, *Bull. Chem. Soc. Jpn.* **1978**, *51*, 2091–2097.
- [72] A. Suzuki, *Angew. Chem. Int. Ed.* **2011**, *50*, 6722–6737.
- [73] J. Sakamoto, M. Rehahn, D. Schlüter, in *Des. Synth. Conjug. Polym.*, Wiley-VCH Verlag GmbH & Co. KGaA, **2010**, p. 45–90.
- [74] Z. Bao, W. Chan, L. Yu, *Chem. Mater.* **1993**, *5*, 2–3.
- [75] S. Huo, R. Mroz, J. Carroll, *Org. Chem. Front.* **2015**, *2*, 416–445.
- [76] S.-L. Suraru, J. A. Lee, C. K. Luscombe, *ACS Macro Lett.* **2016**, 724–729.
- [77] A. Aboukassim, C. Chevrot, *Polymer* **1993**, *34*, 401–405.
- [78] J. M. Tour, *Adv. Mater.* **1994**, *6*, 190–198.
- [79] A. C. Grimsdale, K. Müllen, *Adv. Polym. Sci.* **2006**, *199*, 1–82.
- [80] A. C. Grimsdale, K. Müllen, *Adv. Polym. Sci.* **2008**, *212*, 1–48.
- [81] K. Müllen, U. Scherf, *Organic Light Emitting Devices: Synthesis, Properties and Applications*, Wiley-VCH Verlag GmbH & Co. KGaA, Weinheim, Germany, **2005**.
- [82] D. A. Bernardis, G. G. Malliaras, R. M. Owens, *Organic Semiconductors in Sensor Applications*, Springer, Berlin Heidelberg, Germany, **2008**.

## 14 References

---

- [83] C. Brabec, U. Scherf, V. Dyakonov, *Organic Photovoltaics: Materials, Device Physics, and Manufacturing Technologies*, Wiley-VCH Verlag GmbH & Co. KGaA, Weinheim, Germany, **2014**.
- [84] A. C. Grimsdale, K. L. Chan, R. E. Martin, P. G. Jokisz, A. B. Holmes, *Chem. Rev.* **2009**, *109*, 897–1091.
- [85] D. Dean, M. Husband, M. Trimmer, *J. Polym. Sci. Part B Polym. Phys.* **1998**, *36*, 2971–2979.
- [86] K. Friedrich, H. Sue, P. Liu, A. Almajid, *Tribol. Int.* **2011**, *44*, 1032–1046.
- [87] PrimoSpire® SRP, <http://www.solvay.com/en/markets-and-products/featured-products/primospire.html>, **2016**, online; accessed June 08, 2016.
- [88] A. Almajid, K. Friedrich, A. Noll, L. Gyurova, *Plast. Rubber Compos.* **2013**, *42*, 401–406.
- [89] A. Almajid, K. Friedrich, A. Noll, L. Gyurova, *Plast. Rubber Compos.* **2013**, *42*, 123–128.
- [90] A. Almajid, K. Friedrich, A. Noll, L. Gyurova, *Plast. Rubber Compos.* **2014**, *43*, 138–144.
- [91] D. B. Thomas, N. Maljkovic, R. R. Gagné, *Substituted polyphenylenes via supported transition metal catalysis*, **2010**, US7365146.
- [92] G. C. Plithides, S. Sriram, *Fasteners made of a polymer material*, **2010**, WO2010112435 A1.
- [93] K. Friedrich, T. Burkhart, A. A. Almajid, F. Hauptert, *Int. J. Polym. Mater.* **2010**, *59*, 680–692.
- [94] C. P. Frick, A. L. Dirienzo, A. J. Hoyt, D. L. Safranski, M. Saed, E. J. Losty, C. M. Yakacki, *J. Biomed. Mater. Res. A* **2013**, *102*, 3122—3129.
- [95] V. H. O. Wirth, W. Kern, E. Schmitz, *Die Makromol. Chemie* **1963**, *68*, 69–99.

- 
- [96] K. N. Baker, A. V. Fratini, T. Resch, H. C. Knachel, W. Adams, E. Socci, B. Farmer, *Polymer* **1993**, *34*, 1571–1587.
- [97] U. Lauter, W. H. Meyer, G. Wegner, *Macromolecules* **1997**, *30*, 2092–2101.
- [98] V. W. Kern, M. Seibel, H. O. Wirth, *Die Makromol. Chemie* **1959**, *29*, 164–189.
- [99] M. Ballauff, *Angew. Chemie Int. Ed.* **1989**, *28*, 253–267.
- [100] V. W. Kern, H. W. Ebersbach, I. Ziegler, *Die Makromol. Chemie* **1959**, *31*, 154–180.
- [101] A. R. Postema, K. Liou, F. Wudl, P. Smith, *Macromolecules* **1990**, *23*, 1842–1845.
- [102] A. J. Berresheim, M. Müller, K. Müllen, *Chem. Rev.* **1999**, *99*, 1747–1786.
- [103] K. C. Park, L. R. Dodd, K. Levon, T. K. Kwei, *Macromolecules* **1996**, *29*, 7149–7154.
- [104] U. Scherf, K. Müllen, *Die Makromol. Chemie, Rapid Commun.* **1991**, *12*, 489–497.
- [105] K. Chmil, U. Scherf, *Die Makromol. Chemie, Rapid Commun.* **1993**, *14*, 217–222.
- [106] M. B. Goldfinger, T. M. Swager, *J. Am. Chem. Soc.* **1994**, *116*, 7895–7896.
- [107] S. Jakob, A. Moreno, X. Zhang, L. Bertschi, P. Smith, A. D. Schlüter, J. Sakamoto, *Macromolecules* **2010**, *43*, 7916–7918.
- [108] J. Simitzis, L. Zoumboulakis, A. Stamboulis, G. Hinrichsen, *Angew. Makromol. Chemie* **1993**, *213*, 181–196.
- [109] R. B. Seymour, *Conductive polymers*, Plenum Press, **1981**, p. 237.
- [110] J. L. Musfeldt, J. R. Reynolds, D. B. Tanner, J. P. Ruiz, J. Wang, M. Pomerantz, *J. Polym. Sci. Part B Polym. Phys.* **1994**, *32*, 2395–2404.
- [111] N. Kobayashi, S. Sasaki, M. Abe, S. Watanabe, H. Fukumoto, T. Yamamoto, *Macromolecules* **2004**, *37*, 7986–7991.
- [112] S. Y. Hong, D. Y. Kim, C. Y. Kim, R. Hoffmann, *Macromolecules* **2001**, *34*, 6474–6481.
- [113] B. Hohl, L. Bertschi, X. Zhang, A. D. Schlüter, J. Sakamoto, *Macromolecules* **2012**, *45*, 5418–5426.

## 14 References

---

- [114] G. Wittig, G. Lehmann, *Chem. Ber.* **1957**, *90*, 875–892.
- [115] R. Kandre, A. D. Schlüter, *Macromol. Rapid Commun.* **2008**, *29*, 1661–1665.
- [116] S. M. Mathew, J. T. Engle, C. J. Ziegler, C. S. Hartley, *J. Am. Chem. Soc.* **2013**, *135*, 6714–6722.
- [117] S. Mathew, L. A. Crandall, C. J. Ziegler, C. S. Hartley, *J. Am. Chem. Soc.* **2014**, *136*, 16666–16675.
- [118] E. Ohta, H. Sato, S. Ando, A. Kosaka, T. Fukushima, D. Hashizume, M. Yamasaki, K. Hasegawa, A. Muraoka, H. Ushiyama, K. Yamashita, T. Aida, *Nat. Chem.* **2010**, *3*, 68–73.
- [119] V. S. Claesson, R. Gehm, W. Kern, *Die Makromol. Chemie* **1951**, *7*, 46–61.
- [120] R. Kandre, K. Feldman, H. E. H. Meijer, P. Smith, A. D. Schlüter, *Angew. Chemie Int. Ed.* **2007**, *46*, 4956–4959.
- [121] J. Sakamoto, M. Rehahn, G. Wegner, A. D. Schlüter, *Macromol. Rapid Commun.* **2009**, *30*, 653–687.
- [122] M. Rehahn, A.-D. Schlüter, G. Wegner, W. Feast, *Polymer* **1989**, *30*, 1060–1062.
- [123] M. Rehahn, A. Schlüter, G. Wegner, *Die Makromol. Chemie* **1990**, *191*, 1991–2003.
- [124] A. de Meijere, F. Diederich, *Metal-Catalyzed Cross-Coupling Reactions*, 2 Ed., Wiley-VCH Verlag GmbH & Co. KGaA, Weinheim, Germany, **2004**.
- [125] N. Miyaura, in *Top. Curr. Chem. Cross-Coupling React.*, vol. 219, Springer, Berlin Heidelberg, **2002**, p. 11–59.
- [126] J. Louie, J. F. Hartwig, *J. Am. Chem. Soc.* **1995**, *117*, 11598–11599.
- [127] J. A. Casares, P. Espinet, G. Salas, *Chem. Eur. J.* **2002**, *8*, 4843–4853.
- [128] A. Gillie, J. K. Stille, *J. Am. Chem. Soc.* **1980**, *102*, 4933–4941.
- [129] A. J. J. Lennox, G. C. Lloyd-Jones, *Angew. Chemie Int. Ed.* **2013**, *52*, 7362–7370.

- [130] R. M. Kandre, F. Kutzner, H. Schlaad, A. D. Schlüter, *Macromol. Chem. Phys.* **2005**, *206*, 1610–1618.
- [131] A. Ludemann, R. M. Anemian, A. Julliard, *Polymer mit aldehydgruppen, umsetzung sowie vernetzung dieses polymers, vernetztes polymer sowie elektrolumineszenzvorrichtung enthaltend dieses polymer*, **2010**, WO2010097155.
- [132] M. S. Ober, D. R. Romer, J. B. Etienne, T. J. Pulikkottil, *Aromatic polyacetals and articles comprising them*, **2013**, US20150025278.
- [133] A. D. Schlüter, *J. Polym. Sci. Part A Polym. Chem.* **2001**, *39*, 1533–1556.
- [134] B. Deffner, D. Schlüter, *Polym. Chem.* **2015**, *6*, 7833–7840.
- [135] H. Komber, S. Müllers, F. Lombeck, A. Held, M. Walter, M. Sommer, *Polym. Chem.* **2014**, *5*, 443–453.
- [136] S. K. Weber, F. Galbrecht, U. Scherf, *Org. Lett.* **2006**, *8*, 4039–4041.
- [137] A. Yokoyama, H. Suzuki, Y. Kubota, K. Ohuchi, H. Higashimura, T. Yokozawa, *J. Am. Chem. Soc.* **2007**, *129*, 7236–7237.
- [138] Z. Zhang, P. Hu, X. Li, H. Zhan, Y. Cheng, *J. Polym. Sci. Part A Polym. Chem.* **2015**, 1457–1463.
- [139] E. Elmalem, A. Kiriya, W. T. S. Huck, *Macromolecules* **2011**, *44*, 9057–9061.
- [140] K. Kosaka, Y. Ohta, T. Yokozawa, *Macromol. Rapid Commun.* **2015**, *36*, 373–377.
- [141] C. Adamo, C. Amatore, I. Ciofini, A. Jutand, H. Lakmini, *J. Am. Chem. Soc.* **2006**, *128*, 6829–6836.
- [142] M. Moreno-Mañas, M. Pérez, R. Pleixats, *J. Org. Chem.* **1996**, *61*, 2346–2351.
- [143] H. G. Kuivila, J. F. Reuwer Jr., J. A. Mangravite, *Can. J. Chem.* **1963**, *41*, 3081–3090.
- [144] J. Lozada, Z. Liu, D. M. Perrin, *J. Org. Chem.* **2014**, *79*, 5365–5368.

## 14 References

---

- [145] L. Metzler, T. Reichenbach, O. Brügger, H. Komber, F. Lombeck, S. Müllers, R. Hanselmann, H. Hillebrecht, M. Walter, M. Sommer, *Polym. Chem.* **2015**, *6*, 3694–3707.
- [146] J. Murage, J. W. Eddy, J. R. Zimbalist, T. B. McIntyre, Z. R. Wagner, F. E. Goodson, *Macromolecules* **2008**, *41*, 7330–7338.
- [147] R. A. Widenhoefer, H. A. Zhong, S. L. Buchwald, *J. Am. Chem. Soc.* **1997**, *119*, 6787–6795.
- [148] R. A. Bowie, O. C. Musgrave, *Chem. Soc. Chem. Commun.* **1963**, *5*, 3945–3949.
- [149] K. Kong, C. Cheng, *J. Am. Chem. Soc.* **1991**, *1*, 6313–6315.
- [150] F. E. Goodson, T. I. Wallow, B. M. Novak, *Macromolecules* **1998**, *31*, 2047–2056.
- [151] J. Frahn, B. Karakaya, A. Schäfer, A.-D. Schlüter, *Tetrahedron* **1997**, *53*, 15459–15467.
- [152] T. I. Wallow, B. M. Novak, *J. Org. Chem.* **1994**, *59*, 5034–5037.
- [153] W. H. Carothers, *Chem. Rev.* **1931**, *8*, 353–426.
- [154] P. J. Flory, *Chem. Rev.* **1946**, *39*, 137–197.
- [155] H. Jacobson, W. H. Stockmayer, *J. Chem. Phys.* **1950**, *18*, 1600–1606.
- [156] M. Gordon, W. B. Temple, *Die Makromol. Chemie* **1972**, *152*, 277–289.
- [157] J. A. Semlyen, *Mech. Polyreactions-Polymer Charact.* **1976**, *21*, 41–75.
- [158] H. R. Kricheldorf, G. Schwarz, *Macromol. Rapid Commun.* **2003**, *24*, 359–381.
- [159] C. Wutz, H. R. Kricheldorf, *Macromol. Theory Simulations* **2012**, *21*, 266–271.
- [160] R. F. T. Stepto, D. R. Waywell, *Die Makromol. Chemie* **1972**, *152*, 263–275.
- [161] H. R. Kricheldorf, S. Böhme, G. Schwarz, *Macromolecules* **2001**, *34*, 8879–8885.
- [162] H. R. Kricheldorf, M. Rabenstein, M. Maskos, M. Schmidt, *Macromolecules* **2001**, *34*, 713–722.

- [163] S. P. Jakob, Ph.d. thesis, ETH Zürich, **2013**.
- [164] B. E. Huff, W. Zhang, *t-Butyldimethylchlorosilane*, John Wiley & Sons, Ltd, **2001**.
- [165] R.-D. Rusu, A. D. Schlüter, *RSC Adv.* **2014**, *4*, 57026–57034.
- [166] B. Avitia, E. MacIntosh, S. Muhia, E. Kelson, *Tetrahedron Lett.* **2011**, *52*, 1631–1634.
- [167] M. Rehahn, A.-D. Schlüter, G. Wegner, W. Feast, *Polymer* **1989**, *30*, 1054–1059.
- [168] K. Ziegler, *Berichte der Dtsch. Chem. Gesellschaft (A B Ser.* **1934**, *67*, A139–A149.
- [169] J. Li, H. Fu, P. Hu, Z. Zhang, X. Li, Y. Cheng, *Chemistry* **2012**, *18*, 13941–13944.
- [170] S. Vanhee, R. Rulkens, U. Lehmann, C. Rosenauer, M. Schulze, W. Köhler, G. Wegner, *Macromolecules* **1996**, *29*, 5136–5142.
- [171] B. Freeman, A. Hill, *ACS Symp. Ser.* **1998**, *710*, 306–325.
- [172] H. Higuchi, Z. Yu, A. M. Jamieson, R. Simha, J. D. McGervey, *J. Polym. Sci. Part B Polym. Phys.* **1995**, *33*, 2295–2305.
- [173] Z. Mo, H. Zhang, *J. Macromol. Sci. Part C Polym. Rev.* **1995**, *35*, 555–580.
- [174] L. Mandelkern, *Crystallization of polymers*, vol. 38, Cambridge University Press, Cambridge, **1964**.
- [175] W. I. Lee, M. F. Talbott, G. S. Springer, L. A. Berglund, *J. Reinf. Plast. Compos.* **1987**, *6*, 2–12.
- [176] T. Fütterer, T. Hellweg, G. H. Findenegg, J. Frahn, A. D. Schlüter, C. Böttcher, *Langmuir* **2003**, *19*, 6537–6544.
- [177] C. A. Daniels, *Polymers: Structure and Properties*, Technomic Pub. Co, Lancaster, **1989**.
- [178] H. Yu, A. D. Schlüter, B. Zhang, *Macromolecules* **2014**, *47*, 4127–4135.
- [179] N. Murthy, R. Bray, S. Correale, R. Moore, *Polymer* **1995**, *36*, 3863–3873.

## 14 References

---

- [180] P. Smith, P. J. Lemstra, J. P. L. Pijpers, A. M. Kiel, *Colloid Polym. Sci.* **1981**, *259*, 1070–1080.
- [181] G. Dingemans, C. A. A. van Helvoirt, D. Pierreux, W. Keuning, W. M. M. Kessels, *J. Electrochem. Soc.* **2012**, *159*, 277–285.
- [182] E. Pretsch, P. Bühlmann, M. Badertscher, *Spektroskopische Daten zur Strukturklärung organischer Verbindungen*, 5th Ed., Springer-Verlag, Berlin, Heidelberg, **2010**.
- [183] D. R. Coulson, L. C. Satek, S. O. Grim, *Inorg. Synth.* **2007**, *13*, 121–124.
- [184] C. A. Tolman, W. C. Seidel, D. H. Gerlach, *J. Am. Chem. Soc.* **1972**, *94*, 2669–2676.
- [185] A. P. Hammersley, S. O. Svensson, M. Hanfland, A. N. Fitch, D. Hausermann, *High Press. Res.* **1996**, *14*, 235–248.



## 15 Acknowledgements

First of all I want to thank Prof. A. Dieter Schlüter for setting out this interesting and diverse topic, which gave me the chance to work on the boarder between polymer synthesis and materials science. Further I want to thank him for his constant patience, support, advice and fruitful discussions during the last years.

Prof. Jan Vermant and Prof. Massimo Morbidelli are gratefully acknowledged for taking the time to evaluate this thesis and for being a member in the PhD committee. In addition I would like to thank both of them for granting me access to their lab equipment in order to investigate my polymers.

Further I would like to thank Prof. Paul Smith and Dr. Kirill Feldmann, especially for the help and discussions about the tensile tests on my polymers.

In addition I would like to give special thanks to Prof. Anja Kröger-Brinkmann, for supporting us with the static light scattering results.

I would like to express my gratitude to Gregor Hofer, Dr. Julia Dshemuchadse and Dr. Thomas Weber for performing X-ray diffraction measurements on my polymer films and the patience it took to interpret the results.

Also I want to thank Dr. Thomas Schweizer not only for being a permanent contact person for all kinds of technical issues, but also for constantly putting great effort in keeping the GPC machines running and calibrated. For the better part of this work GPC was a vital method for me and without this support it wouldn't have been possible.

The entire mass spectrometry service group at the Laboratory of Organic Chemistry, ETH Zürich is greatly acknowledged for measuring countless mass spectra and constant advice about choosing the right method.

A very special thanks I want to give to all my lab mates over the last tree years. Especially

## 15 Acknowledgements

---

Chiara, Marco, Payam and Leon who were there nearly every day sharing the successes and giving support during frustrating moments. I'm also very grateful for all the fun we had outside the lab during skiing, dinners, wine fairs and partying.

In addition I want to thank Sandra, Chiara, Vivian and Danial for reading through this thesis.

I also would like to thank my students Sètuhn Jimaja and Pascal Jurt, who both contributed experimentally to this work. I really enjoyed working with you and I wish you all the best for your future.

Last but not least, I want to thank the whole Schlüter group for giving me a warm welcome in the beginning of my PhD and for the great working environment we had during my time at ETH.

Also outside of work I received a lot of support from friends and family, especially I want to mention the "Munich connection" (Thorsten, Philipp, Hannes, Miri, Sarah, Isy, Oli). The great times with you always allowed me to refresh my mind when ever it was necessary and I hope we will also have great fun in the future.

Last but not least I want to thank my parents and my family without whom I would not be where I'm now. The knowledge of having a place where I can always go during hard times gave me the strength to reach my goals during my whole education.

---

## Curriculum vitae

**Name** Bernd Deffner  
**Address** Glärnischstrasse 11  
CH-8800 Thalwil  
**Nationality** German  
**Email** bernd.deffner@mat.ethz.ch  
**Phone** +41(0) 78 906 003 0  
**Date of Birth** October 10, 1986

---

### Education

---

06/2013 – 10/2016 **Doctor of Science, ETH Zürich, Switzerland**  
Synthesis and properties of poly(*m,p*-phenylene)s  
Supervision: Professor A. D. Schlüter

04/2008 – 05/2013 **Masters Degree in Chemistry**  
**Johannes Gutenberg-University of Mainz, Germany**

09/2012 – 05/2013 **Master thesis at ETH Zürich**  
Synthesis of monodisperse oligofluorenes.  
Supervision: Professor A. D. Schlüter

08/2011 – 02/2012 **Research project, Cornell University**  
Synthesis and lithography of polymer brushes.  
Supervision: Professor C. K. Ober

10/2006 – 03/2008 **Intermediate diploma in applied chemistry**  
**Technical University Nürnberg**

11/2005 – 07/2006 **Civilian Service**

09/2003 – 07/2005 **Technical diploma, Technical secondary school Ansbach**

---

### Work experience

---

05/2011 – 08/2011 **Internship, BASF SE Ludwigshafen, Germany**  
Synthesis of monomers from renewable resources.  
Up-scaling of the syntheses to a kilogram scale.

## Curriculum Vitae

---

11/2010 – 03/2011 and 08/2009 – 03/2010	<b>Research assistant, Max-Planck-Institut for polymer research Mainz, Germany</b> Synthesis of model compounds for sensitivity enhancement in NMR via parahydrogen induced polarization. MRI and NMR experiments with hyperpolarized $^{129}\text{Xe}$ .
08/2010 – 10/2010	<b>Internship, Grindeks Riga, Latvia</b> Synthesis of active pharmaceutical ingredients. Up-scaling of the syntheses to a kilogram scale.
08/2008 – 10/2008	<b>Internship, Boehringer Ingelheim Vienna, Austria</b> Syntheses of active pharmaceutical ingredients

## Additional skills

---

Languages	German (Mother tongue), English (fluent)
IT	Microsoft Office, Origin, ChemBioOffice, MestReNova, TopSpin, SciFinder, Reaxys, Matlab, LaTeX, POV-Ray
Further education	General Management, Patent law, Macroeconomics, Business administration

## Prizes and Scholarships

---

06/2015	<b>Chemistry Travel Award of the Swiss academy of Science</b>
since 10/2011	<b>BASF European Talent pool</b>
09/2012 – 05/2013	<b>Erasmus Scholarship during master thesis</b>
04/2011 – 05/2013	<b>Scholarship of the German federal ministry of education and research</b>
08/2011 – 03/2012	<b>ISAP Scholarship of the German academic exchange service</b>

## Extracurricular activities

---

since 08/2014	<b>President and treasurer of the job platform eth-gethired</b>
since 09/1996	<b>Trumpet player in different brass bands</b>
06/2006 – 07/2006	<b>Volunteer FIFA world cup 2006</b>

---

## Publications

Parts of this thesis have already been published.

### Articles

---

Bernd Deffner, A. Dieter Schlüter, „Robust procedure for large scale synthesis of a high molar mass, unsubstituted poly(*m,p*-phenylene)”, **2015**, *Polymer Chemistry*, 6, 7833-7840.

### Oral presentations

---

Bernd Deffner, A. Dieter Schlüter, “High molecular weight poly(*m,p*-phenylene)s derived by Suzuki polycondensation: synthesis, processing and testing”, **December 2015**, *Pacificchem*, Honolulu.

Bernd Deffner, A. Dieter Schlüter, “High molecular weight poly(*m,p*-phenylene)s derived by Suzuki polycondensation: synthesis, processing and testing”, **September 2015**, *Fall meeting of the Swiss chemical society*, Lausanne.

Bernd Deffner, A. Dieter Schlüter, “High molecular weight poly(*m,p*-phenylene)s by Suzuki-Miyaura cross-coupling polymerization“, **November 2014**, 5. *Symposium on Academic Exchange and Collaborative Research*, Zürich.

Bernd Deffner, A. Dieter Schlüter, “Poly(*m,p*-phenylene) based materials via Suzuki polycondensation“, **August 2014**, *BASF International summer course*, Ludwigshafen.

### Poster presentations

---

Bernd Deffner, Anja Kroeger, Gregor Hofer, A. Dieter Schlüter, “Molecular weight determination and mechanical behavior of 300 kDa poly(*m,p*-phenylene) synthesized by Suzuki polycondensation”, **July 2016**, *Warwick polymer conference 2016*, Warwick

Bernd Deffner, A. Dieter Schlüter, “Poly(*m,p*-phenylene) based Materials via Suzuki Polycondensation”, **September 2014**, *Fall meeting of the Swiss chemical society*, Zürich

Bernd Deffner, A. Dieter Schlüter, “Poly(*m,p*-phenylene) based Materials via Suzuki Polycondensation”, **June 2014**, *Swiss chemical society annual meeting of the division of polymers, colloids and interfaces*, Dübendorf